

Copyright
by
Will Sherman Slaughter
2010

**The Thesis Committee for Will Sherman Slaughter
Certifies that this is the approved version of the following thesis:**

Stability of Polymers Used for Enhanced Oil Recovery

**APPROVED BY
SUPERVISING COMMITTEE:**

Supervisor:

Gary A. Pope

Kishore K. Mohanty

Stability of Polymers Used for Enhanced Oil Recovery

by

Will Sherman Slaughter, BSCE

Thesis

Presented to the Faculty of the Graduate School of

The University of Texas at Austin

in Partial Fulfillment

of the Requirements

for the Degree of

Master of Science in Engineering

The University of Texas at Austin

May 2010

Dedication

To my lovely wife, Amy.

Acknowledgements

It is difficult to express in words how grateful I am for receiving the opportunity I was given to finish the journey that began seven years ago. First and foremost, I would like to thank my supervisor, Dr. Gary Pope. I am forever indebted to you for your guidance and support. Your unending drive to promote chemical EOR is inspiring, and I am grateful to have been a part of your research team. Next, I would like to express my gratitude to David Levitt, literally without whom none of this would have been possible. I truly appreciate everything you have done for me.

I would also like to thank my other committee member, Dr. Kishore Mohanty. I appreciate your devotion to the field; UT Austin is truly fortunate to have you. I am extremely lucky to have been able to associate with two great scientists in Dr. Larry Britton and Dr. Upali Weerasooriya. Thank you both for your stimulating conversations of all things chemistry. I would like to extend a special thanks to Maurice Bourrel, as well as everyone at Total in Lacq, for accepting me for the non French-speaking Texan that I am.

Other researchers that I would like to thank are Chris Britton, Do Hoon Kim, and Jith Liyanage. It would be impossible for the lab to run without you guys. Much of the work that our lab does would not be possible without the help of a great technical and administrative staff: Tony Bermudez, Glem Baum, Gary Miscoe, Joanna Castillo, Esther Barrientes, and Kiki Peckham. Thank you all for your help.

I would also like to acknowledge the financial support of the sponsors of the Chemical EOR JIP for the Center for Petroleum and Geosystems Engineering at the

University of Texas at Austin. A special thanks goes to Chevron for extending a job offer for me to continue the work I absolutely love doing.

Dr. Pope's group would not be successful without the collaborative work of many graduate and undergraduate students. People who have had a direct impact on the work in this research and deserve to be recognized include Robin Weatherl, Gina Cahill, Thilini Mudiyansele, Matt Dean, Siamak Chabokrow, Hyun Tae Yang, Sriram Solairaj, Vinay Sahni, Oluwaseun Magbagbeola, Kyle Tippley, Stephanie Adkins, and Sophie Dufour.

I would like to thank the two people who have shown unconditional love and support for any decision I have ever made: my parents Joan and Kenneth Slaughter. I would also like to thank my brother, Matt, and my sister, Jodi, for their support.

Finally, I would like to thank my lovely wife, Amy. Thank you for always being there for me.

May 2010

Abstract

Stability of Polymers Used For Enhanced Oil Recovery

Will Sherman Slaughter, M.S.E.

The University of Texas at Austin, 2010

Supervisor: Gary A. Pope

The purpose of this work was to study polymer degradation mechanisms as well as ways to mitigate it. In the area of chemical stability, defined as divalent cation tolerance of acrylic polymers as hydrolysis increases, use of the n-vinyl pyrrolidone (NVP) monomer helps to preserve viscosity and tolerate higher calcium concentrations over those polymers without NVP. Also, ethylenediaminetetraacetate tetrasodium salt (EDTA-Na^+_4) is shown to sequester calcium ions at alkaline conditions ($\text{pH} > 10$) and, in the case of lab-aged post-hydrolyzed poly(AM-co-AMPS), helps to retain full viscosity at all calcium concentrations when EDTA is present at a stoichiometric equivalence of calcium.

Many discrepancies exist in the literature concerning the presence or absence of degradation under various field or laboratory conditions. Carbonate and bicarbonate, which are typically present in natural waters but often neglected in lab-prepared brines,

prove to be a hidden variable in resolving why Shupe (1981) saw no loss in viscosity when sodium dithionite was added to polymer in the presence of oxygen (with bicarbonates) but others (Knight, 1973 and Levitt and Pope, 2008) observed severe degradation under similar conditions (but without bicarbonates). A commercial HPAM polymer (Flopaam 3630S) has been shown to be stable in the presence of ferrous iron in the absence of oxygen, clarifying an apparent discrepancy in the literature between the results of Yang and Treiber (1985) and Kheradmand (1987).

Dissolved oxygen (DO) levels, and not redox potential (ORP) measurements, are often reported in polymer stability research on oxidative degradation. ORP is shown to be a better measure of the onset of degradation because oxygen is initially being consumed and may not appear until substantial degradation has occurred. Although generally believed to be a detriment to polymer stability in the field, aeration of iron-laden source water prior to hydration of polymer may be beneficial in certain cases where exposure to air is unavoidable. Also, a novel process of safely producing sodium dithionite in the field proves to perform better in terms of long-term polymer stability in anaerobic conditions than the traditional method of using a solution made from powder dithionite.

Finally, a pre-sheared 5 million Dalton HPAM is successfully injected into a 3 mD carbonate reservoir core plug. Remarkably, permeability reduction factors remain at values close to unity. However, pressure data from ASP tertiary corefloods suggest that polymer is not feasible for field injections.

Table of Contents

List of Tables.....	xi
List of Figures	xiv
CHAPTER 1: Introduction.....	1
1.1 Motivation	1
1.2 Description of Chapters.....	3
CHAPTER 2: Literature Review.....	4
CHAPTER 3: Experimental Methodology	15
3.1 General Laboratory Equipment and Materials	15
3.2 Experimental Methodology.....	18
3.2.1 Chemical Stability.....	21
3.2.2 Thermal Stability Experiments.....	26
3.2.3 Coreflooding Experiments	31
CHAPTER 3: Experimental Methodology	15
3.1 General Laboratory Equipment and Materials	15
3.2 Experimental Methodology.....	18
3.2.1 Chemical Stability.....	21
3.2.2 Thermal Stability Experiments.....	26
3.2.3 Coreflooding Experiments	31
CHAPTER 4: Chemical Stability Results & Discussion	38
4.1 Thermal Aging Experiments	38
4.2 Calcium Tolerance Experiments	40
4.3 Discussion	42
CHAPTER 5: Thermal Stability Results & Discussion.....	69
5.1 Experiments With Fe^{++}	69
5.2 Experiments With H_2	73
5.3 Experiments With Sodium Dithionite.....	75

5.4 Observations From the Field.....	82
5.5 Discussion	83
CHAPTER 6: Coreflooding Results & Discussion.....	119
6.1 Polymer Injectivity Tests	119
6.2 Chemical Floods.....	122
6.3 Discussion	126
CHAPTER 7: Conclusions and Recommendations	163
Appendix A	168
Bibliography.....	192
Vita	196

List of Tables

Table 2.1:	E_H and pH of the Natural Environment (Baas Becking (1960) and Shafer and Pirson(1969)).....	14
Table 3.1:	Polymers used in this research	34
Table 3.2:	Redox potential (ORP) of various aqueous solutions	35
Table 3.3:	Background NaCl concentrations for Ca^{++} tolerance experiments ..	36
Table 3.4:	Sample mixing sheet for Ca^{++} tolerance experiments using EDTA.	37
Table 4.1:	2500 ppm SAV 301 in 3% NaCl thermal aging experiments data (85 C)	44
Table 4.2:	2500 ppm SAV 301 in 3% NaCl thermal aging experiments data (100 C)	45
Table 4.3:	2500 ppm SAV 301 in 3% NaCl thermal aging experiments data (126 C)	46
Table 4.4:	2500 ppm Kypam 5 in 3% NaCl thermal aging experiments data (85 C)	47
Table 4.5:	2500 ppm Kypam 5 in 3% NaCl thermal aging experiments data (100 C)	48
Table 4.6:	2500 ppm Kypam 5 in 3% NaCl thermal aging experiments data (126 C)	49
Table 5.1:	Yang and Treiber's Brine Composition (Yang and Treiber (1985))	85
Table 5.2:	Shupe's Brine Composition (Shupe (1981))	86
Table 5.3:	Aging data from 2500 ppm 3630S in 3 wt% NaCl with 100 ppm dithionite from powder.....	87

Table 5.4:	Aging data from 2500 ppm 3630S in 3 wt% NaCl with 100 ppm dithionite from Montbrite 1240.....	88
Table 5.5:	Synthetic Field Brine Composition.....	89
Table 5.6:	Aging data from 2500 ppm 3330S in synthetic field brine with 100 ppm dithionite from Montbrite 1240 and 2 ppm Fe ⁺⁺	90
Table 5.7:	2500 ppm 3630S in 3 wt% NaCl with 100 ppm bisulfite and 2 ppm Fe ⁺⁺ as sulfate data	91
Table 6.1:	k _{air} and ϕ of reservoir core plugs	127
Table 6.2:	Reservoir rock and fluid properties.....	128
Table 6.3:	Formation and injection water make-up.....	129
Table 6.4:	2500 ppm AN 125 VLM in SSHSB, injected and produced viscosities, 25 C	130
Table 6.5:	2500 ppm AN 125 VLM in SSLSB, injected and produced viscosities, 25 C	131
Table 6.6:	Summary of polymer injectivity tests for core plug #341.....	132
Table 6.7:	10,000 ppm AB 305 VLM in SSLSB, injected and produced viscosities, 25 C	133
Table 6.8:	AB 305 MPM & FP 3230S in SSLSB, pre-sheared, sheared and produced viscosities, 25 C.....	134
Table 6.9:	L-9 phase behavior data for varying WOR	135
Table 6.10:	Summary of L-9 coreflood.....	136
Table A.1:	Summary of L-1 coreflood.....	168
Table A.2:	Summary of L-2 coreflood.....	171
Table A.3:	Summary of L-3 coreflood.....	174
Table A.4:	Summary of L-4 coreflood.....	177

Table A.5: Summary of L-5 coreflood.....	180
Table A.6: Summary of L-6 coreflood.....	183
Table A.7: Summary of L-7 coreflood.....	186
Table A.8: Summary of L-8 coreflood.....	189

List of Figures

Figure 4.1: 2500 ppm SAV 301 in 3% NaCl hydrolysis data ageing at 85 C, pH~7	50
Figure 4.2: 2500 ppm SAV 301 in 3% NaCl hydrolysis data ageing at 100 C, pH~7	51
Figure 4.3: 2500 ppm SAV 301 in 3% NaCl hydrolysis data ageing at 126 C, pH~7	52
Figure 4.4: 2500 ppm Kypam 5 in 3% NaCl hydrolysis data ageing at 85 C, pH~7	53
Figure 4.5: 2500 ppm Kypam 5 in 3% NaCl hydrolysis data ageing at 100 C, pH~7	54
Figure 4.6: 2500 ppm Kypam 5 in 3% NaCl hydrolysis data ageing at 126 C, pH~7	55
Figure 4.7: Ca^{++} tolerance with 1.2 wt% NaCl for lab-aged post-hydrolyzed polymers ($\tau \sim 0.6$)	56
Figure 4.8: Ca^{++} tolerance with 3 wt% NaCl for lab-aged post-hydrolyzed polymers ($\tau \sim 0.6$)	57
Figure 4.9: Ca^{++} tolerance with 5 wt% NaCl for lab-aged post-hydrolyzed polymers ($\tau \sim 0.6$)	58
Figure 4.10: Ca^{++} tolerance with 10 wt% NaCl for lab-aged post-hydrolyzed polymers ($\tau \sim 0.6$)	59
Figure 4.11: Ca^{++} tolerance for 2000 ppm PHAMPS (post-hydrolyzed AN 125) in 13.6 wt% NaCl, $\tau \sim 0.55$	60

Figure 4.12: Ca^{++} tolerance for 2000 ppm PHAMPS (post-hydrolyzed AN 125), 1.2 wt% NaCl, with and without 4 wt% EDTA; pH=10.75; $\tau \sim 0.55$; relative viscosity.....	61
Figure 4.13: Ca^{++} tolerance for 2000 ppm PHAMPS (post-hydrolyzed AN 125), 1.2 wt% NaCl, with and without 4 wt% EDTA; pH=10.75; $\tau \sim 0.55$; apparent viscosity.....	62
Figure 4.14: Effect of 4 wt% EDTA on viscosity for 2000 ppm PHAMPS (post-hydrolyzed AN 125) for varying salinities; pH=10.75; $\tau \sim 0.55$; no Ca^{++}	63
Figure 4.15: Effect of increasing EDTA concentration on viscosity for 2000 ppm PHAMPS (post-hydrolyzed AN 125), 1.2 wt% NaCl; pH=10.75; $\tau \sim 0.55$; no Ca^{++}	64
Figure 4.16: EDTA shows little effect on Ca^{++} tolerance at neutral pH using PHAMPS (post-hydrolyzed AN 125), 5 wt% NaCl, 8 EDTA:1 Ca^{++} ; pH=7.2; $\tau \sim 0.55$	65
Figure 4.17: At alkaline conditions, EDTA completely removes effect of Ca^{++} for 2000 ppm PHAMPS (post-hydrolyzed AN 125), 5 wt% NaCl, 8 EDTA:1 Ca^{++} ; pH=11; $\tau \sim 0.55$	66
Figure 4.18: For post-hydrolyzed PAM (FA 920 SH), EDTA shows improvement for Ca^{++} tolerance but not as pronounced as with PHAMPS, 2000 ppm PHPAM, 1.2 wt% NaCl, 8 EDTA:1 Ca^{++} ; pH=11; $\tau \sim 0.55$	67
Figure 4.19: Effect of increasing EDTA concentration on viscosity for 2000 ppm PHPAM (post-hydrolyzed FA 920 SH), 1.2 wt% NaCl; pH=10.75; $\tau \sim 0.55$; no Ca^{++}	68
Figure 5.1: $E_{\text{Ag}/\text{AgCl}}$ as a function of DO in deionized water (DI) at 23 C	92

Figure 5.2: $E_{\text{Ag}/\text{AgCl}}$ as a function of $[\text{Fe}^{++}]$ in DI, 23 C	93
Figure 5.3: 2500 ppm 3630S in 3% NaCl with 2 ppm Fe^{++} and a slow continuous supply of O_2	94
Figure 5.4: 2500 ppm 3630S in 3% NaCl and Yang and Treiber's brine with 2 ppm Fe^{++} and a slow continuous supply of O_2	95
Figure 5.5: 2500 ppm 3630S in 3% NaCl and Yang and Treiber's brine with 2 ppm Fe^{++} and an initial small amount of O_2 (30 ppb) and no more exposure to O_2	96
Figure 5.6: 2500 ppm 3630S in 3% NaCl reduced with H_2 then exposed to O_2	97
Figure 5.7: 2500 ppm 3630S in 3% NaCl reduced with H_2 , dosed with 2 ppm Fe^{++} then exposed to O_2	98
Figure 5.8: Effect of amount of dithionite on 2500 ppm 3630S in 3 wt% NaCl when exposed to O_2	99
Figure 5.9: Effect of degree of hydrolysis on polymer stability when reduced with 100 ppm dithionite and exposed to O_2	100
Figure 5.10: Effect of bicarbonate (as seen in Shupe (1981) brine) on 2500 ppm 3630S in 3 wt% NaCl reduced with 100 ppm dithionite and exposed to O_2	101
Figure 5.11: Effect of DTPA on 2500 ppm 3630S in 3 wt% NaCl when dosed with 100 ppm dithionite and exposed to O_2	102
Figure 5.12: $E_{\text{Ag}/\text{AgCl}}$ and viscosity of 2500 ppm FA 920 SH in 3 wt% NaCl reduced with 100 ppm dithionite and exposed to O_2	103
Figure 5.13: $E_{\text{Ag}/\text{AgCl}}$ and viscosity of 2500 ppm FA 920 SH in 3 wt% NaCl reduced with 100 ppm dithionite initially under N_2 then exposed to O_2	104

Figure 5.14: $E_{Ag/AgCl}$ and viscosity of 2500 ppm 3630S in 3 wt% NaCl reduced with 100 ppm dithionite and exposed to O_2	105
Figure 5.15: $E_{Ag/AgCl}$ and viscosity of 2500 ppm 3630S in 3 wt% NaCl reduced with 100 ppm dithionite initially under N_2 then exposed to O_2	106
Figure 5.16: $E_{Ag/AgCl}$ and viscosity of 2500 ppm AN 923 in 3% NaCl reduced with 100 ppm dithionite and exposed to O_2	107
Figure 5.17: $E_{Ag/AgCl}$ and viscosity of 2500 ppm AN 923 in 3 wt% NaCl reduced with 100 ppm dithionite initially under N_2 then exposed to O_2	108
Figure 5.18: $E_{Ag/AgCl}$ and viscosity of 2500 ppm ALP 99 in 3% NaCl reduced with 100 ppm dithionite and exposed to O_2	109
Figure 5.19: $E_{Ag/AgCl}$ and viscosity of 2500 ppm ALP 99 in 3 wt% NaCl reduced with 100 ppm dithionite initially under N_2 then exposed to O_2	110
Figure 5.20: $E_{Ag/AgCl}$ and viscosity of 2500 ppm 3630S in 3 wt% NaCl deoxygenated then reduced with 100 ppm dithionite initially under N_2 then exposed to O_2	111
Figure 5.21: $E_{Ag/AgCl}$ and viscosity of 2500 ppm 3630S in 3% NaCl reduced with dithionite (using Montbrite 1240) initially under Ar then exposed to O_2	112
Figure 5.22: 2500 ppm 3630S in 3% NaCl reduced with dithionite (using powder) viscosity data for aged samples at various temperatures.....	113
Figure 5.23: 2500 ppm 3630S in 3% NaCl reduced with dithionite (using Montbrite 1240) viscosity data for aged samples at various temperatures	114
Figure 5.24: 2500 ppm 3330S in synthetic brine with 100 ppm dithionite (using Montbrite 1240) and 2 ppm Fe^{++} viscosity data for aged samples at various temperatures	115

Figure 5.25: 2500 ppm 3630S in 3% NaCl with bisulfite and 2 ppm Fe ⁺⁺ viscosity data for aged samples at various temperatures.....	116
Figure 5.26: Degradation experienced in the field when iron-laden source water is allowed to aerate after addition of polymer, 2 different polymer concentrations.....	117
Figure 5.27: In the case where contact with air during polymer hydration is unavoidable, degradation is lower if source brine is aerated prior to addition of polymer	118
Figure 6.1: High salinity polymer injectivity test brine flood pressure drop (#332); 69 C; 2 ft/day.....	137
Figure 6.2: High salinity polymer injectivity test polymer flood pressure drop, 2500 ppm AN 125 VLM in SSHSB (#332); 69 C; 1 & 2 ft/day.....	138
Figure 6.3: 2500 ppm AN 125 VLM in SSHSB, injected viscosity profile at 25 C	139
Figure 6.4: Low salinity polymer injectivity test polymer flood pressure drop, 2500 ppm AN 125 VLM in SSLSB (#332); 69 C; 1, 2, & 3 ft/day	140
Figure 6.5: 2500 ppm AN 125 VLM in SSLSB, viscosity profile at 25 C.....	141
Figure 6.6: Low salinity polymer injectivity test brine flood pressure drop (#341); 69 C; 4 ft/day.....	142
Figure 6.7: Low salinity polymer injectivity test polymer flood pressure drop, 10,000 ppm AB 305 VLM in SSLSB (#341); 69 C; 2 ft/day	143
Figure 6.8: 2500 ppm AB 305 MPM in SSLSB, viscosity profile at 25 C	144
Figure 6.9: 2000 ppm FP 3230S in SSLSB, viscosity profile at 25 C.....	145
Figure 6.10: Low salinity polymer injectivity test polymer flood pressure drop, 2500 ppm AB 305 MPM in SSLSB (#341); 69 C; 1.33 ft/day	146

Figure 6.11: Low salinity polymer injectivity test polymer flood pressure drop, 2000 ppm FP 3230S in SSLSB (#341); 69 C; 1.33 ft/day	147
Figure 6.12: L-9 phase behavior plot after 55 days, 10% oil.....	148
Figure 6.13: L-9 phase behavior plot after 55 days, 20% oil.....	149
Figure 6.14: L-9 phase behavior plot after 55 days, 30% oil.....	150
Figure 6.15: L-9 phase behavior plot after 55 days, 40% oil.....	151
Figure 6.16: L-9 phase behavior plot after 55 days, 50% oil.....	152
Figure 6.17: Pressure transducer setup and orientation of core.....	153
Figure 6.18: L-9 brine flood pressure data; 69 C; ~4 ft/day	154
Figure 6.19: L-9 oil flood pressure data (constant pressure); 69 C; 275 psi.....	155
Figure 6.20: L-9 oil flood pressure data (constant flow rate); 69 C; ~1.5 ft/day	156
Figure 6.21: L-9 water flood pressure data; 69 C; ~2.5 ft/day	157
Figure 6.22: FP 3230S in SSLSB, viscosity vs. concentration before and after shearing for 6 min in Waring blender, 25 C.....	158
Figure 6.23: L-9 chemical flood pressure data; 69 C; ~1 ft/day.....	159
Figure 6.24: Oil recovery, saturation, and cut for L-9 chemical flood.....	160
Figure 6.25: pH of effluent for L-9 chemical flood.....	161
Figure 6.26: Ion concentration of effluent for L-9 chemical flood.....	162
Figure A.1: L-1 chemical flood pressure data; 69 C; ~1 ft/day.....	169
Figure A.2: Oil recovery, saturation, and cut for L-1 chemical flood.....	170
Figure A.3: L-2 chemical flood pressure data; 69 C; ~1 ft/day.....	172
Figure A.4: Oil recovery, saturation, and cut for L-2 chemical flood.....	173
Figure A.5: L-3 chemical flood pressure data; 69 C; ~2 ft/day.....	175
Figure A.6: Oil recovery, saturation, and cut for L-3 chemical flood.....	176
Figure A.7: L-4 chemical flood pressure data; 69 C; ~2 ft/day.....	178

Figure A.8: Oil recovery, saturation, and cut for L-4 chemical flood.....	179
Figure A.9: L-5 chemical flood pressure data; 69 C; ~1 ft/day.....	181
Figure A.10: Oil recovery, saturation, and cut for L-5 chemical flood.....	182
Figure A.11: L-6 chemical flood pressure data; 69 C; ~2 ft/day.....	184
Figure A.12: Oil recovery, saturation, and cut for L-6 chemical flood.....	185
Figure A.13: L-7 chemical flood pressure data; 69 C; ~2 ft/day.....	187
Figure A.14: Oil recovery, saturation, and cut for L-7 chemical flood.....	188
Figure A.15: L-8 chemical flood pressure data; 69 C; ~2 ft/day.....	190
Figure A.16: Oil recovery, saturation, and cut for L-8 chemical flood.....	191

CHAPTER 1: INTRODUCTION

The research presented in this work was a part of the ongoing chemical enhanced oil recovery research at the University of Texas at Austin. The main focus of this work was to identify the methods to retard or prevent degradation to the acrylic polymers that are used for mobility control. In the following sections, the motivation for this work and description of all the chapters are provided.

1.1 MOTIVATION

One of the main goals of this research was to clarify many of the discrepancies that exist in literature published on polymer stability. For instance, Shupe (1981) reports that addition of dithionite to polymer in the presence of air results in minimal loss of viscosity after 3 hours while others (Knight, 1973 and Levitt and Pope, 2008) report that the degradation will be rapid and severe in the continual presence of oxygen. Elsewhere, Yang and Treiber (1985) reported that in presence of ferrous iron with oxygen absent no degradation was observed, whereas Kheradmand (1987) noted that degradation was severe under similar conditions.

Independent verification is necessary for new products. Polymer companies such as SNF Floerger are continuously seeking to provide better polymers that can prevent degradation without the use of additives. SNF claims that their SAV line of polymers, n-vinyl pyrrolidone (NVP) ter-polymers, can withstand higher temperatures without complete hydrolysis and exhibit better chemical stability, or more specifically tolerance to divalent cations. It is important to test these claims in order to validate the use of these improved products.

Also, in the area of chemical stability of polymer, Levitt (2009) reports that the solution and subsequent dissolution of silica may have affected the results. Some of Levitt's experiments were repeated during this research, but care was taken to eliminate exposure to glassware during polymer hydration at elevated pH.

Another goal of this research was to study a novel process for safely producing sodium dithionite in the field. Effects of sodium dithionite on polymer stability under simulated reservoir conditions are well known, but this is using the sodium dithionite as a powder. Fears exist in the field as to the safety factor involved with using powder dithionite because it is listed as pyrophoric, or has the capability to explode. A safe way of producing dithionite in the field is mixing sodium borohydride with sodium bisulfite, but the effect of this process on polymer rheology has not been studied. Identical tests were performed using each of the two methods available for dithionite production. If similar effects were observed, then handling of sodium dithionite in the field would no longer be a concern.

Opportunities to visit two full-field polymer injections prompted an unorthodox question: in situations where a polymer hydration or dilution brine is in reduced conditions, contains a significant amount of iron, and where subsequent exposure to oxygen is unavoidable, might it be better to aerate brine prior to the addition of polymer in order to avoid later degradation? Experiments were conducted to test this hypothesis.

Finally, core flooding is a necessary step in developing a successful chemical formulation. For this research, a difficult reservoir was evaluated for the feasibility of chemical enhanced oil recovery. The characteristics which make this a difficult reservoir are: very low permeability (< 3 mD), moderately high temperature (69 C), extremely saline and hard formation brine (220,000 ppm TDS, ~80,000 ppm divalent cations), and

an uncertainty of injection water (either 10,000 ppm TDS or 200,000 ppm TDS). Both polymer injectivity tests and chemical flooding were conducted for this reservoir.

1.2 DESCRIPTION OF CHAPTERS

A discussion of the literature results is presented in Chapter 2. Chapter 3 presents a description of the experimental apparatus and methodology used in this research. Chapter 4 discusses the results of the chemical stability experiments. This includes polymer hydrolysis studies and calcium tolerance experiments. Chapter 5 presents the results from thermal stability experiments which include studies involving interactions between polymer in the presence of a number of combinations of the following: oxygen, iron, sodium dithionite, and sodium carbonate/bicarbonate. Chapter 6 outlines the coreflooding experiments which were conducted for this research. The summary and conclusions as well as recommendations for future work are presented in chapter 7.

CHAPTER 2: LITERATURE REVIEW

Polymer is the most important constituent in chemical flooding because it provides the mobility control necessary for improved sweep efficiency, and without it, no amount of surfactant can economically recover oil (Sorbie, 1991 and Lake, 1989). Acrylic polymers, such as hydrolyzed polyacrylamides (HPAMs), are susceptible to degradation through many means widely present in the field. The causes of degradation and ways to mitigate it have been studied extensively for many years because maintaining polymer stability is crucial to the success of a chemical flood. Discrepancies are inevitable, and much of this research was motivated on attempting to clarify these.

The terms chemical stability and thermal stability were first defined by Muller (et al., 1980, and 1981a). Chemical stability refers to the chemical hydrolysis, which results in an increase in degree of hydrolysis (or more generally, anionicity), increased sensitivity to precipitation with divalent cations, and either an increase or decrease in viscosity, depending on salinity. Thermal stability is the oxidative degradation of polyacrylamide-based polymers used in the context of enhanced oil recovery, in which the acrylic backbone is cleaved by a radical mechanism, resulting in a reduction of molecular weight and a corresponding drop in viscosity.

Chemical Stability

Polymers hydrolyze with increased temperature and with a deviation in pH from neutral. Polymer hydrolysis has been detailed extensively in literature. Muller et al. (1981a, 1981b) studied the effects of several electrolytes (NaCl, CaCl₂, MgCl₂) on polymer viscosity with degree of hydrolysis (τ) ranging from 0 to 0.49. Muller et al.

reported that a critical τ of 0.3 exists above which precipitation can occur and the concentration of divalent cations necessary to show an onset of precipitation depends on τ . Davidson and Metzner (1982) showed that in the presence of divalent cations, polymer solutions will precipitate when aged at 90 C as the polymer hydrolyzes. It was also noted that precipitation of polymer in sea water becomes an issue after 200 days at 70 C.

Zaitoun and Potie (1983) also studied the precipitation of hydrolyzed PAM in the presence of calcium. They reported that above $\tau \sim 0.3$ (for 30 C and at 80 C), precipitations with calcium can occur. The amount of calcium necessary in order for precipitation above this value of τ decreases as τ increases. As τ approaches 1, or when HPAM becomes PAA (poly(acrylic acid)), the amount of calcium necessary for precipitation is the molar equivalence to carboxylate (or acrylate) monomers. Interestingly, the critical degree of hydrolysis is independent of polymer concentration. One last major finding of Zaitoun and Potie is that more calcium can be tolerated as the background concentration of NaCl increases.

Levitt (2009) conducted extensive experiments on salinity tolerance and divalent cation tolerance of many commercially available polymers. Polymers were tested both as they come from the supplier (initial degree of hydrolysis) as well as at increasing levels of degree of hydrolysis above the critical number of $\tau = 0.35$. He noted that for PAM and poly(AM-co-AMPS), values of $\tau \sim 0.6$ (or in the case of AMPS, total anionicity, σ) can be seen in samples that are aged at neutral pH at 85 C for more than 200 days as well as in samples which are hydrated in 0.3 M NaOH for 7-10 days at 23 C. This proved to be advantageous because now large stocks of post-hydrolyzed polymer solution could be prepared so that many scans (both varying NaCl and Ca^{++}) could be conducted on the same sample of polymer at the same degree of hydrolysis.

Levitt also found that calcium tolerance depends on the amount of NaCl present. One somewhat surprising artifact of ageing polymer at elevated pH and at increased temperature in borosilicate glass ampoules, is that the solution and subsequent dissolution of silica may inadvertently skew results. Although this was not necessarily observed at low temperature (23 C), Levitt recommended that the calcium tolerance experiments be revisited without the use of glassware when polymer solutions are at an elevated pH.

Notwithstanding the above observation, Levitt (2009) found that there was no difference in the cloud point, or the concentration of calcium necessary to show an onset of turbidity, of both post-hydrolyzed PAM or post-hydrolyzed poly(AM-co-AMPS). The major difference was that leading up to the cloud point, poly(AM-co-AMPS) retained much higher viscosities for all background NaCl concentrations. With limited experiments, he showed that post-hydrolyzed poly(AM-co-ATBS-co-NVP) outperformed both post-hydrolyzed PAM and post-hydrolyzed poly(AM-co-AMPS) in both amount of calcium necessary to precipitate as well as viscosity retained.

It should be noted that the term above, ATBS (sodium acrylamido tertio butyl sulfonate), is a more general description of the monomer commonly referred to as AMPS (2-acrylamide 2-methyl propane sulfonate). ATBS is one monomer that has been researched and identified as a way to make acrylamide more chemically stable because it is a sulfonate with more tolerance to divalent cations than a carboxylate. Moradi-Araghi et al. (1987), Taylor and Nasr-El-Din (1995), and Martin et al. (1983) looked into this as well as other methods of stabilize the effects of salinity tolerance and precipitation due to divalent cations. Another monomer that was identified was the previously mentioned n-vinyl pyrrolidone (NVP) monomer. The mechanism associated with NVP is that protects acrylamide from hydrolysis and helps to prevent the cleaving of the AMPS monomer at sustained elevated temperatures. This is important because both Levitt (2009) and Parker

and Lezzi (1993) report that the AMPS monomer will hydrolyze completely at a temperature of 100 C within 100 days. One last method discussed by the above authors that is relevant to this work is a comb-like steric hindrance which prevents a polymer from collapsing completely in the presence of high salinity. Because the above is an HPAM, it is likely that at high temperatures the benefits of the steric hindrance may be lost due to increased hydrolysis.

Ethylenediaminetetraacetate (EDTA) is a powerful chelating agent that is being investigated for polymer stability. It is hypothesized that EDTA can sequester calcium ions and eliminate the negative effect that they impose on polymer. EDTA has been used for many years in the oilfield as a scale inhibitor and to remove formation damage from waterflooded wells (Dria, 1988 and Shaughnessy and Kline, 1983). Both report that not only will EDTA dissolve scale but it will chelate the cations (both calcium and iron) and keep them in solution. However, Xie (1997) reports that using a chelating agents (EDTA in particular) can lead to degradation of polymer when iron (II) and oxygen are present. Upon closer inspection, the form of EDTA that is being used by Xie is of neutral form. The efficacy of EDTA to sequester divalent cations depends on pH because in the complexation with EDTA, multivalent ions compete with the protons to bind to the EDTA molecule. For this research, the tetrasodium salt (EDTA-Na^+_4) was used which is the most alkaline form.

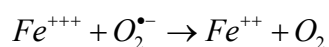
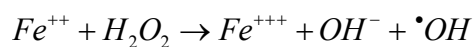
One final thought on chemical stability is that results of tests comparing different polymers at similar degrees of anionicity but for different molecular weights or different initial degrees of hydrolysis should be done with caution. This is to say that the results of a calcium scan for a post-hydrolyzed (initially unhydrolyzed) PAM is not necessarily a direct comparison to a post-hydrolyzed ter-polymer of acrylamide, AMPS, and NVP of the same final degree of anionicity. More simply, it has been reported by several authors

(notably Kheradmand (1987) when comparing his results to those found by Muller) that copolymers of acrylamide (AM) and acrylate (AA) tend to form a less random and more block-like polymer when compared to that of a polyacrylamide that is post-hydrolyzed. This tacticity (or co-tacticity) will affect the exact way in which a polymer chain containing both monomers is arranged. This will in turn affect the way in which divalent cations attract to any given part on the polymer chain because of the competing neighboring effects. For instance, a polymer chain that the acrylate moieties are randomly dispersed will be more likely to experience greater effect from Ca^{++} than a co-polymer which will contain a great number of acrylate “blocks”.

Thermal Stability

It is well known that EOR polymers can be susceptible to oxidative degradation through almost any combination of the following: exposure to high temperature, presence of oxygen; presence of residual impurities from the polymerization process; presence of $\text{Fe}^{++}/\text{Fe}^{+++}$; and misuse of oxygen scavengers (Yang and Treiber, 1985). However, the literature can be contradictory with respect to explaining the degradation of polymer when only 1 or 2 of these factors are present.

One mechanism that is known to cause oxidative degradation in organic compounds when iron (II) is allowed to oxidate to iron (III) was first identified by Fenton (1897). The following equations are a simplification of the reactions that occur and presented as a schematic only to show that free radicals are.



These reactions produce free radicals that are capable of abstracting hydrogen from the polymer backbone and with repeated abstraction will cause a cleavage of the backbone. This scission effectively cuts the polymer molecule in half and reduces the viscosity drastically.

Pye (1967) seems to be the first to identify that iron can degrade HPAM when he discovered that sodium dithionite, if used correctly, can prevent this from happening. Since this discovery, many researchers have studied how iron (II and/or III) affects the viscosity of polymers in the presence/absence of oxygen, but no general consensus has been reached. For instance, Yang and Treiber (1985) reports that if only a small amount of O₂ (5 ppm) is present with ferrous iron in polymer and then sealed in ampoules, slight degradation occurs and then no further. Kheradmand (1987), on the other hand, reported that degradation under similar conditions was severe.

Where inconsistencies have surfaced, it appears likely that this is due to a focus on oxygen and iron concentrations, to the neglect of the oxidation-reduction potential (ORP) and other factors affecting iron solubility, such as pH and the presence of carbonate and bicarbonate ions, which more directly affect the ability of iron to redox cycle. For instance, Ramsden and McKay (1986) found that pH is a key factor in Fenton-type degradation of polyacrylamide.

Another inconsistency in the literature relates to the degradation that occurs when sodium dithionite is added to a solution containing oxygen. Sodium dithionite has been investigated for many years due to its ability to reduce iron from the ferric to the ferrous state, and polymer stability has been demonstrated in its presence, for instance by Pye (1967). However degradation has been reported in some (though not all) cases upon addition of dithionite to polymer solutions containing oxygen or when polymer solutions

containing sodium dithionite are subsequently re-exposed to oxygen, which is one concern regarding its use in the field.

Several authors (Knight, 1973 and Levitt and Pope, 2008) report that the use of the oxygen scavenger sodium dithionite will severely and rapidly degrade polymer in the continual presence of O₂. Yang and Treiber (1985) showed that degradation under similar conditions is moderate. However, Shupe (1981) reports that addition of dithionite to polymer in the presence of air results in minimal loss of viscosity after 3 hours. One significant difference between the experimental procedures of the above authors is the presence of small amounts of carbonate and bicarbonate, corresponding to a natural water source, in the brine used by Shupe.

Several authors have analyzed polymers for residual impurities, iron, and other additives such as sodium carbonate. Shupe (1981) used Dow Pusher 500, which he reports as having more than 5 ppm iron in the powder form, which would result in ~5-10 ppb iron in an aqueous solution containing 2000 ppm polymer. Muller (1981) showed that residual impurities left over from the synthesis of polymer remains unstabilized and this could lead to degradation of the polymer in the presence of oxygen.

It was hypothesized by Levitt (2009) that the ability or inability of low levels of iron to redox cycle plays a role in the inconsistencies in the literature, and that this is controlled by the redox potential as well as the factors affecting iron solubility, such as the presence of carbonate and bicarbonate ions. Polymer inevitably encounters iron in the field. It has also been shown that ppb levels of iron are left over from the polymerization process (Shupe, 1981). Most field brines contain carbonate and/or bicarbonate, though these are often left out of reconstituted brines in the laboratory. Additionally, in laboratory experiments relating to polymer stability, oxygen can either be removed by purging with a purified inert gas that displaces oxygen, such as argon or

nitrogen, or by purging with hydrogen, which reacts with oxygen and can also lower the redox potential.

The beneficial effect of even low levels of carbonate ion is in accordance with the theory that the very low levels of iron present in polymer solutions play a catalytic role in the degradation experienced when sodium dithionite is added. If this is indeed the case, it was hypothesized that a chelator that can reduce the redox cycling of iron, such as diethylene triamine pentaacetic acid (DTPA), could also have a beneficial effect. While DTPA can not prevent the oxidation of iron (II) to iron (III), it is believed to prevent the subsequent reduction of iron (III), and hence halts the iron-catalyzed Haber-Wiess mechanism (Cohen and Sinet, 1982).

Zobell (1946) studied the E_H , pH, and poisoning capacity of marine sediments and found that pH increased and E_H as well as poisoning capacity decreased with increasing sediment depth. Baas Beeking et al. (1960) performed a comprehensive review of E_H and pH measurements made in natural environments, and Shafer and Pirson (1969) performed a similar study on reservoir fluids. Their combined results are summarized in Table 2.1. As was generally observed by Zobell, E_H decreases and pH increases with increasing exposure to decomposition and dissolved minerals. Meteoric water is close to the E_H of water in equilibrium with atmospheric oxygen and is slightly acidic though weakly buffered, whereas marginal marine sediments and connate waters are strongly buffered by the presence of bicarbonate and are under increasingly reduced conditions associated with burial and decomposition of organic matter. Shafer and Pirson (1969) suggest that the reducing conditions present in the reservoir are set by the SO_4/H_2S redox couple. Zobell notes that preliminary measurements in petroleum reservoirs show more strongly reducing conditions but less poise than marine sediments, though as no experimental

details are reported it is impossible to know if, for example, H_2S was liberated during sampling.

In sum, whereas waters exposed to the atmosphere, including sea water, contain dissolved oxygen and are typically slightly to strongly positive in E_{H} , brines produced from reservoirs and aquifers are typically slightly to strongly reduced. The reservoir may be thought of as anaerobic and highly reduced, though possibly not strongly poised at its very low E_{H} . This last point may be of interest in the case where oxygenated water has been injected into a reservoir for decades.

Coreflooding Experiments

Martin (1974) looked at injecting polymer into a low permeability reservoir. He injected Calgon Polymer 454 (a slightly cross-linked HPAM) into both a 4 mD sandstone as well as an 8 mD limestone containing oil. He cautions that the core test data suggests that high molecular weight polymers may encounter problems in the reservoir. This is evident by the ever increasing polymer permeability resistance factors throughout the flood. Martin suggests that pore size distribution and not permeability will be the determining factor of whether a polymer can successfully be injected into low permeability reservoirs. He recommends that lower molecular weight polymers be studied for use in these reservoirs.

Coreflooding is used as a selection tool in the lab as a way to test a chemical formulation in either surrogate or reservoir rocks. It is a one-dimensional flow experiment that simulates oil recovery in the reservoir. Results from core floods should not be taken as an analog for what will happen in the reservoir because of many complicating factors that exist in the reservoir, which include areal sweep, heterogeneity and thief zones. The procedure for coreflooding is described in great detail by many

investigators including the recent studies by Jackson (2006), Levitt (2006), Flaaten (2007), and Sahni (2009).

Table 2.1: E_H and pH of the Natural Environment (Baas Becking (1960) and Shafer and Pirson(1969))

Environment	E_H (V)	pH
Meteoric waters	0.4 to 0.8	3 to 7
Sea water	-0.2 to 0.5	6 to 9
Marginal marine sediments	-0.3 to 0.5	6 to 9
Uncontaminated connate waters	-0.3 to 0	6 to 8
Reservoir brines (except oil sands)	-0.4 to -0.1	6 to 8

CHAPTER 3: EXPERIMENTAL METHODOLOGY

This chapter presents a description of the experimental apparatus and methodology used in this research. The chapter is divided into several sections. The first two segments detail general laboratory equipment and materials common to all experiments and all analytical equipment. Another section explains the general polymer hydration technique. Experimental methodology is described in the last three sections which are divided into chemical stability, thermal stability, and coreflooding.

3.1 GENERAL LABORATORY EQUIPMENT AND MATERIALS

This section describes the experimental equipment and materials common to all experiments. Experimental equipment includes mass balances, water deionizer, stir plates, and ovens. Materials include electrolytes, polymers, and other chemicals.

Mass balances

All experiments were conducted on a mass basis, so mass balances were used for measuring liquids and powders. For quantities smaller than 10 grams, an Ohaus Discovery mass balance with a precision of 0.0001 g was used. For larger quantities, a Denver Instruments mass balance with a precision of 0.01 g was used. Mass balances were also used to determine the pore volume of core plugs.

Water Deionizer

Deionized water (DI) was used for all experiments. A Nanopure™ filter system was used to de-ionize the water. This filter uses a recirculation pump and monitors the water resistivity to indicate whether the ions have been removed. Distilled water was fed into the system and deionized water was obtained at the outlet.

Stir plates& overhead mixers

Generally, a Corning PC-420D magnetic stirring hot plate along with a Teflon coated magnetic stir bar was used to mix brine polymer solutions. An IKA RW 20 Digital overhead mixer was used in cases when polymer solutions were too viscous to properly mix with a stir plate.

Convection ovens

Several Binder benchtop and Blue M freestanding convection ovens were used for thermal aging experiments as well as for core floods conducted at reservoir temperature. Mercury thermometers and oven temperature gauges helped to maintain a constant temperature with minimal fluctuation.

Electrolytes

Salts such as NaCl, CaCl₂, and MgCl₂*6H₂O were used to create synthetic brines in the lab. Other salts such as sodium carbonate, sodium bicarbonate, sodium dithionite, and sodium bisulfite were used as chelating agents and oxygen scavengers. Ferrous and

ferric chloride and sulfate were used in some of the oxidative degradation experiments to simulate the exposure to iron seen in the field. All of these materials were supplied by Fisher Scientific.

Polymers

Polymers used in this research were supplied by SNF Floerger and Hengju. They are of powder, granular form and have a moisture content of approximately 12 wt%. All of the polymers used are acrylamide-based (AM) and have molecular weights ranging from 0.5 million to over 20 million Daltons as reported by their respective manufacturers. Most are co- or ter-polymers with functional groups like acrylate (AA), 2-acrylamido 2 methylpropane sulfonate (AMPS), and n-vinyl pyrrolidone (NVP). Table 3.1 lists the polymers that were used for this research.

Other Chemicals

Surfactants supplied by Shell Chemical and Stepan were used in the coreflooding experiments. Montbrite 1240, sodium borohydride, is a chemical manufactured by Montgomery Chemicals. Montbrite 1240 is used along with sodium bisulfite to create sodium dithionite. Two specific chelating agents were used in different experiments. Diethylene triamine pentaacetic acid (DTPA) is a chelating agent was supplied by Total Petrochemicals. DTPA is thought to be able to prevent the reduction of ferric iron (Fe^{+++}). Ethylenediaminetetraacetate tetrasodium salt (EDTA-Na_4^+), supplied by Harcross, is a very strong chelating agent that was used for sequestering divalent cations.

3.2 EXPERIMENTAL METHODOLOGY

This section describes the systematic approach to all of the experiments. First, some of the methods common to all experiments are detailed. Then there are three subsections: Chemical Stability, Thermal Stability, and Coreflooding.

Polymer Hydration

Polymer solutions for all laboratory experiments were hydrated in the same manner. Polymer hydration was similar to that described by Foshee et al. (1976) with a few exceptions. A beaker containing some brine solution placed on a magnetic stir plate. The speed was set to 500 rpm in order to obtain a good vortex, and polymer was sprinkled slowly into solution while being blanketed with some inert gas such as nitrogen or argon. After solutions became clear, the speed was reduced to 200-300 rpm. Polymers were hydrated for 16-24 hours on the stir plate, and then placed in the refrigerator in a sealed container capped with argon or nitrogen in the headspace in order to prevent any degradation.

Viscosity

For most of the experiments, a Contraves LS-30 with a temperature bath set to 25 C was used to measure viscosities. For some experiments (which are noted), a Brookfield viscometer with UL adapter was used. For experiments that, due to the presence of a reducing agent were potentially susceptible to degradation in the presence of oxygen, the viscometer was blanketed with nitrogen or argon through a hole drilled in

the bottom of the wind guard. A TA Instruments ARES-LS 1 viscometer was used in cases where elevated temperature measurements were necessary or when measuring oil viscosities.

Screen Factor (SF)

Screen factor as described by Jennings (1971) and Schurz (1972) was used to show the onset of degradation. Polymer solutions were passed through a series of 5, 100-mesh screens packed at the bottom of a glass funnel with an elongated neck. This simulates flow through porous media. The time required to pass between two markings on the neck was compared to that of water flowing through the same apparatus. The value reported is a non-dimensional number relative to water.

pH and Redox Potential ($E_{Ag/AgCl}$)

pH and redox potential (ORP) are measured for all experiments. Redox potential can be expressed as $E_{Ag/AgCl}$ or E_H . The relationship between $E_{Ag/AgCl}$ and E_H is given by

$$E_H = E_{Ag/AgCl} + 200 \text{ mV}$$

The $E_{Ag/AgCl}$ and calculated E_H of aqueous solutions under a variety of conditions are given in Table 3.2. An Accumet pH probe (Model No. 13-620-290) and $E_{Ag/AgCl}$ probe (No. 13-620-81) were used to measure these properties in all polymer solutions. A Thermoscientific Orion 5-Star meter was used to record the values.

Dissolved Oxygen (DO)

DO was measured in two different ways depending on the experiment. For experiments where polymer was not used, a Mettler Toledo Model M400 meter with an InPro 6950 O₂ probe was used. This setup was also used in the initial polymer experiments where it was necessary to confirm a low (< 10 ppb) level of DO in the deoxygenated solution. After a procedure was developed and replicated multiple times producing similar low levels of oxygen, this setup was no longer used because of the difficulties with maintaining an oxygen-free environment. DO readings were slow to come to equilibrium using the probe, so for experiments where a quick measurement of DO was necessary, Chemets® 0-40 ppb ampoules were used.

Degree of Hydrolysis, ¹³C NMR

¹³C NMR work was performed by UT Analytical Services Laboratory in the Department of Chemistry and Biochemistry using a Varian Inova 500. This procedure is described in great detail by Levitt (2009). Peaks were established that are associated with each of the moieties and are as follows: 183 ppm for acrylate, 180 ppm for amine, 178.5 ppm for NVP, and 176 ppm for AMPS. Degree of hydrolysis (τ) is defined as the mol fraction of acrylate. For polymers containing AMPS and NVP, total anionicity has shown to be a more appropriate measure (Levitt, 2009). Total anionicity can be expressed as $\tau + \sigma + \nu$, where σ and ν represent the mol fraction of AMPS and the mol fraction of NVP, respectively.

3.2.1 Chemical Stability Experiments

There were two main types of chemical stability experiments. The first set of experiments examined the long-term hydrolysis of polymers aged at different temperatures. The second set of experiments dealt with the stability of post-hydrolyzed polymers in the presence of divalent cations (in this case calcium).

Thermal Aging Experimental Procedure

Reservoirs are anaerobic environments so it is necessary to perform experiments which replicate this. Below is a detailed procedure for these experiments.

1. 2.5 g of polymer is hydrated in 497.5 g of brine consisting of 3 wt% NaCl consistent with the above polymer hydration technique.
2. A 30 g sample from the polymer solution was used to measure viscosity, pH, $E_{Ag/AgCl}$, screen factor, and DO. These measurements were taken as initial values. This sample was not added this back to the initial polymer solution. At this time, the heated column, which is packed with copper turnings to scrub the argon of any residual oxygen, should be turned on.
3. The remaining polymer solution was weighed into a 1 L Erlenmeyer flask and placed on a magnetic stir plate at 200 rpm. The solution was blanketed with argon and sealed with Parafilm.
4. A 200X (times) stock of sodium dithionite was prepared. A final dithionite concentration in the polymer solution of 400 ppm was desired, so this means an 8 wt% solution of dithionite was prepared. Using a 100 mL Erlenmeyer flask, 46 g of DI was weighed and began stirring at 400 rpm under argon blanket and sealed with Parafilm. 4 g

of dithionite was added carefully to the DI after it had been mixing under argon blanket for several minutes. This was allowed to mix until clear solution.

5. A small syringe with a piece of 1/8" nylon tubing attached was flushed argon and left with argon in the syringe. The tubing was inserted above the dithionite solution and the contents of the syringe were expunged into head space of flask. 10 mL of dithionite solution were drawn into the syringe.

6. Based on the weight of the polymer solution, 1/200 of dithionite stock was added to the polymer solution to get desired final concentration. This means if the polymer weighed 1000 g, 5 mL of dithionite stock was added.

7. The polymer solution was resealed, and the mixing speed was increased to 350 rpm and let mix for 10 min. While the polymer was mixing, custom-made 20 mL borosilicate ampoules were prepared with the nylon fitting and brown o-ring and set aside. A 150 mL syringe with a similar setup described above was flushed with argon similar to the procedure for the small syringe, leaving some argon inside. Also, the manifold was set to the vacuum setting.

8. 110 mL of polymer solution was then drawn into the syringe. This was difficult, as it must be done slowly as to not accidentally draw air in or even shear the polymer.

9. An ampoule was flushed with argon for 30 sec. Then, the line from syringe was inserted into the ampoule, and filled with polymer solution to 1 inch below neck. The polymer tube was removed first, and then the argon line was quickly removed making sure to place the thumb over the top of the ampoule immediately to prevent oxygen from entering.

10. The ampoule was quickly screwed into the manifold. The valve was opened for a few seconds to evacuate head space then closed.

12. Step 11 was repeated for the next six ampoules. When manifold was full, all the valves were opened while still under vacuum. A good vacuum was achieved when the pressure gauge read 30 in Hg. The manifold was then switched to argon until the pressure gauge read 10 psi. This is one cycle. This cycle was repeated 2 more times (for a total of 3 cycles). With the manifold still on argon, all valves were closed and the manifold was switched to vacuum.

13. The valve to first ampoule is opened so that it was under vacuum. A spot was chosen 1/2 inch below the plastic fitting and gently heated evenly around the ampoule using a methane-oxygen torch. As soon as a dimple formed, the flame was immediately removed for a few seconds. The flame was moved to the opposite side of ampoule from dimple and heated again until another dimple forms. This was done until the neck was completely collapsed. The area was rigorously heated while gently pulling down on the ampoule until it broke away. Care must be taken to not heat through the seal. In previous experiments, the curve created by the seal was a weak spot, so as soon as it broke away, the ampoule was followed with the flame in order to slowly remove from the heat. This is repeated for the rest of the ampoules on the manifold.

14. Ampoules are then labeled and placed in several ovens (as well as at room temperature or 23 C) to age and removed at logarithmic time intervals.

Cracking Ampoules and Sampling Procedure

After ampoules were removed from the oven and allowed to cool to room temperature, they were cracked open and measured for the solution viscosity, DO, pH, and $E_{\text{Ag}/\text{AgCl}}$. It was necessary to move as quickly as possible to get measurements before

oxygen was allowed to affect the polymer sample. The viscometer was blanketed with argon and zeroed. Next a glass pipette was flushed with argon.

As soon as the ampoule was cracked open, a DO ampoule was cracked immediately followed by a sample removed with the pipette. The redox probe was inserted into the ampoule as the viscosity measurement was taken. After the redox measurement, a pH reading was taken.

In cases where hydrolysis was being studied, this procedure was repeated two more times. All three samples were combined and filtered through 100,000 MW Millipore ultrafiltration membranes in an Amicon stirred cell. The retentate was loaded into a 5 mm NMR tube and centrifuged to remove air bubbles before having an NMR measurement taken.

Divalent Cation Tolerance Experiments

This set of experiments focused on the susceptibility of hydrolyzed polymer ($t > 0.3$) to precipitate in the presence of divalent cations. Calcium was the cation of concern for these experiments.

The method employed in this research was similar to that developed by Levitt (2009) except that a few improvements stemmed from observations made about silica solubility possibly affecting results. Scans were conducted for two purposes: to determine calcium ion concentration to achieve the ‘cloud point’ (onset of precipitation) and to determine the 50% viscosity loss.

For all experiments, a 1000 g stock of polymer solution was hydrated in 0.3 M NaOH for 10 days in 4L Nalgene polypropylene screw-top bottles. The use of NaOH allowed the polymer solution to achieve pH~11, which was sufficient to post-hydrolyze

the polymer to $\tau \sim 0.6$. A concentration of polymer was chosen such that sufficient viscosity could be measured after a four-fold dilution.

Next the solution was neutralized with 1000 g of 0.3 M HCl. The resulting salinity of the polymer solution was 1.2 wt% NaCl. Sometimes, a small titration (less than 50 g of 0.3 M HCl or 0.3 M NaOH) was necessary to adjust the solution to pH 7 \pm 0.2. After neutralization, a sample was used for a degree of hydrolysis measurement using NMR.

A 22 wt% solution of CaCl_2 was prepared as a calcium stock. This corresponded to a calcium ion concentration of 80,000 ppm. Smaller stocks were diluted from this in order to have predetermined Ca^{++} concentrations when added to polymer in a 1:40 ratio. For instance, 0.5 g of a calcium stock called '100' could be added to 19.5 g of polymer and the final Ca^{++} concentration in solution would be 100 ppm.

Because calcium tolerance was studied as a function of total dissolved solids (TDS), several background NaCl concentrations were chosen which can be seen in Table 3.3. 200 g of polymer stock was added to 200 g of brine in order to get the desired NaCl concentration.

After sufficient time to homogenize the mixture, a calcium scan was performed. 0.5 g of DI was added to 19.5 g of polymer solution in a 40 mL glass, screw-top vial and allowed to mix on a rocker plate for at least 1 hour. This sample was used as a control for all other samples to be compared to. This step was repeated for all Ca^{++} concentrations up to and including 2000 ppm using the various calcium stocks.

Any Ca^{++} concentration higher than 2000 ppm required more than 0.5 g of the 80,000 ppm Ca^{++} stock. Another blank would be prepared with the equivalent amount of DI added. For example, if the desired Ca^{++} concentration in solution was 5000 ppm, the 1.25 g of 80,000 ppm Ca^{++} stock was added to 19.5 g of the polymer solution. A control

sample consisting of 1.25 g of DI in 19.5 g of polymer was prepared so that a relative viscosity measurement could be obtained.

Use of EDTA as a Sequestering Agent

Several experiments were conducted using EDTA to sequester the calcium in order to minimize its effects on polymer. EDTA is water-soluble so long as only one end of the chain is occupied by a calcium ion. This means that on a molar basis, one EDTA molecule needs to exist for every calcium ion. On a weight basis, this was determined experimentally to be 6 EDTA: 1 Ca^{++} . For these experiments, an 8:1 ratio was used as a safety factor, unless otherwise noted.

The order of addition of each of the components, brine, DI, polymer, EDTA, and calcium stock, became important for this experiment. This means that polymer could not be added before EDTA or the Ca^{++} would react with the polymer first. Table 3.4 is an example mixing sheet showing the order of addition for all of these experiments.

3.2.2 Thermal Stability Experiments

There were three main types of thermal stability experiments. The first set of experiments examined the effect of iron (both ferrous and ferric) on polymer stability. In particular, these experiments were designed to clarify contradictions in the literature concerning the level of degradation of polymers in the absence/presence of oxygen when iron exists.

The second set of experiments also looks to shed some light on discrepancies in literature with respect to oxygen scavengers and their effects on polymer stability when

exposed to oxygen. Sodium dithionite, or hydrosulfite, was the main focus but some experiments used sodium bisulfite as the oxygen scavenger.

The third part of the experimental work presented involves field experiences that demonstrate the importance of redox potential (ORP) in field applications of polymer flooding. Two field experiences are described in which polymer preparation and injection was monitored and various levels of degradation were reported.

Preparation/Addition of Fe^{++}

For those experiments, which involved the addition of Fe^{++} , it was necessary to assure that the iron added was in the reduced state. DI was deoxygenated by bubbling with nitrogen or argon for at least 1 hour. The iron was added, and the solution was continued to bubble with nitrogen or argon until the time that the iron solution was no longer required for the experiment. Thus it can be reasonably assumed that the iron was predominantly in the ferrous form.

Experiments in DI

For the experiments where DO and $E_{Ag/AgCl}$ were monitored in DI, a 1000 mL 5-port spherical vessel was used so that probes could be inserted into the solution. N_2 was bubbled into solution, and when DO was below 5 ppb, it was deemed oxygen-free. N_2 bubbling continued while the ferrous sulfate ($FeSO_4$) was added in small increments. At each step, the solution was allowed to come to equilibrium and $E_{Ag/AgCl}$ and DO were recorded. Each time, DO did not rise above 5 ppb.

Experiments with Polymer and Continuous O₂

Polymer was initially weighed into a 250 mL spherical 3-port vessel. The vessel was then suspended above a stir plate. The top port was plugged with a glass stopper, and the two other ports were sealed with rubber stoppers. A syringe tip hooked up to a N₂ line was inserted into one of the small stoppers, while a 2-meter length of 1 mm inner diameter nylon tubing was inserted into the other small stopper. The tubing served as a vent, which was sufficiently long in order to inhibit oxygen intrusion into the vessel during the experiment.

0.2 bar of N₂ was then bubbled into solution for at least 1 hour. Previous tests showed that ~45 minutes of bubbling polymer with N₂ at 0.2 bar was necessary to achieve less than 30 ppb O₂ in solution with the given apparatus and geometry. It should be noted that in the experiments with DI, DO of less than 5 ppb could be achieved.

Between this first set of experiments and these, the tank of scientific nitrogen was changed and the lowest level of DO that could be achieved was 30 ppb. After 45 minutes of bubbling, the syringe tip was removed from the liquid and allowed to blanket the solution for the duration of the experiment. Then, 2 ppm Fe⁺⁺ as either sulfate or chloride was introduced into solution. Viscosity measurements were taken at different intervals.

Experiments with Polymer and Absence of O₂

The set up was the same as above, but with N₂ bubbling continued for more than 1 hour. Additionally, N₂ was passed through a heated column containing copper turnings to remove any traces of O₂ was used for at least the last 30 minutes of bubbling. DO levels at the end of the 30 minutes were confirmed to be 0 ppb using Chemet® ampoules.

Preparation/Addition of Sodium Dithionite

For experiments involving dithionite, a stock of 10 g/L sodium dithionite was prepared using a method identical to that for which Fe^{++} was prepared.

Experiments in the Presence of O_2

99 g of polymer was poured into a 500 mL screw-top glass jar with the lid removed. This allowed approximately 400 mL of headspace in the containers. The solution was placed on the stir plate on setting 3, the $E_{\text{Ag}/\text{AgCl}}$ probe was placed inside the jar, and an initial reading was recorded. 1 g of sodium dithionite stock was added to the solution to give a concentration of 100 ppm sodium dithionite in the polymer. $E_{\text{Ag}/\text{AgCl}}$ values were recorded as the redox potential dropped to a minimum and rose back again to a steady value.

At 10 minutes, a sample of polymer was removed and viscosity was taken. A few more $E_{\text{Ag}/\text{AgCl}}$ values were taken, but usually showed little change after about 5 minutes after addition of sodium dithionite. Again at 1 hour, a sample was removed and viscosity was taken. Samples were left open to air on the stir plate for no more than 5 hours in order to prevent evaporation. They were then closed with O_2 in the headspace, and placed on the benchtop until the next viscosity measurement was recorded, which happened after 1 day and approximately 1 week.

Experiments in the Absence of O₂

148.5 g of polymer solution was poured into a 250 mL glass Erlenmeyer flask. The solution was then placed on the stir plate on setting 3, the E_{Ag/AgCl} probe was placed into the solution and the headspace was flushed continuously with N₂. Parafilm® was used to prevent exposure to atmospheric oxygen. After about 10 minutes of stirring with an N₂ blanket, an initial E_{Ag/AgCl} measurement was recorded. Polymer solutions had a dissolved oxygen level of 1-2 ppm. 1.5 g of sodium dithionite stock was added to the solution to give a concentration of 10 ppm sodium dithionite in the polymer. E_{Ag/AgCl} values were recorded as the redox potential dropped to a minimum. The polymer solution was left blanketed with N₂ for 1 hour.

After 1 hour, a sample of polymer was removed and the viscosity was taken. The polymer sample was carefully transferred to a 500 mL screw-top glass jar with the lid removed to expose to air. Next, the E_{Ag/AgCl} values were recorded as the sodium dithionite was consumed. After one hour, a sample was taken for a viscosity measurement. Viscosity was also recorded after 1 day and approximately 1 week.

Experiments using H₂ as an Oxygen Scavenger

Like argon, hydrogen displaces oxygen in solution. Unlike argon (but similar dithionite) hydrogen imposes a reduction in redox potential. Two experiments were conducted using hydrogen to scavenge the oxygen: with and without additional Fe⁺⁺.

Experiments with MontBrite 1240

These experiments were designed to test the efficacy of the dithionite created using Montbrite 1240 (sodium borohydride) and sodium bisulfite against powder sodium dithionite. A 10 g/L dithionite stock solution was created by adding 1.4 g of Montbrite 1240 solution (12% borohydride) and 10 g of a 40% active aqueous solution of sodium bisulfite to 454 g of DI.

Experiments were performed in a manner similar to those described in the subsection in this chapter called “Thermal Aging Experimental Procedure.”

3.2.3 Coreflooding Experiments

This section will give a brief overview of the process involved with coreflooding. Coreflooding is described ad nauseam and in great detail in many theses including Jackson (2006), Levitt (2006), Flaaten (2007), and Sahni (2009).

Injectivity Tests

Two distinct types of coreflooding were necessary for this research. Because this reservoir contained rock that was very low in permeability, polymer injectivity tests were first conducted. The purpose of these experiments was to determine if polymer could propagate through the rock. No oil was used for these experiments.

It is important to note that all fluids that were injected in all coreflooding experiments were first filtered through at least a 0.45 μm Millipore membrane. Filter

ratio (FR) as described in Levitt (2009) was the deciding factor for whether a polymer solution could be injected into the core.

Polymer injectivity tests began with a single reservoir core plug of dimensions 2 inch in length and 1.5 inch in diameter potted in epoxy. Three pressure taps, inlet, middle, and outlet, allowed for differential pressure readings throughout the experiment. The core plug was evacuated then saturated with the synthetic injection brine. After the pore volume (PV) of the plug was determined, several pore volumes of the brine were injected until the effluent ran clear. Brine permeability was determined by injecting at a baseline flow rate.

Several polymer solutions were prepared in the synthetic brine and injected at the baseline flow rate. Each time the injected polymer viscosity and the effluent polymer viscosity were compared to determine any possible degradation. Other calculated measurements such as resistance factor (R_f) and permeability reduction factor (R_k) were used to determine the decreased mobility and permeability due to polymer.

In some cases, it was necessary to pre-shear the polymer solution using a Waring blender on low speed for 10-20 seconds. Viscosity and screen factor (SF) before and after shearing were measured to know how much degradation occurred.

Chemical Flooding Tests

The second type of coreflooding experiment conducted involved using chemicals to recover oil to very low residual oil saturations. The type of chemical flood used for these experiments was alkali-surfactant-polymer (ASP) flooding followed by a polymer drive (PD). Because iron was present in the injection lines as well as the columns, sodium dithionite was used throughout all steps. The process is outlined below.

1. Phase behavior and aqueous stability tests – optimum surfactant, co-solvent, and alkali concentrations are determined using different water-to-oil (WOR) ratios. This part of the experimentation is described by Yang (2010).

2. Coreflooding setup – because of the anticipation of high pressures, a stainless steel coreholder was employed as opposed to the method where a core is potted in epoxy. For a detailed description of the setup, please refer to Magbagbeola (2008).

3. Brine flood – the core plugs were saturated with synthetic brine and flushed for several PV until the effluent ran clear. At this point, brine permeability was determined at a baseline flow rate.

4. Oil saturation – the coreholder was flipped over and oil was injected from the top down until no more water could be displaced. The initial oil saturation (S_{oi}), relative oil permeability (k_{ro}), and residual water saturation (S_{wr}) were calculated.

5. Water flood – the coreholder was flipped back to its initial position and synthetic brine was injected until the water cut was 99%. At this point the residual oil saturation to water (S_{orw}) and the relative water permeability (k_{rw}) were calculated.

6. Chemical flood – the optimum formulation as determined by phase behavior tests was injected for 0.3 PV followed by a polymer drive of 2 PV. Effluent samples were collected and analyzed for oil cut, pH, and surfactant concentration. Because of the use of dithionite, it was difficult to measure viscosity and ORP as the exposure to oxygen immediately degraded the polymer.

Table 3.1: Polymers used in this research

Polymer name	Manufacturer	Type	Molecular Weight (MW) (million Dalton)	Degree of Hydrolysis τ
SAV 301	SNF Floerger	ter-polymer of n-vinyl pyrrolidone (NVP), modified acrylamide (AM), and sodium acrylamido tertio butyl sulfonate (ATBS)	unreported	unreported
Kypam 5	Hengju	Sterically hindered 'comb-like' hydrolyzed polyacrylamide (HPAM)	unknown	~ 0.3
FA 920 SH	SNF Floerger	unhydrolyzed polyacrylamide (PAM)		0
AN 125	SNF Floerger	co-polymer of acrylamide (AM) and 2-acrylamide 2-methyl propane sulfonate (AMPS)	5	0.3
FP 3630S	SNF Floerger	hydrolyzed polyacrylamide	20	0.3
FP 3330S	SNF Floerger	hydrolyzed polyacrylamide	8	0.3
FP 3230S	SNF Floerger	hydrolyzed polyacrylamide	5	0.3
AN 125 VLM	SNF Floerger	co-polymer of acrylamide (AM) and 2-acrylamide 2-methyl propane sulfonate	3	0.3
AB 305 MPM	SNF Floerger	hydrolyzed polyacrylamide	2	0.3
AB 305 VLM	SNF Floerger	hydrolyzed polyacrylamide	0.5	0.3

Table 3.2: Redox potential (ORP) of various aqueous solutions

	$E_{\text{Ag/AgCl}}$	E_h
	(mV)	(mV)
10 g/L dithionite in DI	-560	-360
Aq. sol'n of dithionite in air 10 min	20	220
Aq. sol'n of dithionite in air 1 hr	42	242
Aq. sol'n of dithionite in air 25 hr	67	267
Deoxygenated DI	100	300
DI saturated with air (~6 ppm O_2)	200	400

Table 3.3: Background NaCl concentrations for Ca⁺⁺ tolerance experiments

Desired NaCl concentration (wt %)	Polymer NaCl concentration (wt %)	Brine Stock NaCl concentration (wt %)
1.2	1.2	1.2
3	1.2	4.8
5	1.2	8.8
10	1.2	18.8
13.6	1.2	26

Table 3.4: Sample mixing sheet for Ca^{++} tolerance experiments using EDTA

Desired NaCl background concentration 5wt%						
Order of addition:						
	1	2	3	4	5	
Ca^{++} Conc (ppm)	8:1 EDTA: Ca^{++} Desired EDTA conc (ppm)	30% active EDTA (g)	17.6% NaCl Brine (g)	DI (g)	Ca^{++} add (g)	2X stock Polymer (g)
0	0	0	4.875	4.875	0.5 g DI	9.75
100	800	0.052	4.875	4.823	0.5	9.75
500	4000	0.26	4.875	4.615	0.5	9.75
1000	8000	0.52	4.875	4.355	0.5	9.75
1500	12000	0.78	4.875	4.095	0.5	9.75
2000	16000	1.04	4.875	3.835	0.5	9.75
0	0	0	4.875	4.875	0.75 g DI	9.75
3000	24000	1.56	4.875	3.315	0.75	9.75
0	0	0	4.875	4.875	1.25 g DI	9.75
5000	40000	2.6	4.875	2.275	1.25	9.75
0	0	0	4.875	4.875	2 g DI	9.75
7500	60000	3.9	4.875	0.975	2	9.75

CHAPTER 4: CHEMICAL STABILITY RESULTS & DISCUSSION

4.1 THERMAL AGING EXPERIMENTS

Two polymers were tested using this method. SNF Floerger's SAV 301, an n-vinyl pyrrolodine (NVP) modified acrylamide (AM) co sodium acrylamido tertio butyl sulfonate (ATBS) terpolymer (or poly(AM-co-ATBS-co-NVP)) was the first polymer tested. Again, it should be noted that ATBS is a general term for AMPS and can be interchanged. SAV 301 has a molecular weight similar to Flopaam 3230S but the exact mol ratio of the monomers is not disclosed at the request of the manufacturer. The neighboring effect of NVP is generally believed to be helping to protect the other two monomers from hydrolysis as well as improving salt tolerance (Fernandez, 2005 and Moradi-Araghi and Doe, 1987).

Hengju's Kypam 5, a sterically hindered 'comb-like' hydrolyzed polyacrylamide, is the other polymer. One possible mechanism is that a lower molecular weight polymer can be used and the steric hinderance will not allow the polymer to completely collapse at high salinity. This causes it to appear like a larger polymer because the viscosity will be similar to that of a higher molecular weight polymer at a given salinity.

2500 ppm SAV 301 in 3 wt% NaCl was aged at 85 C, 100C, and 126C. Tables 4.1 to 4.3 and Figures 4.1 to 4.3 present the data for the three temperatures. The redox potential ($E_{Ag/AgCl}$) and the dissolved oxygen (DO) levels are measured for every ampoule cracked as a way to check if a leak has developed in the ampoule. A low viscosity coupled with a positive (+) $E_{Ag/AgCl}$ value (or a DO reading of more than a few ppb) indicates that a leak has occurred and the ampoule is discarded. When viewing the data, understand that the relatively high redox potential values at the beginning of the tests

were indicative of a faulty probe and not improperly sealed ampoules. This problem was mitigated and a new probe was used for the remainder of the tests, as revealed in the sudden jump in low values after around 2 weeks.

After 270 days at 85 C, 111% of the viscosity was retained (as compared to the viscosity of the solution after 400 ppm dithionite was added prior to sealing the ampoules). 118% of the viscosity was retained after 180 days at 100 C, and 95 % of the viscosity was retained after 270 days at 126 C. SAV 301 achieved a degree of hydrolysis of 0.6 after 60 days at 85 C, 0.78 after 180 days at 100 C, and 0.92 after 180 days at 126 C. These results show that poly(AM-co-AMPS-co-NVP) can maintain its viscosity for long periods of time even at extremely high temperatures. It also lends credibility to the claim that the NVP monomer may be shielding the other monomers from complete hydrolysis.

It is important to note that the degree of hydrolysis referred to for SAV 301 is slightly different than the traditional value of τ . The value reported is actually the total degree of anionicity. Levitt (2009) defines this as $\tau + \sigma$, where τ is the mol fraction of carboxylate functional groups and σ is the mol fraction of AMPS functional groups. Because SAV 301 is an NVP ter-polymer, one final term, ν , is defined as the mol fraction of NVP functional groups. The total degree of anionicity (or degree of hydrolysis) is calculated as $\tau + \sigma + \nu$.

2500 ppm Kypam 5 in 3% NaCl was also aged at the same temperatures. Tables 4.4 to 4.6 and Figures 4.4 to 4.6 illustrate the effect of temperature and time on both viscosity and degree of hydrolysis. After 270 days at 85 C, 84 % of the initial viscosity was retained. 91 % if the original viscosity was retained after 270 days at 100 C but only 52 % was retained after 270 days at 126 C. Kypam 5 achieved a degree of hydrolysis of

0.89 after 180 days at 85 C. At 100 C, it was fully hydrolyzed sometime before 60 days and it took less than 14 days to completely hydrolyze at 126 C.

The degree of hydrolysis with respect to time aged at temperature agrees with previous reports at all temperatures. Also, these results suggest that above 100 C, viscosity loss will be rapid shortly after the polymer becomes fully hydrolyzed.

4.2 CALCIUM TOLERANCE EXPERIMENTS

These experiments fall into one of two categories: experiments without EDTA and experiments with EDTA.

Experiments without EDTA

Most of these experiments were previously conducted by Levitt (2009) and were repeated in this work. This research served two purposes: determine if solubility of silica skewed results and develop a more systematic approach for calcium scans.

Three polymers were studied using this method: FA 920 SH, an unhydrolyzed polyacrylamide, AN 125, and SAV 301. AN 125 is a copolymer of acrylamide (AM) and 2-acrylamido 2 methylpropane sulfonate (AMPS), or poly(AM-co-AMPS), containing around 25% AMPS and having a molecular weight similar to Flopaam 3330S. In order to avoid confusion, the pre-script PH (for post-hydrolyzed) will denote polymers that were lab-aged at elevated pH causing rapid hydrolysis. FA 920 SH becomes PHPAM, AN 125 becomes PHAMPS, and SAV 301 becomes PHNVP.

For all polymers, the approximate final polymer concentration was 2000 ppm. Scans were conducted for all three polymers at background NaCl concentration of 1.2, 3, 5, and 10 wt%. A scan was done for PHAMPS at 13.6 wt%. Figures 4.7 to 4.11

illustrate the calcium tolerance in the form of relative viscosity retained for increasing Ca^{++} concentration for a constant NaCl background concentration for the first three polymers.

The degree of hydrolysis achieved for each polymer is similar ($\tau \sim 0.6$). As can be seen, the cloud point for the experiments with PHPAM and PHAMPS are similar but the viscosities approaching the onset of precipitation are much better for PHAMPS. This is true for all background salinities. PHNVP always shows better calcium tolerance in both viscosity retention as well as extension of the onset of precipitation. This coupled with the thermal aging results validate that the NVP monomer has potential to solve the calcium tolerance issue for both AM and AMPS monomers.

Experiments using EDTA

Several experiments were designed around the use of EDTA as a sequestering agent for calcium ions. Initially, a stock of PHAMPS existed so first few experiments involve using this polymer. Later experiments were conducted to test the efficacy of EDTA with PHPAM.

Figures 4.12 and 4.13 present the data from an experiment where 2000 ppm PHAMPS in 1.2 wt% NaCl with 4 wt% EDTA is used during each step in the scan. As can be seen, EDTA almost completely reduces the effect of calcium on polymer stability. In Figure 4.13, the viscosity is plotted. One concern with using EDTA is that it will contribute to the total salinity thus on its own reducing viscosity to a point.

The effect the addition of EDTA to polymer viscosity for increasing background NaCl salinities is shown in Figure 4.14, and Figure 4.15 shows the effect of increasing

EDTA on a fixed salinity. Notice that the effect of EDTA on salinity is negligible around 5 wt% NaCl.

This led to using the minimum amount necessary to sequester the calcium in the remaining experiments. The ratio that was selected was 8 EDTA:1 Ca^{++} on a weight basis. It has been determined that EDTA has a maximum pH at which it will sequester calcium. This is due to the fact that at around pH 11, CaOH_2 is the dominate species and will precipitate out even with EDTA in solution.

With this in mind, an experiment was conducted to see if EDTA will effectively sequester calcium at lower pH, closer to pH 7. Figure 4.16 illustrates the results of an experiment where the EDTA solution was neutralized prior to use. It is evident that the solution needs to be at an elevated pH (although the lower limit was not determined) in order for EDTA to sequester calcium. This scan was replicated at pH 11, and the results are displayed in Figure 4.17. The viscosity is virtually independent of the amount of calcium in solution.

Figures 4.18 and 4.19 show the results from a set of experiments were performed using PHPAM and EDTA. While it is apparent that EDTA helps, the effect is not nearly as pronounced as it is with PHAMPS. Also, as with PHAMPS, salinity tolerance is an issue for background salinities below ~5 wt% TDS.

4.3 DISCUSSION

For the calcium tolerance experiments conducted without EDTA, poly(AM-co-ATBS-co-NVP) displayed the best results in both maintaining the highest viscosity and tolerating the most amount of calcium before showing signs of precipitation. Poly(AM-co-AMPS) retained significantly higher viscosity than PAM as it reached the onset of

turbidity, but they both shared similar cloud points, the calcium concentration corresponding to the approach of precipitation, for several NaCl background concentrations. These results suggest that the NVP monomer may be shielding the ATBS monomer. Experiments using EDTA to sequester Ca^{++} ions showed mixed results. When post-hydrolyzed poly(AM-co-AMPS) was used, almost 100% viscosity was retained when EDTA was implemented, and much higher Ca^{++} concentrations were tolerated. This was only true at elevated pH as the scans with neutralized EDTA showed no effect on improving viscosity. Also, salinity tolerance became an issue at low salinities when EDTA was used.

Table 4.1: 2500 ppm SAV 301 in 3% NaCl thermal aging experiments data (85 C)

Time (days)	Viscosity (cP)	$E_{Ag/AgCl}$ (mV)	pH	DO (ppb)	Degree of Anionicity ($\tau+\sigma+v$)
Initial	10.06	22.4	6.91	5000	0.25
After dithionite	9.59	40.1	6.71	4	-
2	8.78	-184.7	6.76	0	0.27
14	9.50	-47.9	6.75	0	-
60	10.28	-117	6.81	0	0.53
180	10.14	-25.53	6.84	0	-
270	10.72	-64.9	6.62	0	-

Table 4.2: 2500 ppm SAV 301 in 3% NaCl thermal aging experiments data (100 C)

Time (days)	Viscosity (cP)	$E_{Ag/AgCl}$ (mV)	pH	DO (ppb)	Degree of Anionicity ($\tau+\sigma+\nu$)
Initial	10.06	22.4	6.91	5000	0.25
After dithionite	9.59	40.1	6.71	4	-
2	10.53	51.45	6.79	0	0.49
14	10.89	-195.3	6.71	0	0.58
60	11.97	-175.8	6.82	0	0.75
180	11.28	-167.5	6.66	0	0.78

Table 4.3: 2500 ppm SAV 301 in 3% NaCl thermal aging experiments data (126 C)

Time (days)	Viscosity (cP)	E _{Ag/AgCl} (mV)	pH	DO (ppb)	Degree of Anionicity ($\tau+\sigma+\nu$)
Initial	10.06	22.4	6.91	5000	0.25
After dithionite	9.59	40.1	6.71	4	-
2	11.7	46.8	6.81	0	0.64
14	11.19	-81.7	6.54	0	0.82
60	13.26	-268.55	6.88	0	0.90
180	10.99	-215.2	6.67	0	0.92
270	9.067	-234.9	6.77	0	-

Table 4.4: 2500 ppm Kypam 5 in 3% NaCl thermal aging experiments data (85 C)

Time (days)	Viscosity (cP)	$E_{Ag/AgCl}$ (mV)	pH	DO (ppb)	Degree of Hydrolysis (τ)
Initial	67.19	-26.4	6.95	5000	0.25
After dithionite	59.10	-369.7	6.77	0	-
2	56.24	-288.33	6.77	0	0.43
14	58.21	-280.2	6.8	0	0.51
60	59.65	36.55	6.8	0	0.53
180	46.80	-191	6.76	0	0.89
270	49.88	-47.7	8.58	0	-

Table 4.5: 2500 ppm Kypam 5 in 3% NaCl thermal aging experiments data (100 C)

Time (days)	Viscosity (cP)	$E_{Ag/AgCl}$ (mV)	pH	DO (ppb)	Degree of Hydrolysis (τ)
Initial	69.56	42.7	6.88	5000	0.25
After dithionite	59.10	-365.4	6.7	0	-
2	54.50	-295.75	6.82	0	-
14	62.65	-278.97	6.8	0	0.60
60	63.20	-248.7	6.82	0	1.0
180	50.14	-55.3	6.85	0	-
270	53.87	-211.47	6.88	0	-

Table 4.6: 2500 ppm Kypam 5 in 3% NaCl thermal aging experiments data (126 C)

Time (days)	Viscosity (cP)	E _{Ag/AgCl} (mV)	pH	DO (ppb)	Degree of Hydrolysis (τ)
Initial	69.86	-22.2	6.9	5000	0.25
After dithionite	59.10	-365.4	6.7	0	-
2	57.42	-276.7	6.87	0	0.88
14	42.26	-209.45	6.88	0	1.0
60	63.20	-248.7	6.82	0	-
180	34.59	-258.06	6.88	0	1.0
270	30.69	-238.27	6.81	0	-

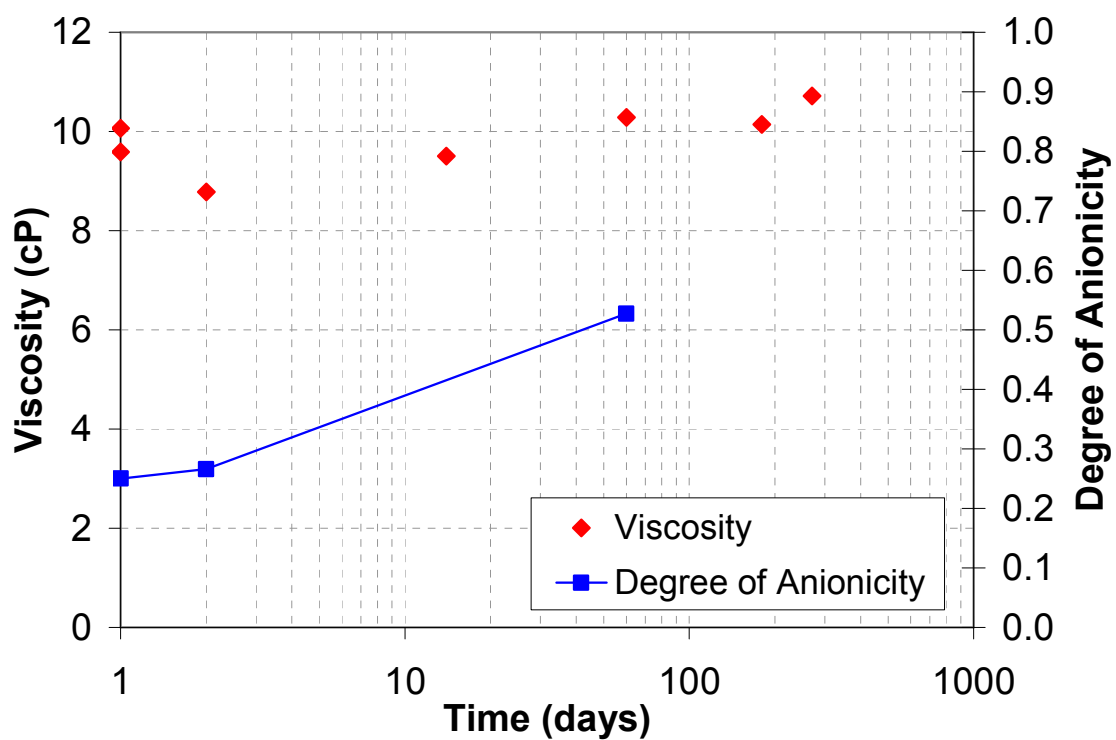


Figure 4.1: 2500 ppm SAV 301 in 3% NaCl hydrolysis data ageing at 85 C, pH~7

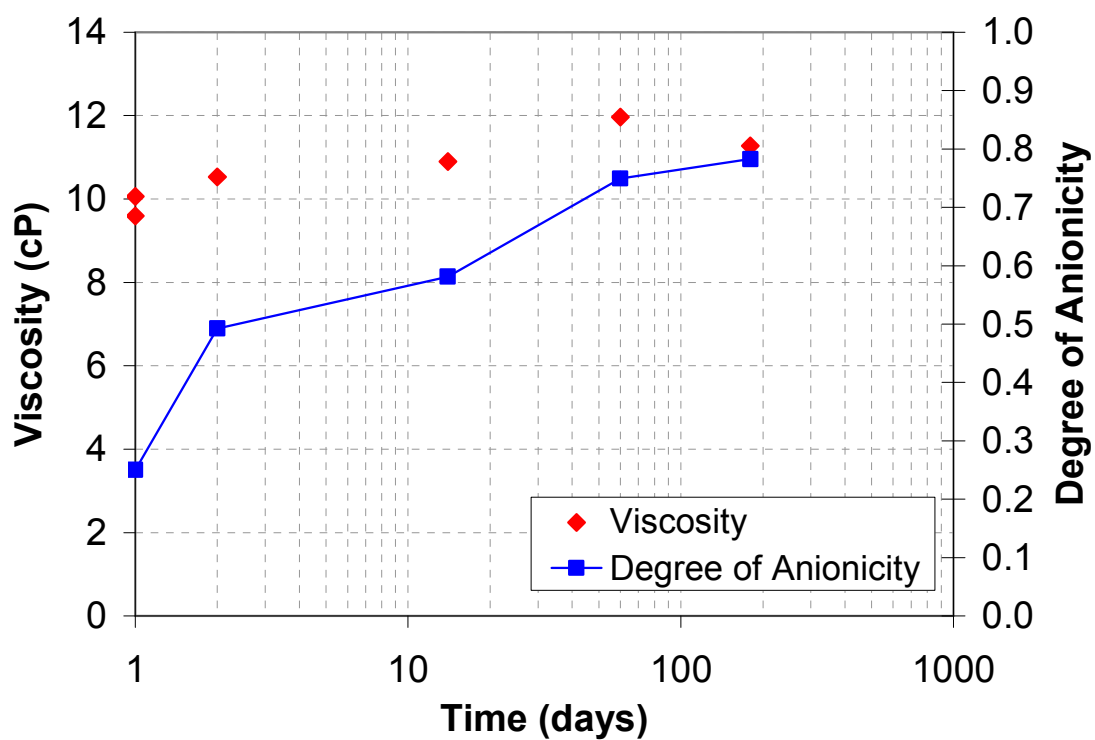


Figure 4.2: 2500 ppm SAV 301 in 3% NaCl hydrolysis data ageing at 100 C, pH~7

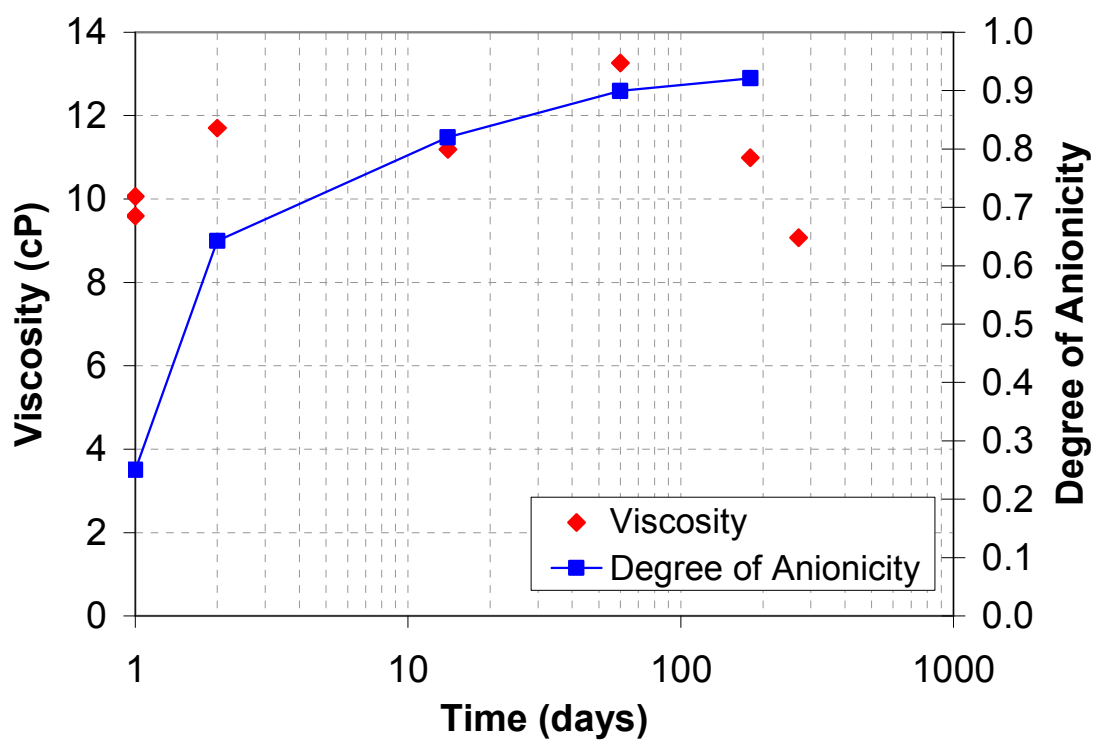


Figure 4.3: 2500 ppm SAV 301 in 3% NaCl hydrolysis data ageing at 126 C, pH~7

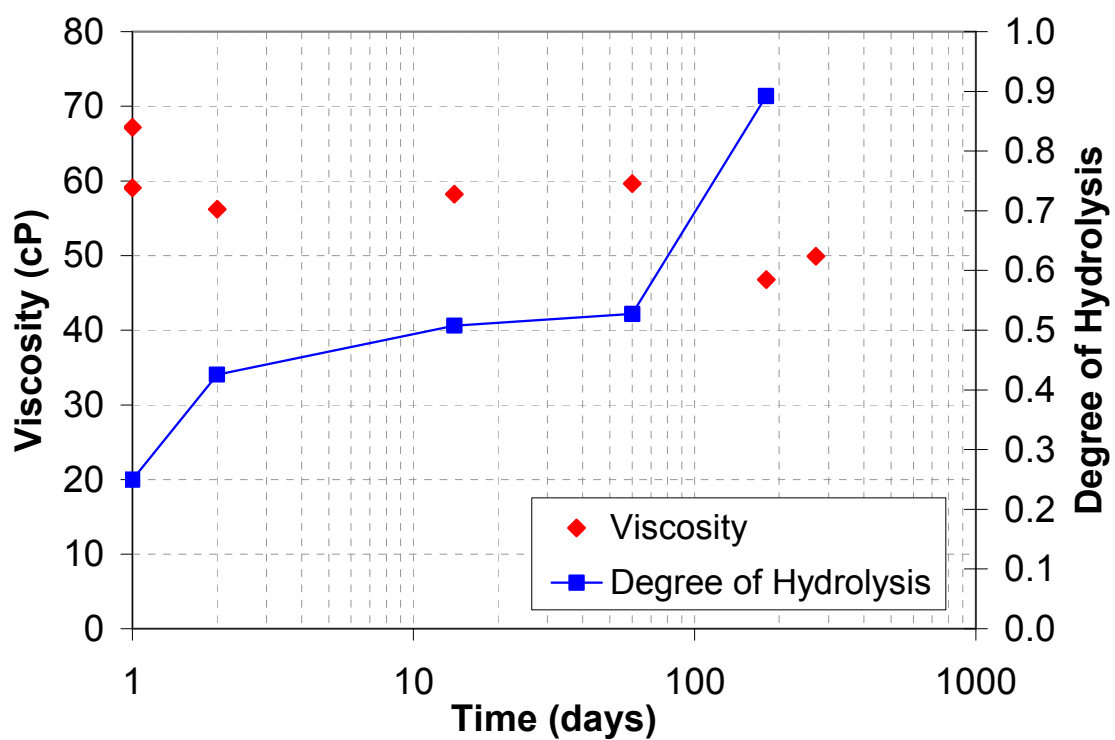


Figure 4.4: 2500 ppm Kypam 5 in 3% NaCl hydrolysis data ageing at 85 C, pH~7

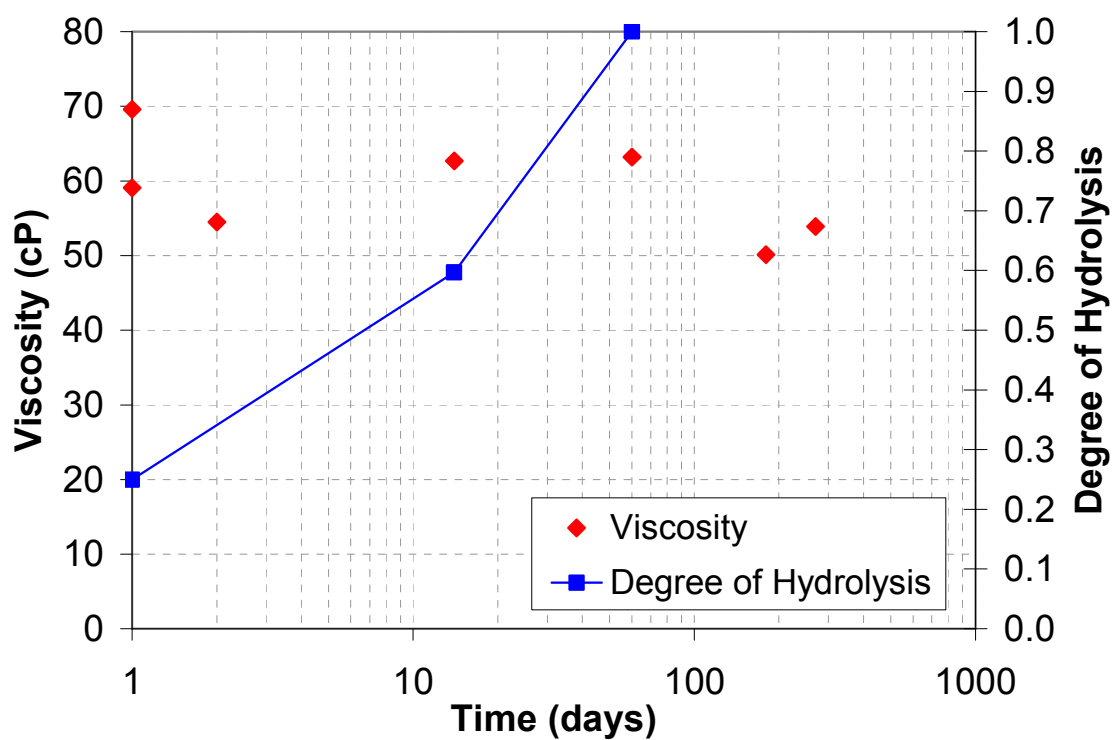


Figure 4.5: 2500 ppm Kypam 5 in 3% NaCl hydrolysis data ageing at 100 C, pH~7

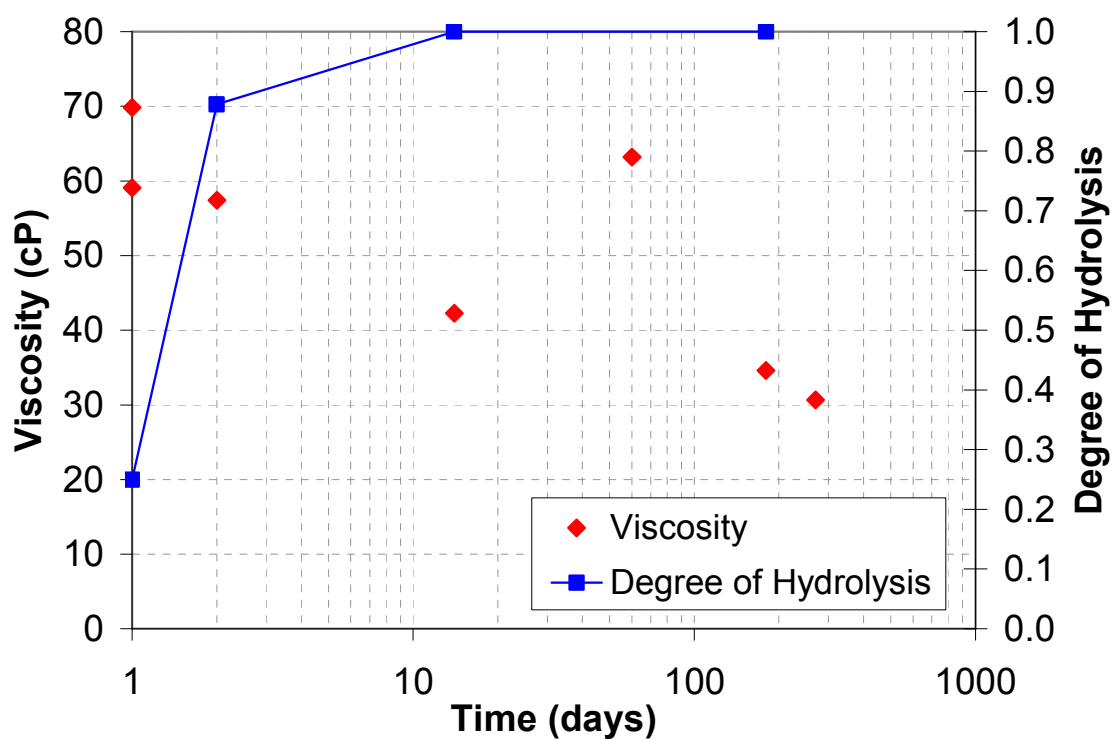


Figure 4.6: 2500 ppm Kypam 5 in 3% NaCl hydrolysis data ageing at 126 C, pH~7

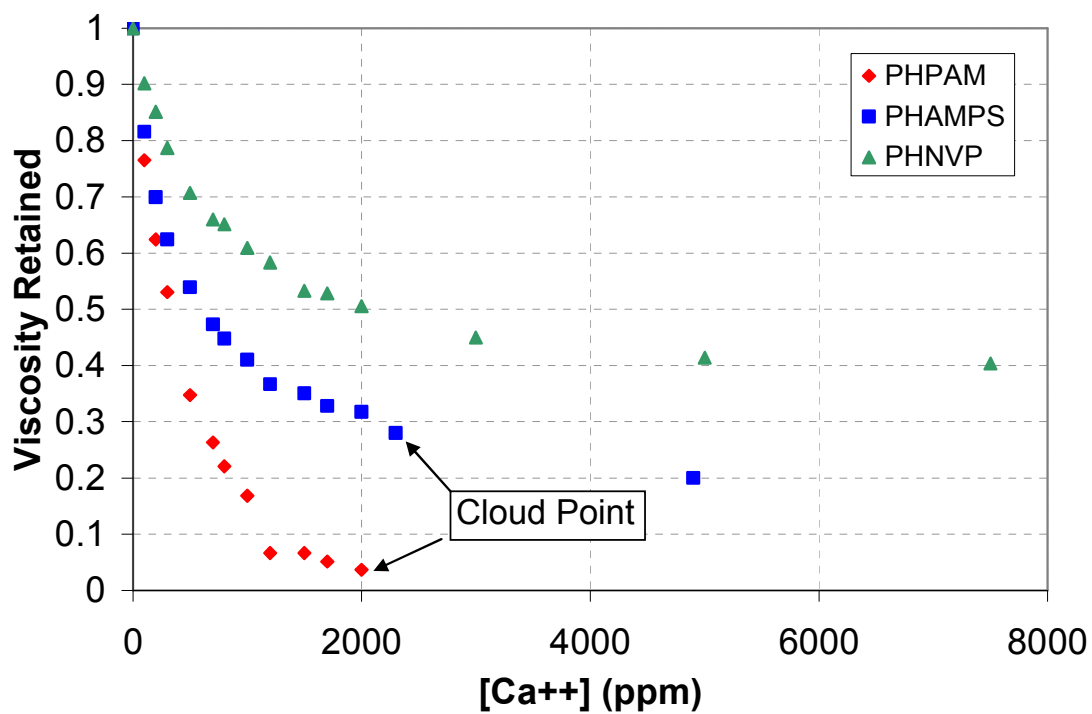


Figure 4.7: Ca^{++} tolerance with 1.2 wt% NaCl for lab-aged post-hydrolyzed polymers ($\tau \sim 0.6$)

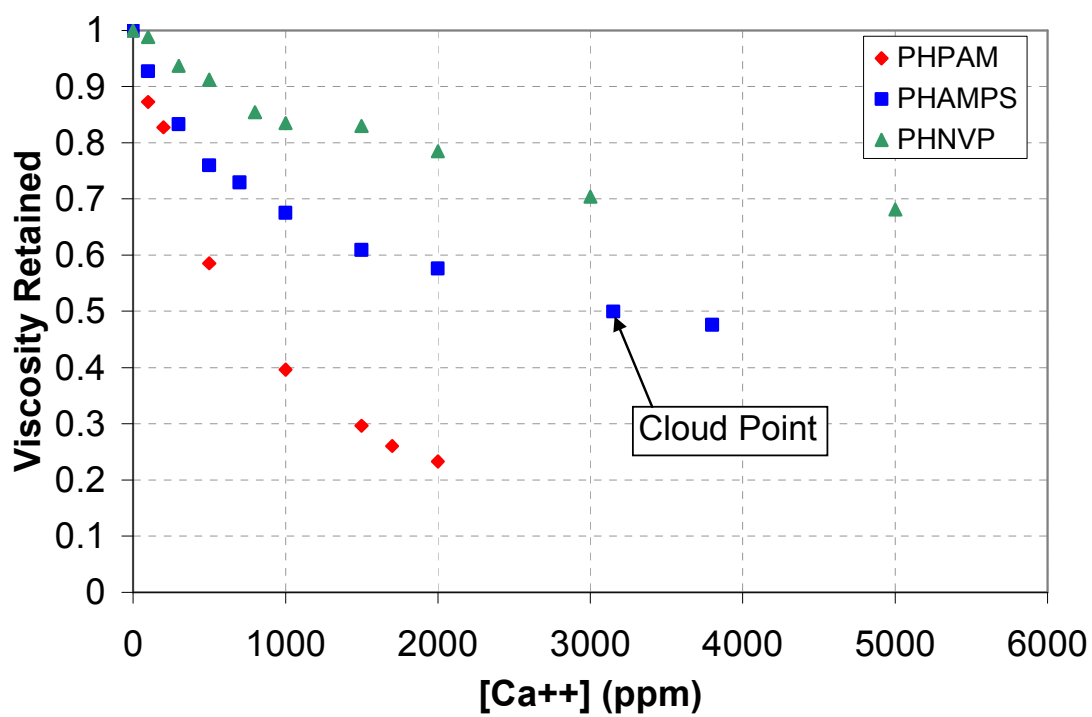


Figure 4.8: Ca⁺⁺ tolerance with 3 wt% NaCl for lab-aged post-hydrolyzed polymers ($\tau \sim 0.6$)

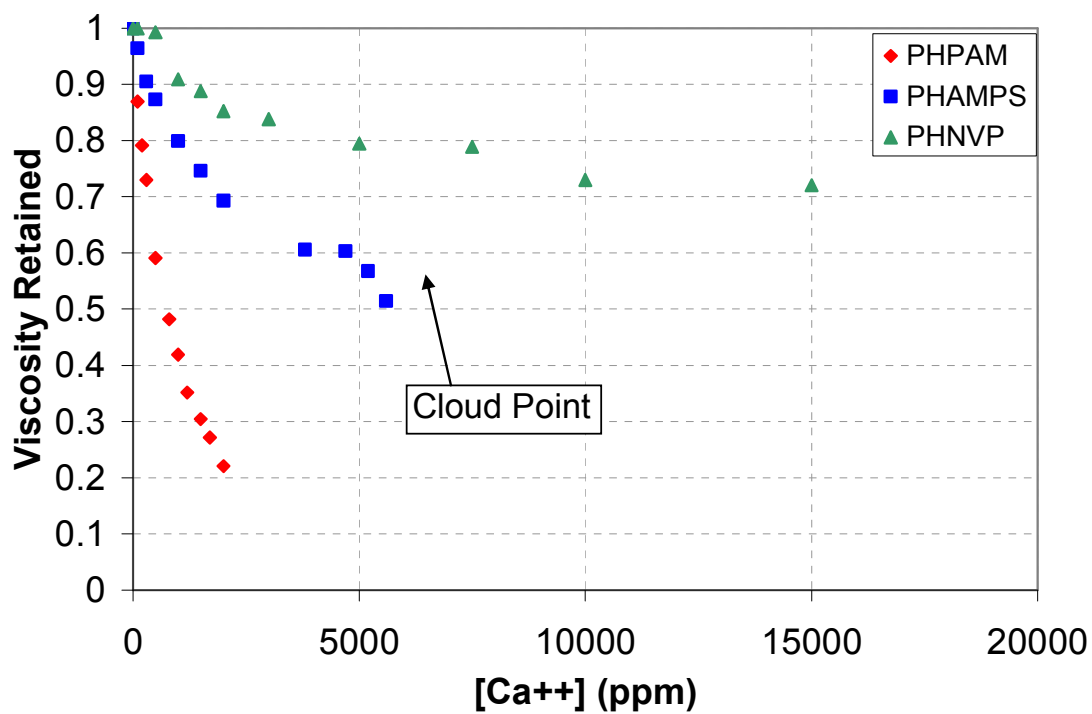


Figure 4.9: Ca^{++} tolerance with 5 wt% NaCl for lab-aged post-hydrolyzed polymers ($\tau \sim 0.6$)

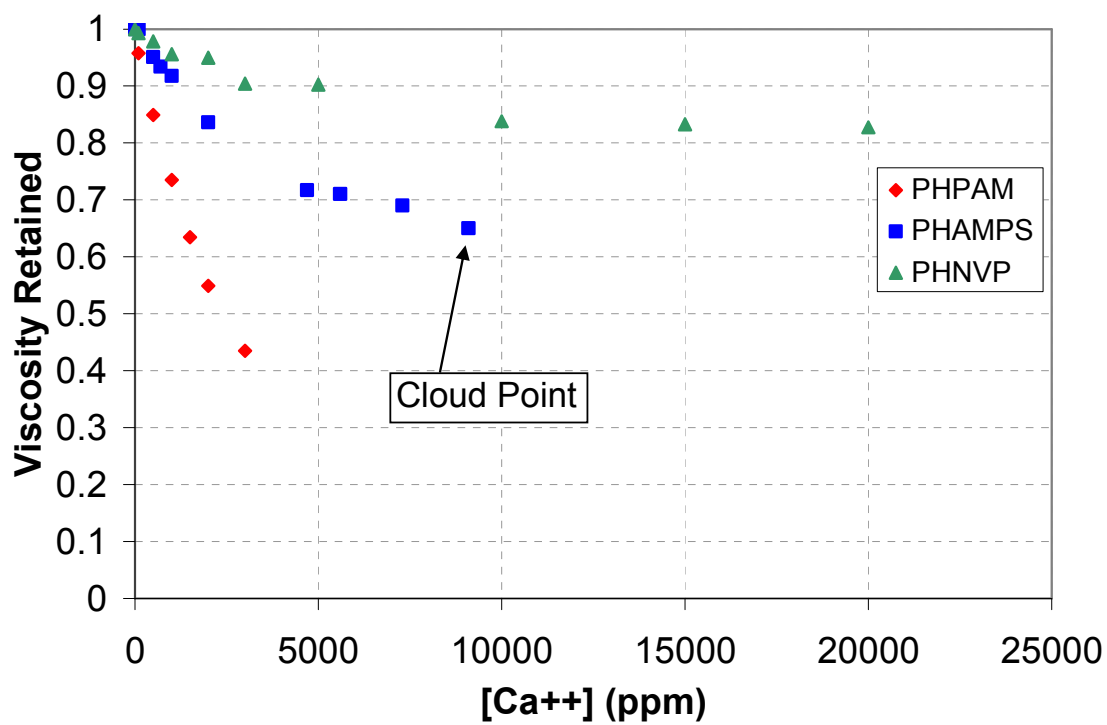


Figure 4.10: Ca⁺⁺ tolerance with 10 wt% NaCl for lab-aged post-hydrolyzed polymers ($\tau \sim 0.6$)

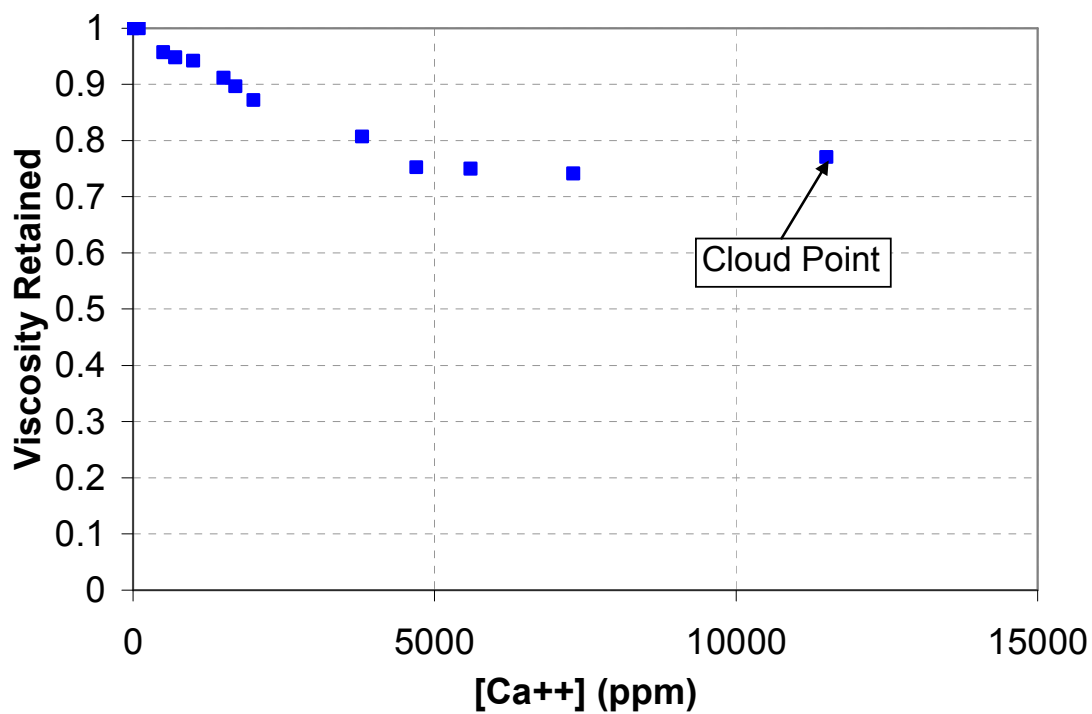


Figure 4.11: Ca^{++} tolerance for 2000 ppm PHAMPS (post-hydrolyzed AN 125) in 13.6 wt% NaCl, $\tau \sim 0.55$

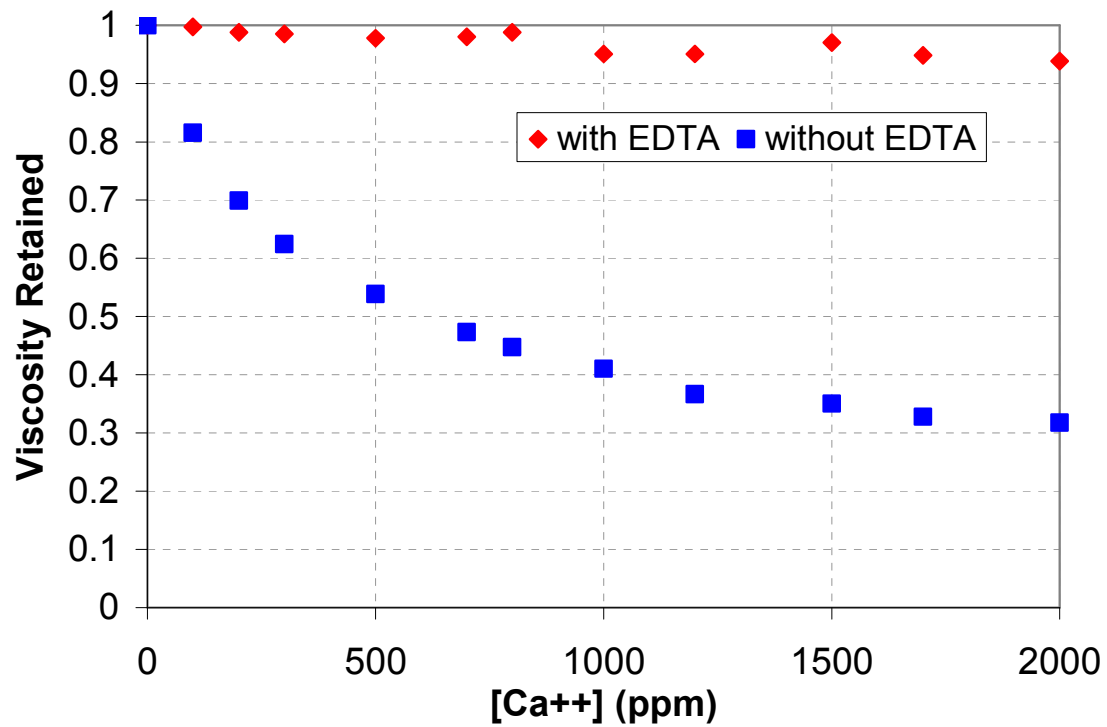


Figure 4.12: Ca⁺⁺ tolerance for 2000 ppm PHAMPS (post-hydrolyzed AN 125), 1.2 wt% NaCl, with and without 4 wt% EDTA; pH=10.75; $\tau \sim 0.55$; relative viscosity

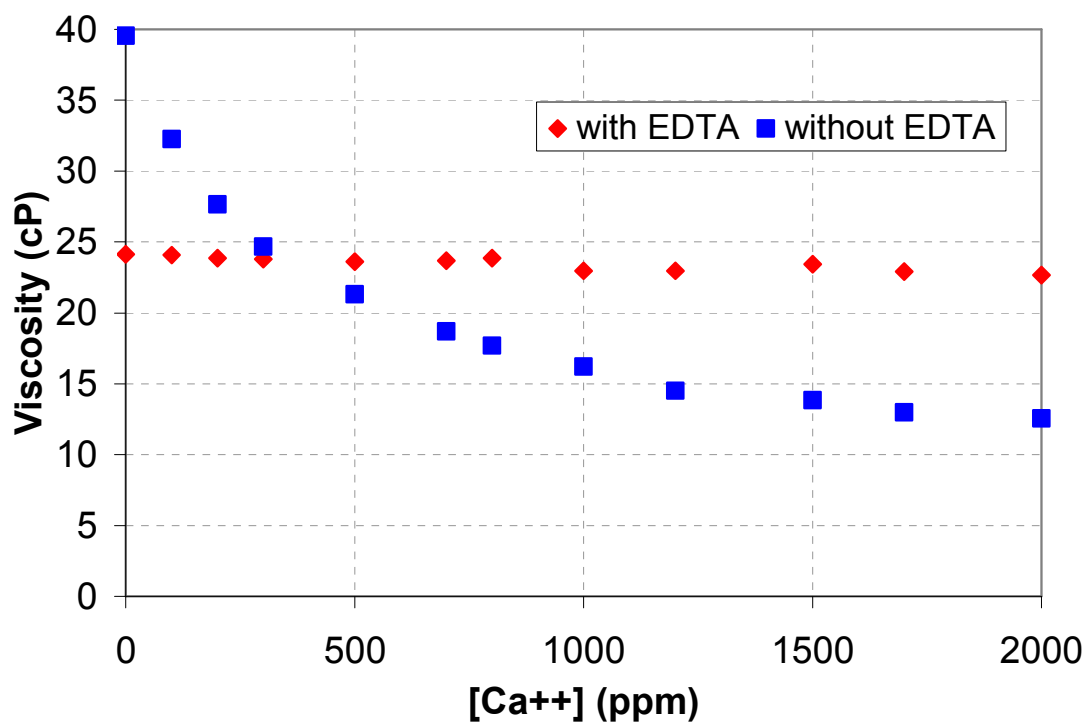


Figure 4.13: Ca⁺⁺ tolerance for 2000 ppm PHAMPS (post-hydrolyzed AN 125), 1.2 wt% NaCl, with and without 4 wt% EDTA; pH=10.75; $\tau \sim 0.55$; apparent viscosity

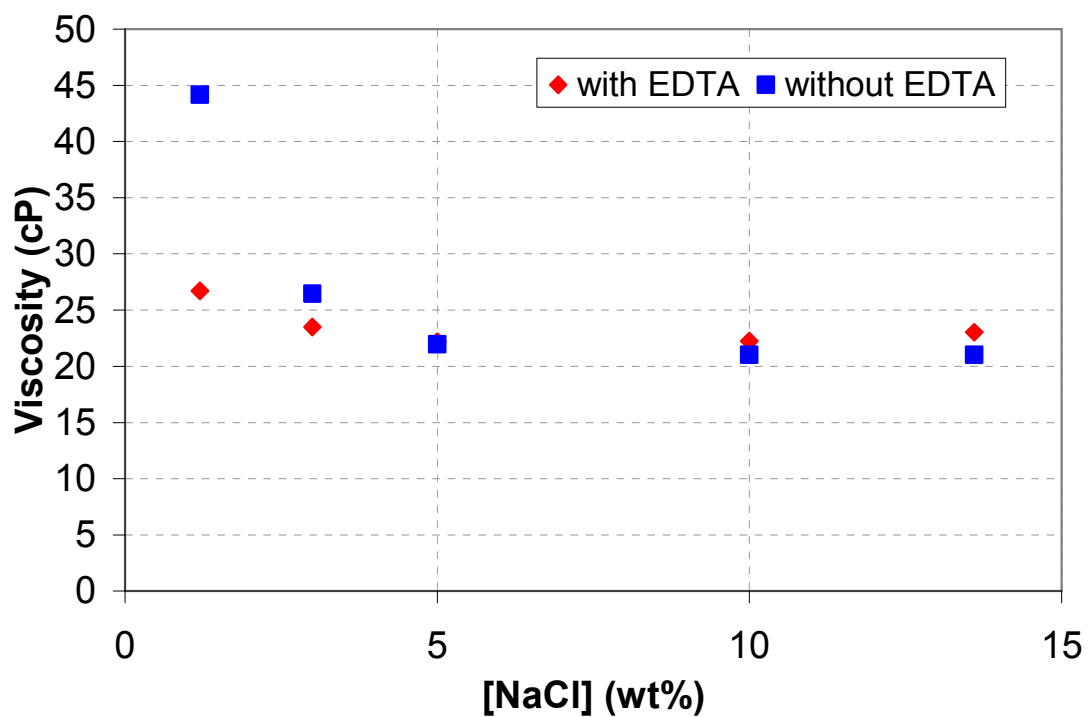


Figure 4.14: Effect of 4 wt% EDTA on viscosity for 2000 ppm PHAMPS (post-hydrolyzed AN 125) for varying salinities; pH=10.75; $\tau \sim 0.55$; no Ca^{++}

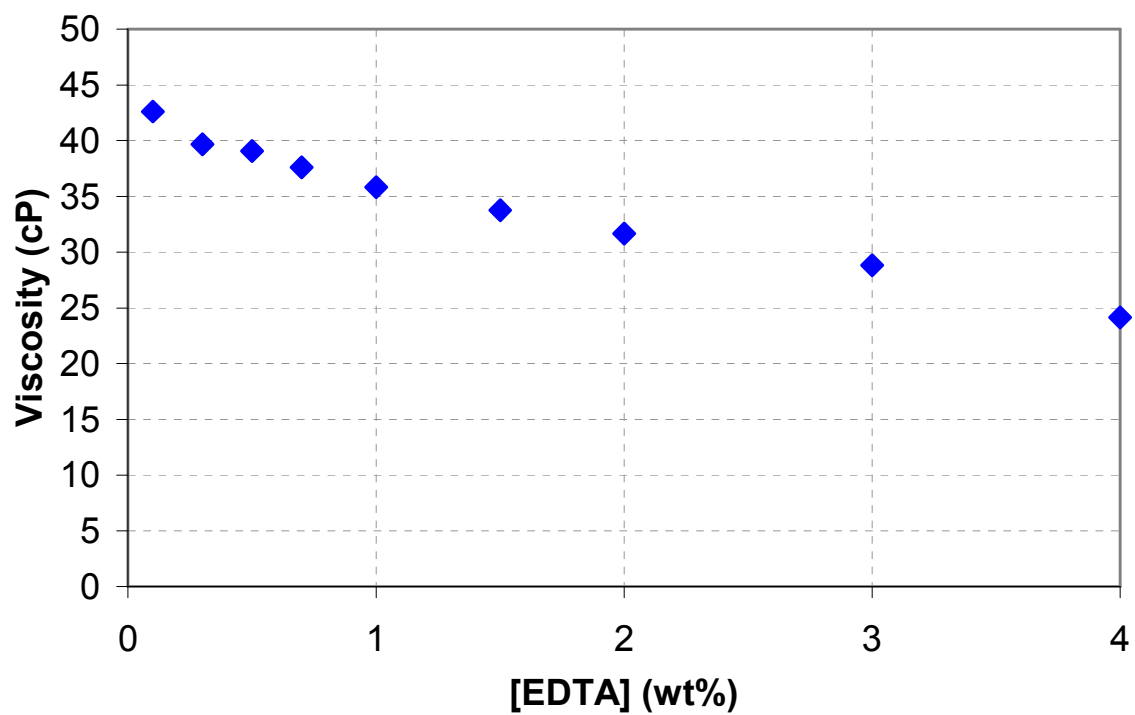


Figure 4.15: Effect of increasing EDTA concentration on viscosity for 2000 ppm PHAMPS (post-hydrolyzed AN 125), 1.2 wt% NaCl; pH=10.75; $\tau \sim 0.55$; no Ca^{++}

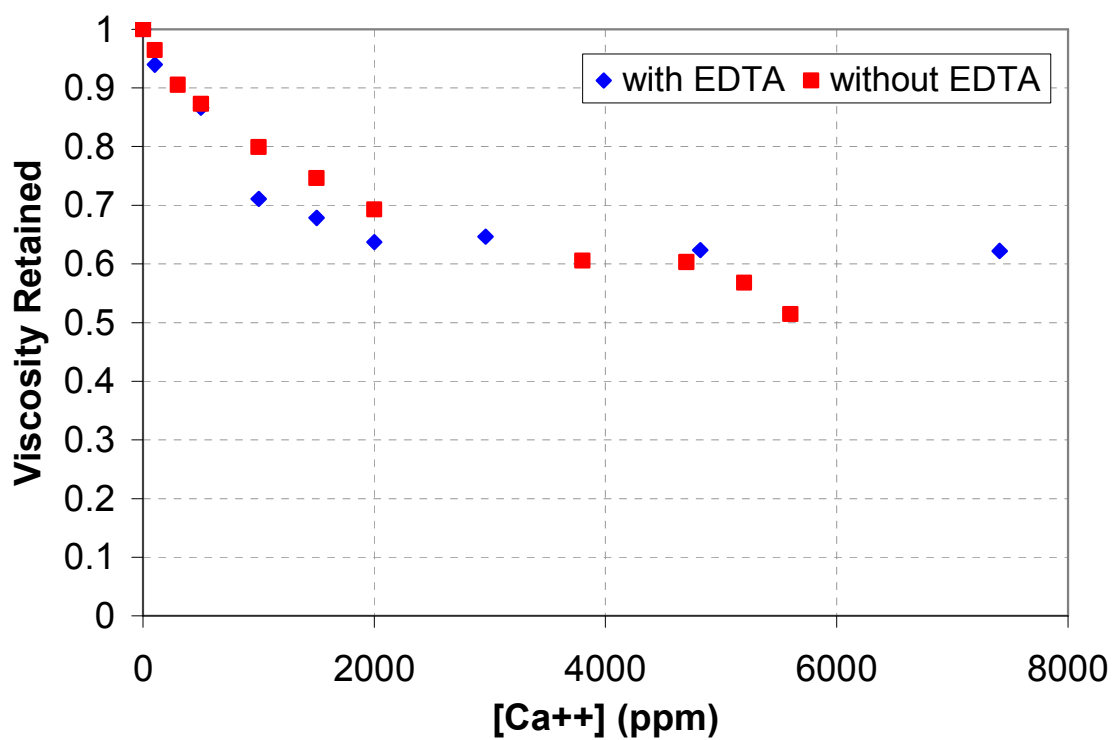


Figure 4.16: EDTA shows little effect on Ca⁺⁺ tolerance at neutral pH using PHAMPS (post-hydrolyzed AN 125), 5 wt% NaCl, 8 EDTA:1 Ca⁺⁺; pH=7.2; $\tau \sim 0.55$

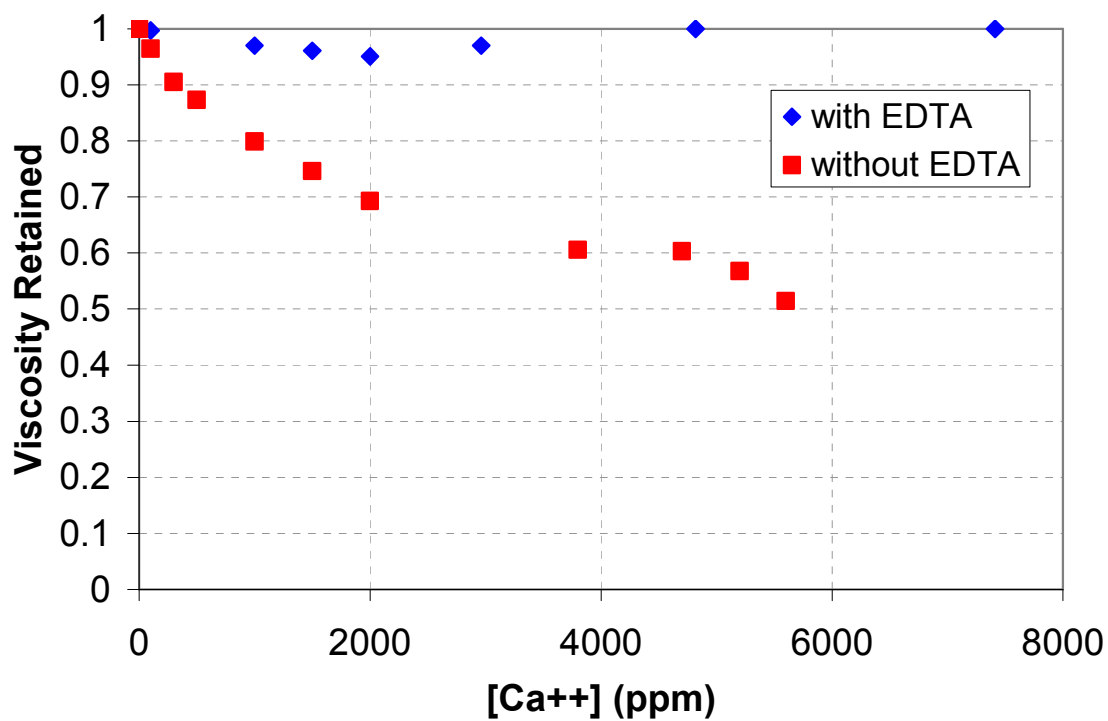


Figure 4.17: At alkaline conditions, EDTA completely removes effect of Ca^{++} for 2000 ppm PHAMPS (post-hydrolyzed AN 125), 5 wt% NaCl, 8 EDTA:1 Ca^{++} ; pH=11; $\tau \sim 0.55$

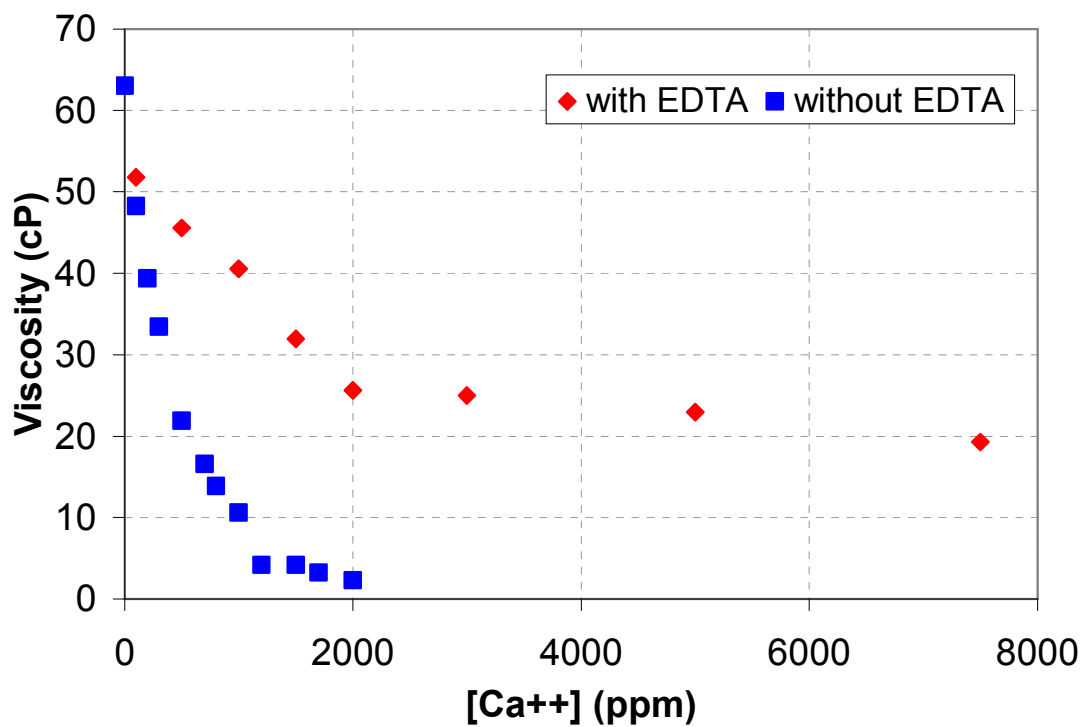


Figure 4.18: For post-hydrolyzed PAM (FA 920 SH), EDTA shows improvement for Ca^{++} tolerance but not as pronounced as with PHAMPS, 2000 ppm PHPAM, 1.2 wt% NaCl, 8 EDTA:1 Ca^{++} ; pH=11; $\tau \sim 0.55$

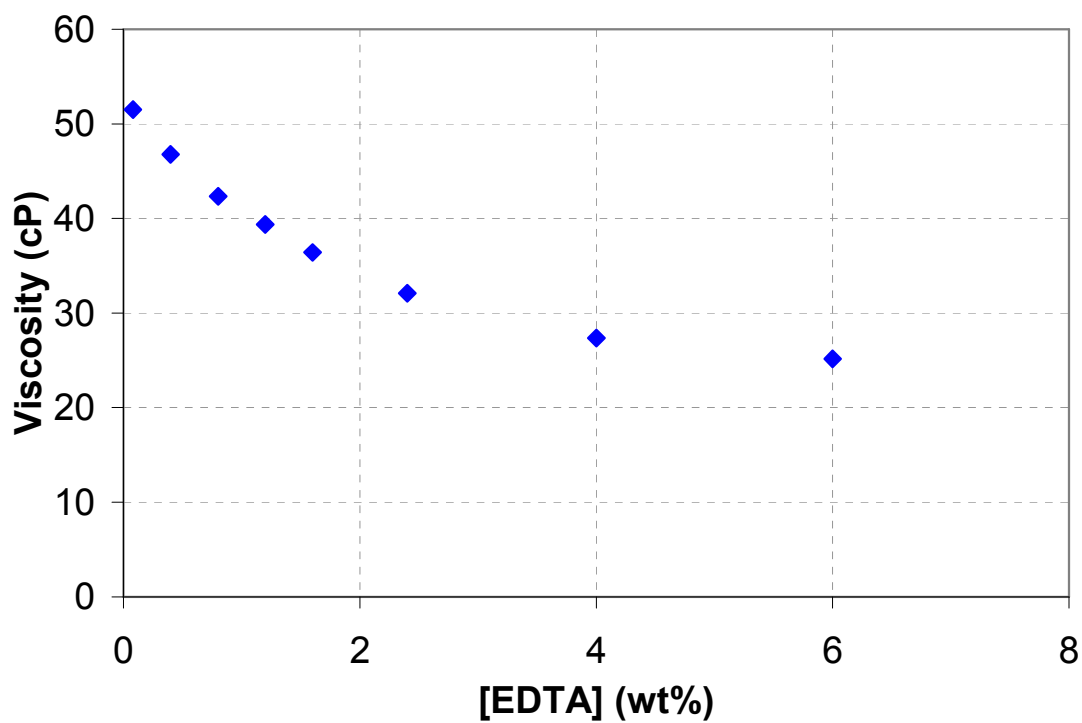


Figure 4.19: Effect of increasing EDTA concentration on viscosity for 2000 ppm PHPAM (post-hydrolyzed FA 920 SH), 1.2 wt% NaCl; pH=10.75; $\tau \sim 0.55$; no Ca^{++}

CHAPTER 5: THERMAL STABILITY RESULTS & DISCUSSION

These experiments involved adjusting several variables in order to better understand how altering redox potential and iron solubility affects polymer stability in the presence of iron. These variables included type of polymer used, method of removal of oxygen (bubbling with argon (or nitrogen), adding sodium dithionite, or bubbling with hydrogen), presence of carbonate/bicarbonate, amount of iron, and method of increasing redox potential after addition of iron (bubbling of air into solution or addition of ferric iron).

5.1 EXPERIMENTS WITH Fe^{++}

Initially experiments were conducted in order to better understand the relationships between dissolved oxygen, iron and redox potential. Figures 5.1 and 5.2 show $E_{\text{Ag}/\text{AgCl}}$ as a function of DO and $E_{\text{Ag}/\text{AgCl}}$ as a function of Fe^{++} . As can be seen from the graphs, for both decreasing DO and increasing Fe^{++} , $E_{\text{Ag}/\text{AgCl}}$ decreases linearly on a semilog plot.

Effect of Fe^{++} on Polymer Solutions with a Small Continuous Supply of O_2

The base case composition for all experiments, unless otherwise noted, was 2500 ppm 3630S in 3% NaCl. A slow, steady degradation was seen when a small, steady supply of oxygen was supplied to a polymer solution containing ferrous iron. Irrespective of which counter ion of ferrous iron was added a similar amount of degradation was observed.

Figure 5.3 presents viscosity loss over time. Yang and Treiber (1985) report that a continuous supply of 30 ppb O_2 to polymer containing 10 ppm ferrous iron will result in 50% viscosity loss after 500 days at 77 °F. For this test, there was a continuous supply of approximately 20-40 ppb O_2 (as confirmed by Chemets® ampoules), and after less than 1 day at 25 °C, there was 28% and 60% viscosity loss at shear rates of 11 and 1.75 sec^{-1} , respectively.

Another experiment was performed with the pH buffered at around 7 using PIPES buffer titrated with NaOH in the polymer solution prior to the addition of iron. Although small viscosity losses were seen upon the addition of iron, it appeared that the PIPES buffer precipitated the iron and caused either flocculation or cross-linking in the polymer. From this point forward experiments were unbuffered, though pH was measured and adjusted with NaOH or HCl if necessary.

Effect of Fe^{++} on Polymer Solutions Containing Bicarbonate with a Small Continuous Supply of O_2

Yang and Treiber (1985) presented some of the most favorable results relating to the stability of polymer solutions in the presence of iron. In light of recent results regarding the beneficial effects of carbonate and bicarbonate on polymer solutions, it seems that some of this earlier work should be revisited. The above experiment with ferrous sulfate was repeated with the Yang and Treiber brine added to the base case polymer. The Yang and Treiber brine composition is detailed in Table 5.1. Figure 5.4 displays the results of this experiment.

As can be seen, there is a significant increase in viscosity after 3 days of mixing in the bicarbonate containing brine. Unfortunately the experiment without bicarbonate was terminated after just one day, so it is impossible to compare the longer term results.

However, over the course of several hours it appears that the additional bicarbonate in the Yang and Treiber brine has no significant effect on the stability of the polymer solution under these conditions. The increase in viscosity may be due to cross-linking of the polymer in the presence of Fe^{+++} , which was indicated by an orange hue of the polymer solution.

Effect of Fe^{++} on Polymer Solutions with a Small Amount of O_2 and no Further

A second relevant case for polymer stability pertains to a solution with a small, initial amount of dissolved oxygen but no further O_2 , as would occur if an iron-free polymer solution saturated with oxygen was injected into an anaerobic reservoir containing iron. In an experiment with 5 ppm dissolved oxygen, Yang and Treiber observed 20% viscosity loss in the first 20 days but then no more.

An experiment was performed similar to that of Yang and Treiber. Yang and Treiber's brine was added to the base case polymer composition. Dissolved oxygen was lowered to 30 ppb by bubbling with N_2 . Fe^{++} was added as a sulfate salt as above, then the polymer solutions were carefully transferred to ampoules, which were kept sealed and under vacuum on the ampoule sealing manifold. Less than 10% viscosity loss was observed after about 2 days, as presented in Figure 5.5. Experiments are still under observation, however the degradation observed thus far is greater than would be expected given the results of Yang and Treiber with far more dissolved oxygen. Nevertheless degradation was less than the previous experiment, where a small continual supply of oxygen was supplied.

Effect of Fe^{++} on Polymer Solutions in the Absence of O_2

Another discrepancy in the literature involves the stability of polymer in the presence of iron (II) and the absence of oxygen. In their experiments without O_2 in the presence of 10 ppm Fe^{++} , Yang and Treiber (1985) report that a polymer solution retained 99% of its viscosity after 500 days at 25 C and has 260% of its original viscosity after 90 days at 93 C. It should be noted that Yang and Treiber report pre-shearing their polymer in a Waring™ blender at 25% power for 30 seconds, making the polymer less sensitive to subsequent degradation, and starting polymer viscosity was only around 5 cP. Kheradmand (1987) on the other hand reports over a 50% loss of viscosity in 60 days when an HPAM is aged at 80 C in the presence of 5 ppm Fe^{++} under oxygen free conditions. Additionally, Kheradmand reports viscosity loss after 1 hour at 80 C as a function of Fe^{++} concentration. At 1 ppm degradation is negligible, whereas at 2.5 ppm and 5 ppm significant degradation is observed in this short time. However Kheradmand also reports that degradation was minimal after his polymer was purified. While Yang and Treiber used Cyanatrol 960, a commercial polymer, Kheradmand used a lab-prepared sample with higher reported monomer content. Both authors reported vacuum/purge cycling, and measured less than 5 ppb dissolved oxygen. Kheradmand reports the use of argon, whereas Yang and Treiber do not report which gas was used.

In an attempt to reconcile these results, a solution of 2500 ppm 3630S in 3% NaCl was deoxygenated to non-detectable levels, and 2 ppm Fe^{++} was added as $FeSO_4$ from a similarly deoxygenated mother solution, except that nitrogen used for this mother solution was not scrubbed with a heated column of copper. The polymer was then carefully transferred to glass ampoules, which were vacuum/purge cycled with scrubbed nitrogen both before and after the transfer. Samples were then broken for measurement

while nitrogen was used to blanket the viscometer and purge the transfer syringe. Only 10% degradation was seen after 188 days at room temperature, both with and without the presence of the divalent constituents and bicarbonate present in Yang and Treiber's brine.

While it was originally theorized that either the presence of bicarbonate or perhaps the use of hydrogen as the unreported purging gas led to the improved stability that Yang and Treiber reported, it now appears that differing results are due to differences in impurities in the authors' polymers, with Yang and Treiber's results with a commercial polymer more relevant to Flopaam 3630S.

It should be noted that several unsuccessful attempts were made to perform this experiment before a method was developed which allowed transfer and sealing of samples without oxygen contamination. When degradation was observed oxygen was also present. In one case 80% of viscosity was lost, though only 50-100 ppb of oxygen was present in the ampoule when opened. A previous experiment, identically performed to that described above except without a heated copper column in place to remove oxygen impurities from the nitrogen supply, resulted in extensive degradation. In this attempt dissolved oxygen contents of 5-20 ppb were measured in the polymer whilst it was bubbled with nitrogen. The successfully preserved samples read 0 ppb using Chemets 0-40 ppm dissolved oxygen ampoules, both before sealing and when opened. This is noted to emphasize the severity of degradation that can occur with minimal amounts of oxygen present, as will be discussed in further detail later in this chapter.

5.2 EXPERIMENTS WITH H₂

It was further theorized that the mechanism by which sodium dithionite (which are discussed in the following sub-section) causes polymer degradation involved the

reduction of iron present as impurities, which subsequently reacted with oxygen in a Fenton-type reaction. Thus the lowered solubility of iron (II) might interrupt the ability of these impurities to redox cycle. In order to test this theory, it was necessary to impose a change in redox potential similar to that seen when sodium dithionite is added to a polymer solution in the presence of oxygen. This was achieved by bubbling a polymer solution with hydrogen gas, then re-exposing it to oxygen.

Reducing the Redox Potential without the Use of Dithionite

While the low E_H achieved was similar to that with sodium dithionite, no degradation was seen, as illustrated in Figure 5.6. Thus the change in E_H alone cannot explain degradation related to the use of sodium dithionite, so at this point we are unable to say that it is redox cycling of iron impurities, rather than a direct reaction between oxygen and dithionite possibly catalyzed by iron, which causes degradation. Additionally it was noted that the rise in E_H upon reintroduction of air was much slower than when E_H was lowered using sodium dithionite.

Effect of Fe^{++} on Polymer Solutions Reduced with H_2

The above experiment was also duplicated with oxygen removal by bubbling the polymer solution with hydrogen, but 2 ppm Fe^{++} (as sulfate) was added when solution was at low E_H . Ampoules were not flame sealed for safety reasons, and viscosity was measured with a Contraves LS-30 viscometer. Degradation one hour after addition of Fe^{++} was insignificant, as shown in Figure 5.7. A sample was allowed to oxidize by slowly stirring in the atmosphere, and both viscosity and E_H were monitored. As seen in

Figure 5.7, initial oxidation increased the E_H but did not cause viscosity loss. Once E_H passes around 0 Volts, viscosity begins declining.

5.3 EXPERIMENTS WITH SODIUM DITHIONITE

Several experiments were completed with the purpose of determining the nature and extent of degradation reactions associated with the simultaneous or subsequent presence of sodium dithionite and oxygen in a polymer solution. These tests included varying the following: polymer type, amount of dithionite added, initial exposure to O_2 or N_2 , addition of chelator or antioxidant, and level of initial DO.

Effect of Amount of Sodium Dithionite

The first tests to be carried out were to show the effects of increasing amounts of sodium dithionite on polymer viscosity. 20, 100, or 400 ppm of sodium dithionite were added to 2500 ppm Flopaam 3630S in 3% NaCl in the presence of approximately 2-4 ppm dissolved oxygen resulting from hydration of the polymer under atmosphere. No attempt was made to exclude oxygen. Figure 5.8 shows the viscosity decrease as a function of time after exposure to O_2 . It can be concluded that increasing sodium dithionite concentration increases viscosity loss in the range examined. Additionally, most of the viscosity loss occurs within 1 day of exposure to O_2 .

Effect of Degree of Hydrolysis

Figure 5.9 compares the degradation of the 4 polymers used in the dithionite experiments. Unhydrolyzed polyacrylamide (FA 920 SH) exhibited the least degradation

while fully hydrolyzed PAM, or polyacrylic acid (ALP 99), showed the greatest viscosity loss.

Little can be said about the difference in viscosity loss seen between the 2 partially hydrolyzed polyacrylamides (FP 3630S and AN 923). Both are of similar degree of hydrolysis ($\tau = 0.3$). It is uncertain if the antioxidant that is in 3630S (the only difference between the 2 polymers besides molecular weight) is to be attributed to the difference in viscosity loss that is seen.

Effect of Bicarbonate/Carbonate and Sodium Dithionite in Presence of O₂

After a reexamination of the results of Shupe (1981), Yang and Treiber (1985) and Knight (1973), it was hypothesized that the differing amounts of sodium carbonate and bicarbonate in Shupe's brine led to the significantly lower degradation observed. Shupe reports that 100 ppm sodium dithionite mixed in polymer in the presence O₂ shows only a 3% loss (at 14.7 sec⁻¹) after 15 minutes of mixing, and 12% loss after 3 hours with an additional 100 ppm of sodium dithionite added to the solution.

An effort was made to reconcile Shupe's findings with those of others who have reported more extensive degradation, and in particular to test the hypothesis that the presence of carbonate and bicarbonate are responsible for the difference. 2500 ppm 3630S was hydrated in a brine of 3% NaCl, 1313 ppm NaHCO₃, and 248 ppm Na₂CO₃. While 3% NaCl was chosen to correspond with the rest of the experimental program, the amounts of carbonate and bicarbonate correspond to the amounts stated by Shupe, plus an additional 100 ppm of sodium carbonate thought to be present in Shupe's polymer stock based upon analysis by Kheradmand (1987). The actual makeup of Shupe's brine is tabulated in Table 5.2. 100 ppm of sodium dithionite was added to the polymer solution

with no attempt to exclude oxygen for the first day, and with only Parafilm™ covering the vessel to prevent evaporation after that. Results are presented in Figure 5.10.

Viscosity loss after 10 minutes and 1 hour in the brine containing carbonate and bicarbonate (7% for both at 11 sec^{-1}) were similar to that seen by Shupe, whereas viscosity loss in the NaCl only brine was around 25%, inline with the extensive degradation oft-reported elsewhere. Viscosity continued to decrease in the carbonate containing sample under continued oxygen exposure, and after 7 days viscosity loss was 22% (at 11 sec^{-1}). It should be noted that this is still considerably less viscosity loss than the tests done without carbonate where the viscosity loss was more than double after 7 days at 46% (at 11 sec^{-1}). Thus it appears that the presence or absence of low levels of carbonate and bicarbonate, as seen in natural brines, can have a significant effect on the degradation seen when sodium dithionite is added to polymer solutions in the presence of oxygen, and this resolves the conflict in the literature concerning the extent of degradation when dithionite is added to polymer solutions without proper exclusion of oxygen.

Effect of Chelators on Polymer Stability

The beneficial effect of even low levels of carbonate presented above are in accordance with the theory that the very low levels of iron present in polymer solutions play a catalytic role in the degradation experienced when sodium dithionite is added. If this is indeed the case, it was hypothesized that a chelator that can reduce the redox cycling of iron, such as diethylene triamine pentaacetic acid (DTPA), could also have a beneficial effect. While DTPA can not prevent the oxidation of iron (II) to iron (III), it is

believed to prevent the subsequent reduction of Fe (III), and hence halts the iron-catalyzed Haber-Wiess mechanism (Cohen and Sinet, 1982).

In order to test this theory, 10 ppm DTPA (from a 40% active aqueous solution of DTPA neutralized with potassium salts) was added to the base case polymer. 100 ppm of sodium dithionite was mixed with the polymer solution in the presence of O₂. Figure 5.11 illustrates that, although there is some immediate degradation upon addition of dithionite, degradation stops almost immediately, consistent with the theory that the Haber-Wiess mechanism is halted after the first oxidation of the iron.

Other Observations Regarding Dissolved Oxygen, Redox Potential, and Polymer Stability

Several experiments were conducted where the only variables were polymer type and time to exposure to oxygen. The four polymers used for this experiment were an unhydrolyzed polyacrylamide (FA 920 SH), two partially hydrolyzed polyacrylamides with a degree of hydrolysis of about 0.3 (AN 923 and 3630S), and a fully hydrolyzed polyacrylamide, or polyacrylic acid (ALP 99). Exposure to oxygen was either immediate or after 1 hour. The experiments where a delay in the exposure to oxygen occurred were blanketed with nitrogen for 1 hour. ORP was measured continuously and viscosity was measured at periodic time intervals. Figures 5.12-5.19 display the results.

E_{Ag/AgCl} values decreased by approximately 600 mV after addition of sodium dithionite in each experiment regardless if oxygen is being rigorously excluded initially. The total time for the redox potential to return to a steady state value was approximately 10 minutes in the experiments where there was no attempt to exclude O₂. A steady state redox potential of approximately -550 mV was reached in each of the experiments where

N₂ was used to exclude O₂. In each experiment, a steady state value was reached approximately 20 minutes after exposure to air.

In all of the experiments, the viscosity loss after 1 hour of mixing was less for those blanketed with N₂ initially. However, in every one of these experiments, when the solution was then exposed to O₂, 1 hour later the viscosity loss matched exactly with the viscosity loss of those experiments that were exposed to O₂ initially. This is exhibited in the graphs by use of a baseline. It can be concluded that the amount of time spent at a low negative redox potential and that the time taken to reach steady state redox potential once exposed to O₂ have no effect on the severity of degradation.

In all of the previous experiments using sodium dithionite, some level of DO existed (approximately 2-4 ppm). For the next experiment, polymer was deoxygenated by bubbling N₂ into solution for a sufficient time to be anaerobic. The base case of 2500 ppm 3630 in 3% NaCl was used. Once deoxygenated, the procedure was the same as all other experiments where the solution was initially blanketed with N₂. Figure 5.20 illustrates the results from this experiment.

There is less degradation when the polymer is initially deoxygenated and then exposed to O₂ after sometime. This is interesting because with all previous experiments, the delay in exposure to O₂ by at first blanketing with N₂ did not have an effect on the severity of degradation.

Use of Montbrite 1240 to Produce Dithionite

Montbrite 1240 (sodium borohydride) mixed with sodium bisulfite creates sodium dithionite and sodium metaborate. Initially, an experiment was done to replicate the above experiments where dithionite was added to polymer mixing under nitrogen (this

time argon) then exposed to the atmosphere. 100 ppm dithionite from the Montbrite 1240 and sodium bisulfite solution was added to 2500 ppm 3630S in 3 wt% NaCl. ORP was constantly monitored and viscosity measurements were taken periodically. Figure 5.21 depicts the time-elapsd measurements for this experiment. Notice that the time until a significant rise in E_H is quite a bit longer when compared to the identical experiment using powder dithionite. Also, the 60% viscosity retained after 72 hours is better than that of the powder dithionite. It should be noted that the stock solution of dithionite after 2.5 hours of mixing under an argon blanket was still at a much reduced state as indicated by an ORP measurement.

The above experiment showed that the short-term effect of the dithionite created by this novel process closely matched that of the traditional method of using powder dithionite. The real test would be to study the long-term effects of the dithionite using Montbrite 1240 on polymer stability as compared to the powder dithionite. This is because polymer must maintain its viscosity for many months as it propagates the reservoir. Two identical solutions of 2500 3630S in 3 wt% NaCl were dosed with 100 ppm dithionite from the two different methods. Several ampoules were sealed and placed at several temperatures to age for increasing time periods. At logarithmic intervals, ampoules were removed from the ovens, cracked, and measurements were taken. Tables 5.3 and 5.4 as well as Figures 5.22 and 5.23 detail the results of these two experiments.

One more experiment was conducted with the Montbrite 1240 using 2500 ppm 3330S in synthetic field brine with 2 ppm Fe^{++} as sulfate added before sealing ampoules and aging at a range of temperatures. The constitution of the synthetic field brine is listed in Table 5.5. The iron was added to simulate iron expected to come into contact with the polymer solution as it is being injected into the reservoir. Results for this experiment are illustrated in Table 5.6 and Figure 5.24.

The results from these three experiments show that at worst the dithionite created by Montbrite 1240 and sodium bisulfite performs that same as the dithionite using the traditional powder with respect to polymer stability. In viewing the redox potential data, it appears that the dithionite produced using Montbrite 1240 is more robust than the method using powder, as is evident by the consistently lower values for all temperatures and time steps. Also notice that the pH values are higher for all samples using the Montbrite 1240 method. If this is due to the production of sodium metaborate as claimed, this could prove to be a welcomed side effect as sodium metaborate has shown some helpful qualities with respect to polymer stability (Flaaten et al, 2008 and Levitt and Pope, 2008). With the added benefit that Montbrite 1240 is a much safer method to produce dithionite, this should quiet concerns over the use of dithionite in the field.

Effectiveness of Sodium Bisulfite as an Oxygen Scavenger

Sodium (or ammonium) bisulfite is the most widely used oxygen scavenger in the field. This is because it has been used for many years and it is much safer to handle than sodium dithionite. The problem with bisulfite is that it requires a transition metal in order to scavenge oxygen from solution. In addition, it is not a reducing agent. An experiment was designed to test the hypothesis that use of bisulfite and the subsequent exposure to iron will not protect the polymer from degradation. 2500 ppm 3630 in 3 wt% NaCl was dosed with 100 ppm bisulfite. Additionally, 2 ppm Fe^{++} as sulfate was added prior to sealing ampoules and aging. The results for this experiment are shown in Table 5.7 and Figure 5.25.

The viscosity of the polymer was not significantly affected by using bisulfite instead of dithionite. This was unexpected as DO was still detected for some time after

sealing. One explanation could be that based on the redox potential measurements, is that there is simply not enough iron in solution to redox cycle. This is because the dominant species at an $E_{\text{Ag/AgCl}} \sim 100$ mV would be Fe^{+++} and the solubility of Fe^{+++} in water is extremely low. More work needs to be conducted by simulating what would actually occur in the field, which is continuous exposure to fluids at a reduced state.

5.4 OBSERVATIONS FROM THE FIELD

Two field injections at low temperature were observed in which source brines from an aquifer originally containing between 0.3 and 0.5 ppm of iron were used to hydrate polymer powder in a hydration system open to the atmosphere. In order to support iron concentrations this high, the brines were necessarily in a somewhat reduced state and oxygen free to begin with. In one case, the brine was inadvertently aerated as sodium chloride was added in order to adjust the salinity to optimal for a surfactant injection before polymer was added using a wetting head. As polymer left the hydration tank, sodium dithionite was slipstreamed into the polymer so that the subsequent contact with iron would not cause polymer degradation. In a second case, in which starting E_{H} was measured around 0 V, polymer was added to the brine as it arrived from a distribution system to a wetting cone, which was the first significant exposure the water had to the atmosphere. In both cases the polymer was then stirred in a hydration tank for around an hour, and samples were taken in order to observe viscosity and filtration behavior prior to injection.

The polymer solution that had been aerated before the addition of polymer had a viscosity that was constant over the course of several hours and comparable to measurements made under laboratory conditions. Conversely, the polymer hydrated in a still-reduced brine had around half of the viscosity of a similar solution prepared in the

laboratory, and viscosity continued to drop at such a rate that filtration tests were impossible because of the extent of degradation over the course of the ten-minute test. These observations prompted an unorthodox question: in situations where a polymer hydration or dilution brine is in reduced conditions, contains a significant amount of iron, and where subsequent exposure to oxygen is unavoidable, might it be better to aerate brine prior to the addition of polymer in order to avoid later degradation?

Results testing this hypothesis are given in Figures 5.26 and 5.27. In Figure 5.26, polymer is allowed to hydrate in the presence of oxygen in source water laden with iron (without pre-aeration). The two lines represent estimated polymer concentrations. As is shown, as much as 42 % of viscosity is lost after just 2 hours of mixing. Figure 5.27 gives results of the test where source brine was allowed to aerate prior to polymer hydration for increasing time. The results show that the longer that iron-laden source water is allowed to aerate, the less degradation occurs.

In this case attention would still need to be given to ensure degradation did not occur immediately as oxygenated polymer encountered an iron-bearing formation. For instance, sodium dithionite could be slipstreamed into the polymer as mentioned above.

5.5 DISCUSSION

Carbonate and bicarbonate ions have been shown to have been a hidden factor in degradation experiments involving the addition of sodium dithionite to polymer solutions without the exclusion of oxygen. A commercial HPAM polymer (Flopaam 3630S) has been shown to be stable in the presence of ferrous iron in the absence of oxygen.

The sensitivity study on polymer stability with respect to sodium dithionite produced some interesting results. After exposure to oxygen, a polymer's degree of hydrolysis plays a role in amount of degradation when dithionite is present. Delayed

exposure to oxygen seems to have no effect on the level of degradation. The rapid cessation of degradation when DTPA is present, which can be explained by the chelator's ability to prevent further redox cycling of iron, supports the theory that redox cycling of trace amounts of iron play a decisive role in the degradation of the polymer backbone.

Aqueous solutions of sodium borohydride (Montbrite 1240) mixed with sodium bisulfite to produce sodium dithionite and sodium metaborate has proven to be a superior method to that of the traditional use of powder sodium dithionite. The degradation experienced is equivalent, but the benefit that it is much safer to handle than powder makes it the preferred choice in the field as an oxygen scavenger.

The results of the experiment with sodium bisulfite as an oxygen scavenger are puzzling. It is apparent that the experiment was not a good representation of what would occur in the field, which would be a non-reduced solution continuously encountering reduced fluids, so further tests should be conducted with this in mind.

Exposing reduced brines to oxygen as polymer is hydrated or afterwards risks serious degradation to the polymer, even when iron concentrations are less than 1 ppm. One method to mitigate this is oxygenation of the brine before polymer is added, however care must be taken to ensure subsequent degradation is not caused by the injection of a polymer solution containing oxygen into a formation containing iron.

Table 5.1: Yang and Treiber's Brine Composition (Yang and Treiber (1985))

Component	Concentration
NaHCO ₃	365 ppm
MgCl ₂ * 7 H ₂ O	231 ppm
CaCl ₂ * 2 H ₂ O	279 ppm
Na ₂ B ₄ O ₇ * 10 H ₂ O	7 ppm

Table 5.2: Shupe's Brine Composition (Shupe (1981))

Component	Concentration
NaCl	2052 ppm
NaHCO ₃	1313 ppm
Na ₂ CO ₃	248 ppm*
*additional 100 ppm of sodium carbonate thought to be present in Shupe's polymer stock based upon analysis by Kheradmand	

Table 5.3: Aging data from 2500 ppm 3630S in 3 wt% NaCl with 100 ppm dithionite from powder

	Viscosity	DO	E _{Ag/AgCl}	pH	notes
	(cP)	(ppb)	(mV)		
	Initial Measurements				
before dithionite	42.33	3000	38.3	6.26	
last ampoule	39.07	0	-340.8	5.99	
	2 day				
23 C	38.13	0	-370	5.96	
62 C	37.65	0	-233	6.03	
85 C	25.57	7.5	-123	6.19	possible leak
100 C	19.54	50	-79	6.5	possible leak
	14 day				
23 C	35.87	0	-150	5.87	
62 C	38.36	0	-149.1	6.31	
85 C	39.25	0	-162.2	6.47	
100 C	41.56	0	-201.6	6.98	
	60 day				
23 C	38.42	0	-190.6	5.94	
62 C	37.24	0	-183.7	6.22	
85 C	42.27	0	-128.3	6.64	
100 C	38.72	0	-255.6	7.1	

Table 5.4: Aging data from 2500 ppm 3630S in 3 wt% NaCl with 100 ppm dithionite from Montbrite 1240

	Viscosity	DO	$E_{Ag/AgCl}$	pH	notes
	(cP)	(ppb)	(mV)		
	Initial Measurements				
before dithionite	40.85	6000	33.9	6.31	
last ampoule	42.33	0	-500	6.8	
	2 day				
23 C	39.31	0	-370	6.73	
62 C	25.16	0	-50.6	6.59	
85 C	40.32	0	-297.3	7.03	possible leak
100 C	42.98	0	-300	7.63	possible leak
	14 day				
23 C	40.26	0	-388	6.8	
62 C	39.01	0	-234.4	7.13	
85 C	40.43	0	-260.7	7.49	
100 C	47.36	0	-268.9	7.62	
	60 day				
23 C	39.90	0	-287.8	6.77	
62 C	44.10	0	-290.2	7.31	
85 C	48.54	0	-318.6	7.46	
100 C	42.27	0	-292.5	7.32	

Table 5.5: Synthetic Field Brine Composition

Component	Concentration
NaHCO_3	236 ppm
$\text{MgCl}_2 \cdot 7 \text{H}_2\text{O}$	204 ppm
$\text{CaCl}_2 \cdot 2 \text{H}_2\text{O}$	201 ppm
Na_2SO_4	111 ppm

Table 5.6: Aging data from 2500 ppm 3330S in synthetic field brine with 100 ppm dithionite from Montbrite 1240 and 2 ppm Fe⁺⁺

	Viscosity	DO	E _{Ag/AgCl}	pH	notes
	(cP)	(ppb)	(mV)		
	Initial Measurements				
before dithionite	125.8	4000	35.8	7.35	
last ampoule	116.92	0	-420	7.33	
	2 day				
23 C	116.33	0	-450	7.35	
85 C	98.57	0	-301	8.18	possible leak
100 C	115.74	0	-328	8.56	possible leak
	14 day				
23 C	114.85	0	-562.3	7.37	
85 C	126.39	0	-311.4	8.44	
100 C	163.98	0	-282.7	8.45	
	60 day				
23 C	109.52	0	-417.3	7.7	
85 C	143.56	0	-320.9	8.69	
100 C	164.87	0	-234.6	8.64	

Table 5.7: 2500 ppm 3630S in 3 wt% NaCl with 100 ppm bisulfite and 2 ppm Fe⁺⁺ as sulfate data

	Viscosity	DO	E _{Ag/AgCl}	pH	notes
	(cP)	(ppb)	(mV)		
	Initial Measurements				
before bisulfite	42.33				
last ampoule	37.89	>100	100	5.73	
bisulfite stock after 2 hrs mixing			100		
	2 day				
23 C	37.30	>100	99	5.68	
62 C	34.22	>100	87.7	5.7	
85 C	14.09	>>100	110.5	5.39	possible leak
100 C	31.20	40	79.3	6.15	
	14 day				
23 C	35.05	15	90.1	5.56	
62 C	35.1	10	78.2	5.99	
85 C	36.53	5	65.4	6.18	
100 C	41.4	0	25.1	6.73	
	60 day				
23 C	36.47	5	46.8	5.6	
62 C	31.73	0	-70.9	5.92	
85 C	30.96	2	-69.7	6.25	
100 C	33.09	0	-170.3	6.84	

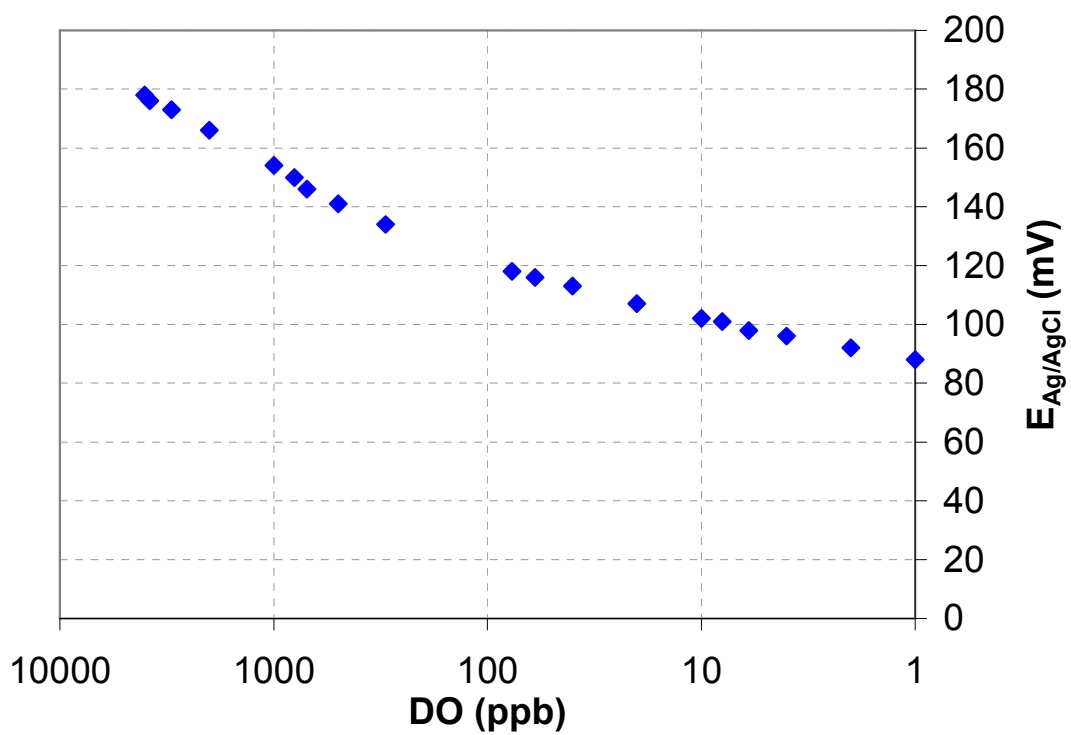


Figure 5.1: $E_{Ag/AgCl}$ as a function of DO in deionized water (DI) at 23 C

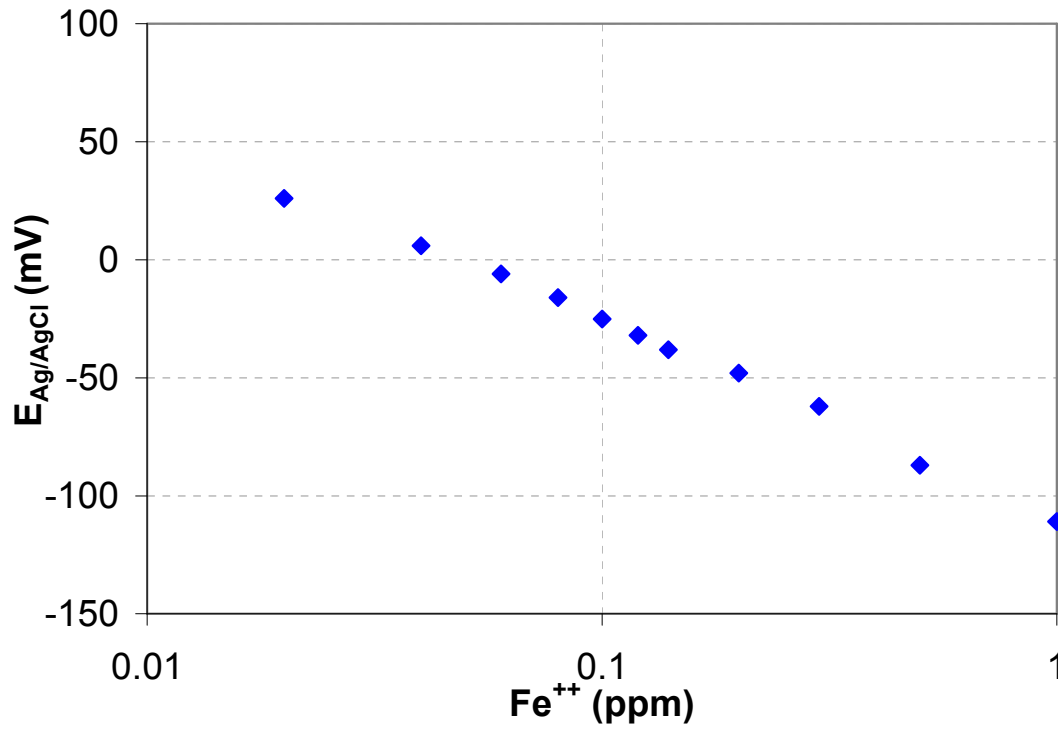


Figure 5.2: $E_{\text{Ag/AgCl}}$ as a function of $[\text{Fe}^{++}]$ in DI, 23 C

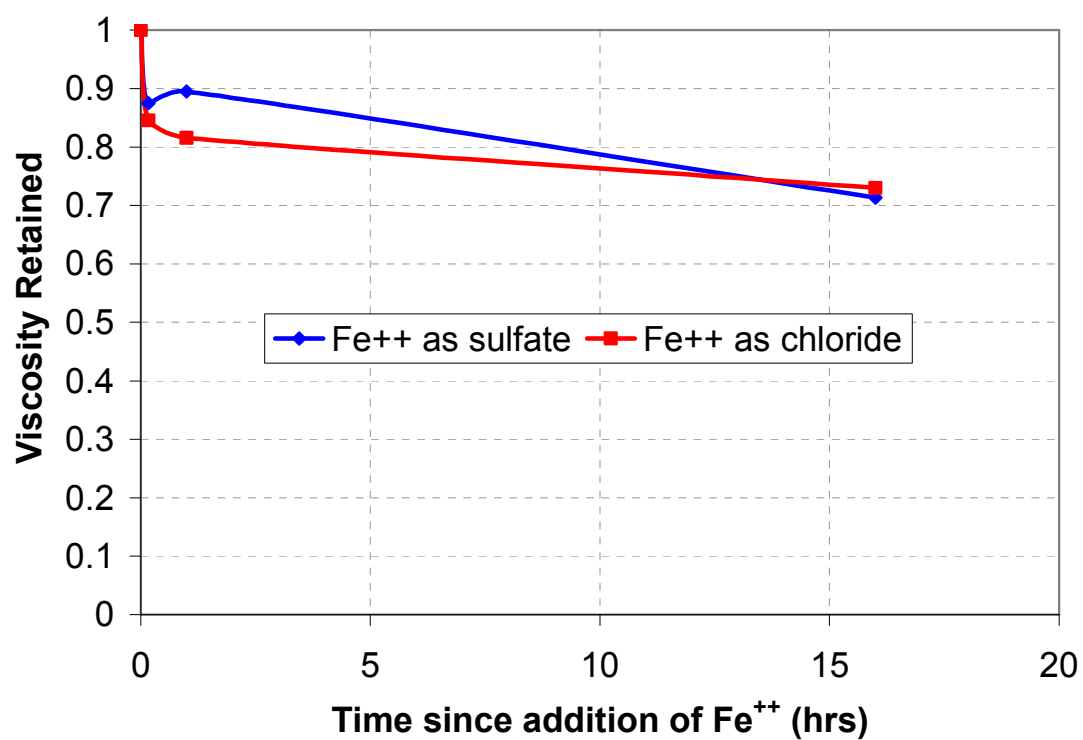


Figure 5.3: 2500 ppm 3630S in 3% NaCl with 2 ppm Fe⁺⁺ and a slow continuous supply of O₂

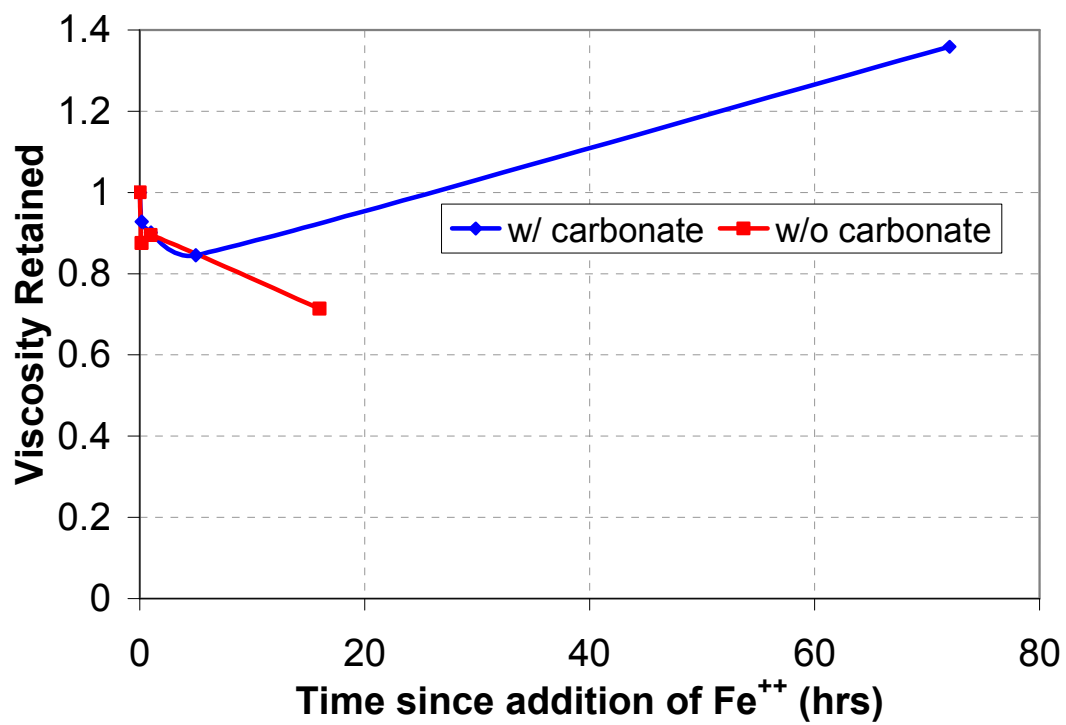


Figure 5.4: 2500 ppm 3630S in 3% NaCl and Yang and Treiber's brine with 2 ppm Fe^{++} and a slow continuous supply of O_2

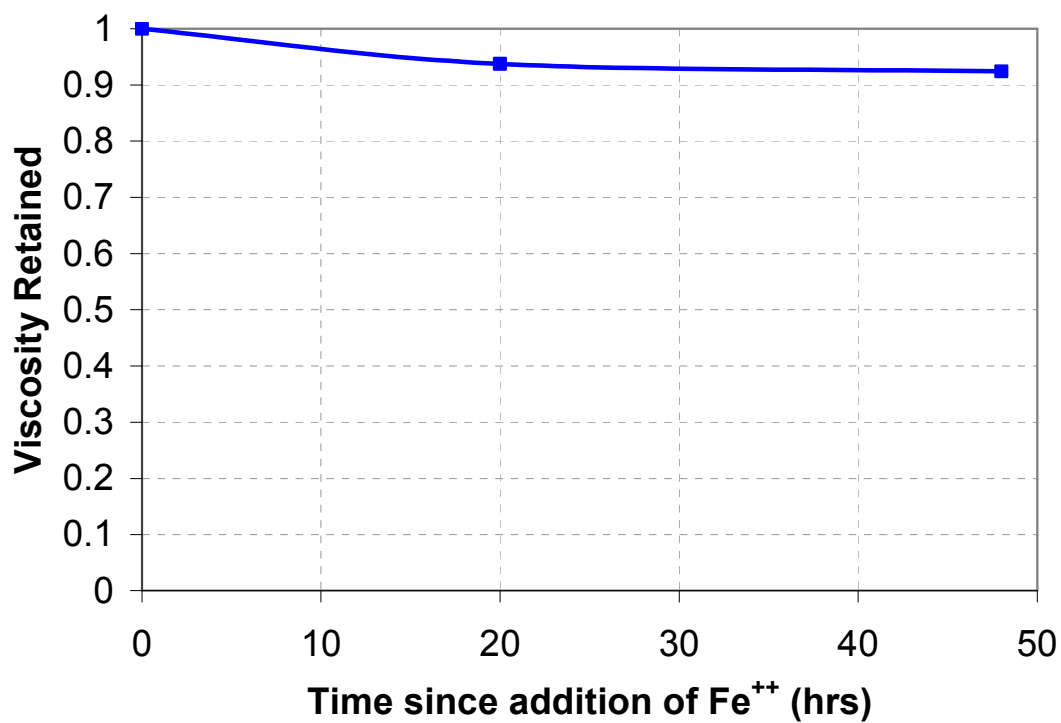


Figure 5.5: 2500 ppm 3630S in 3% NaCl and Yang and Treiber's brine with 2 ppm Fe^{++} and an initial small amount of O_2 (30 ppb) and no more exposure to O_2

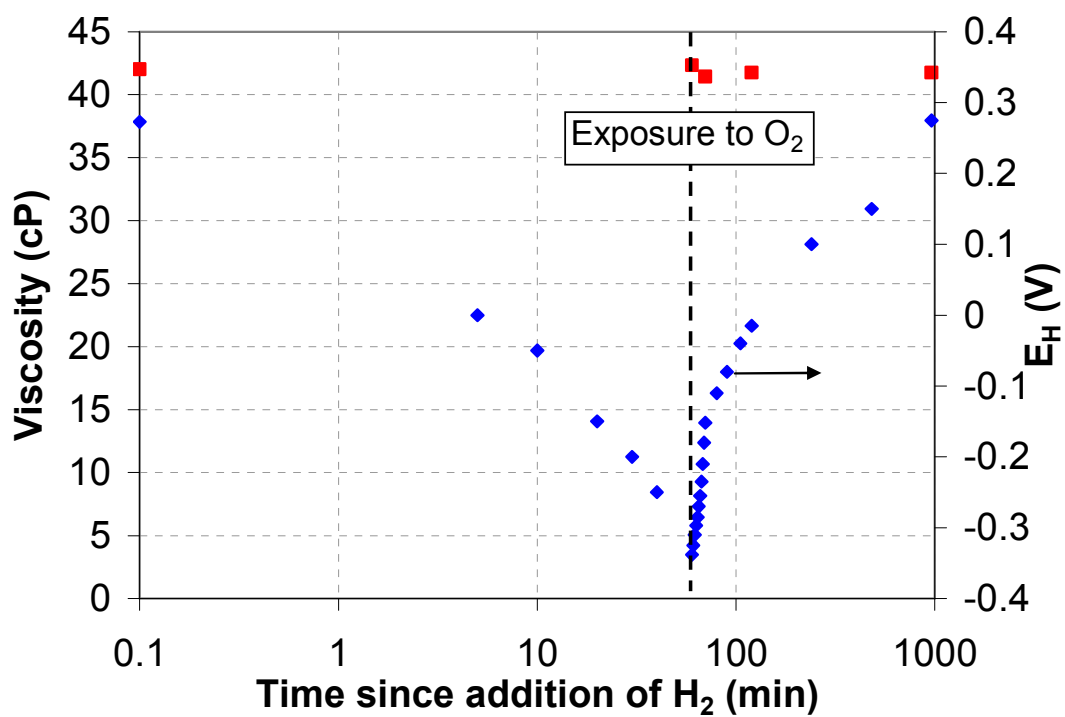


Figure 5.6: 2500 ppm 3630S in 3% NaCl reduced with H₂ then exposed to O₂

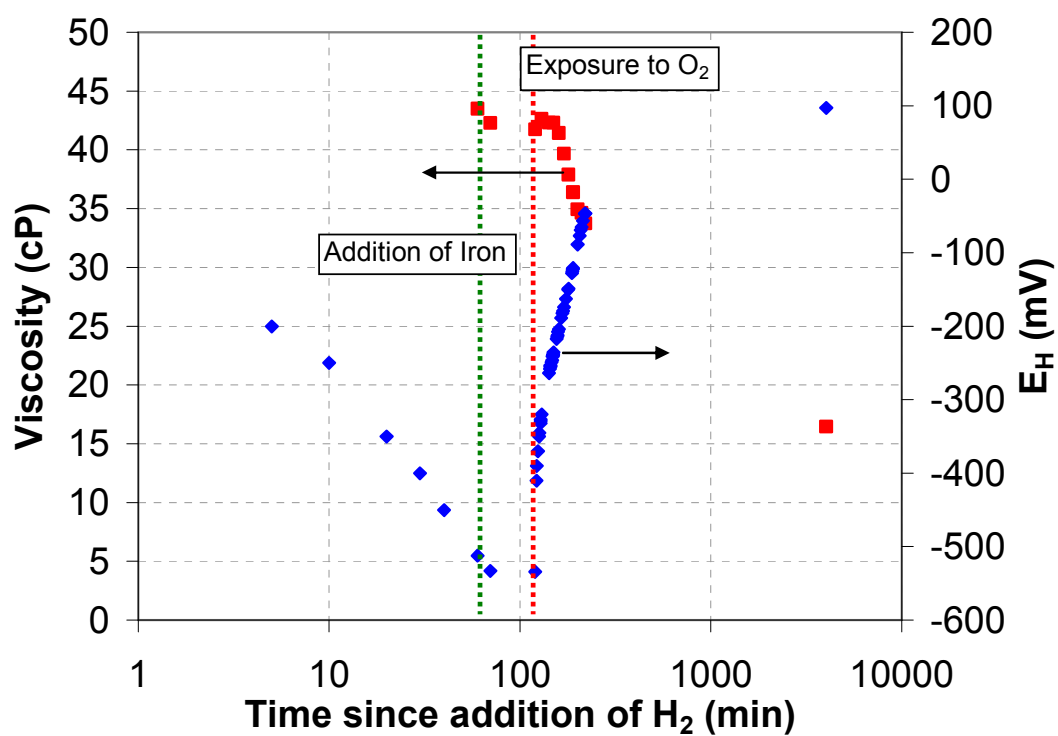


Figure 5.7: 2500 ppm 3630S in 3% NaCl reduced with H₂, dosed with 2 ppm Fe⁺⁺ then exposed to O₂

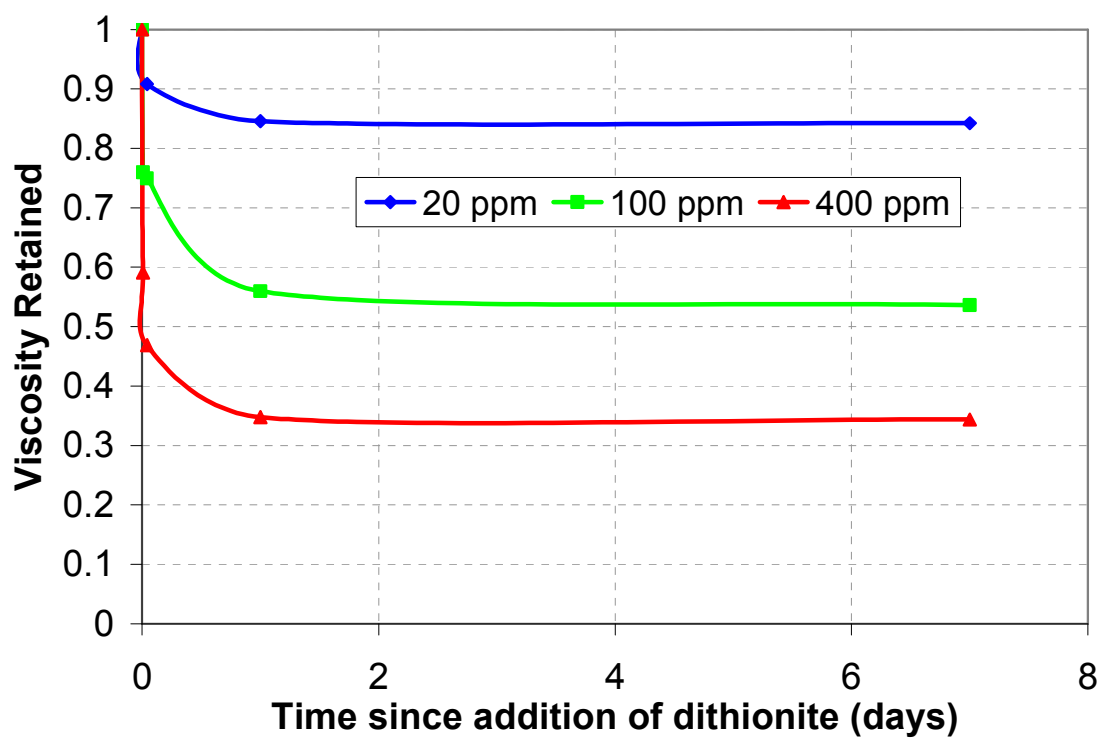


Figure 5.8: Effect of amount of dithionite on 2500 ppm 3630S in 3 wt% NaCl when exposed to O₂

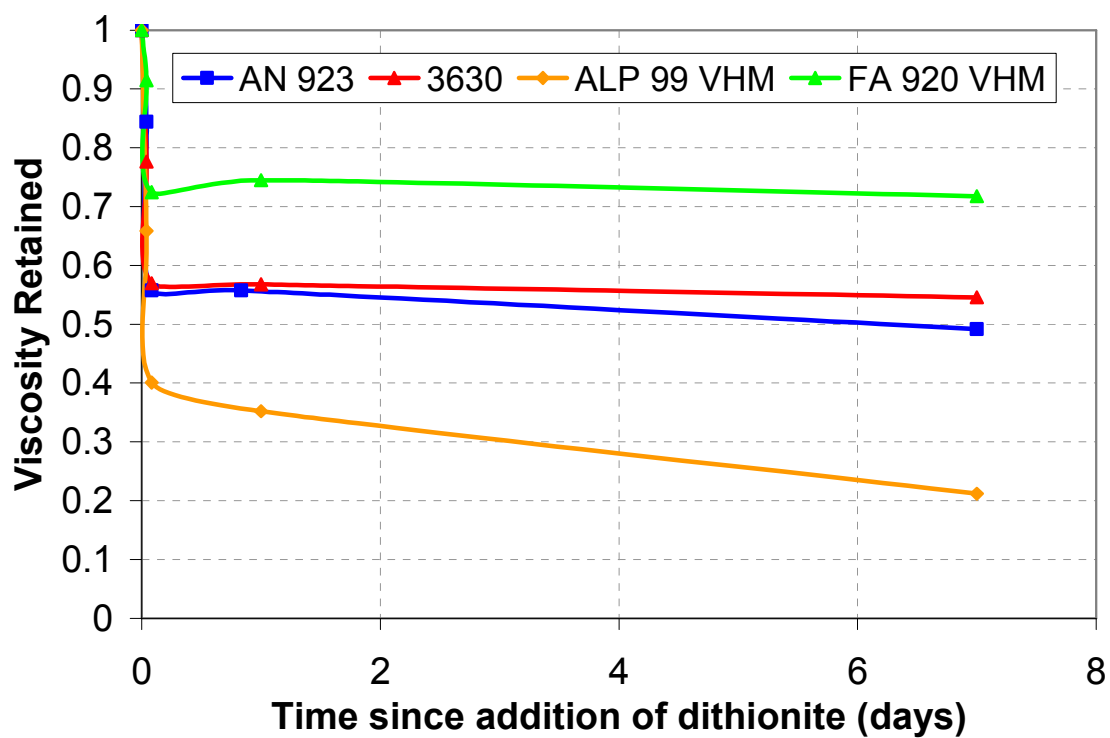


Figure 5.9: Effect of degree of hydrolysis on polymer stability when reduced with 100 ppm dithionite and exposed to O₂

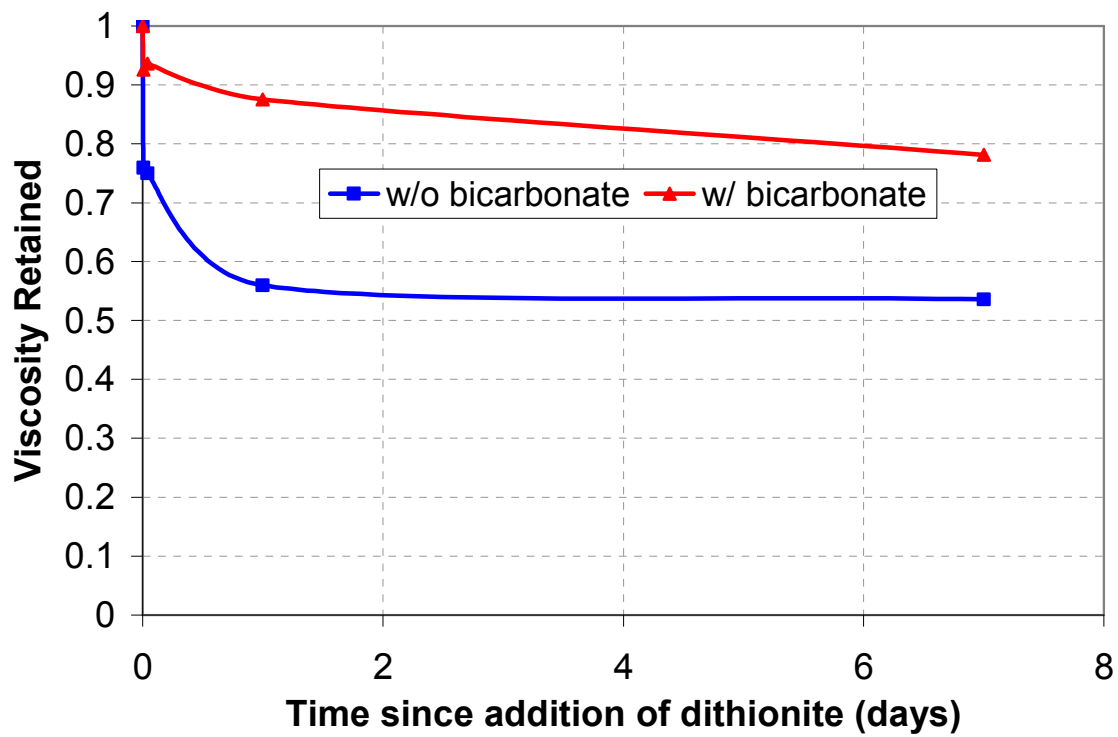


Figure 5.10: Effect of bicarbonate (as seen in Shupe (1981) brine) on 2500 ppm 3630S in 3 wt% NaCl reduced with 100 ppm dithionite and exposed to O₂

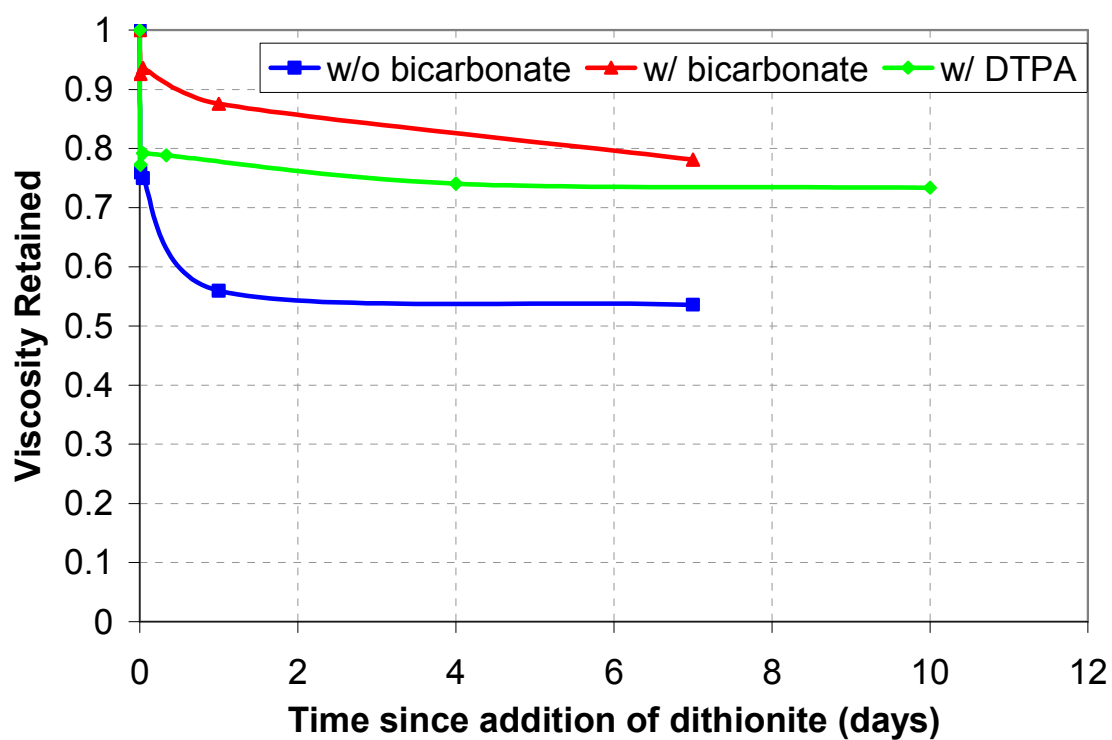


Figure 5.11: Effect of DTPA on 2500 ppm 3630S in 3 wt% NaCl when dosed with 100 ppm dithionite and exposed to O₂

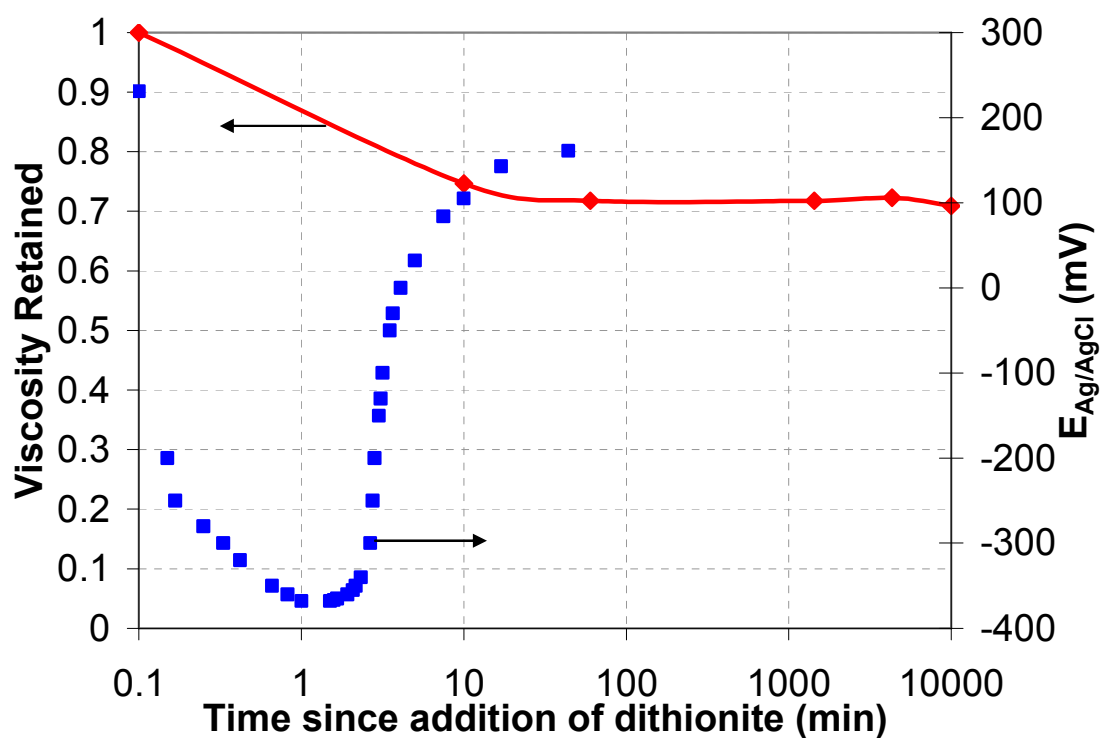


Figure 5.12: $E_{Ag/AgCl}$ and viscosity of 2500 ppm FA 920 SH in 3 wt% NaCl reduced with 100 ppm dithionite and exposed to O_2

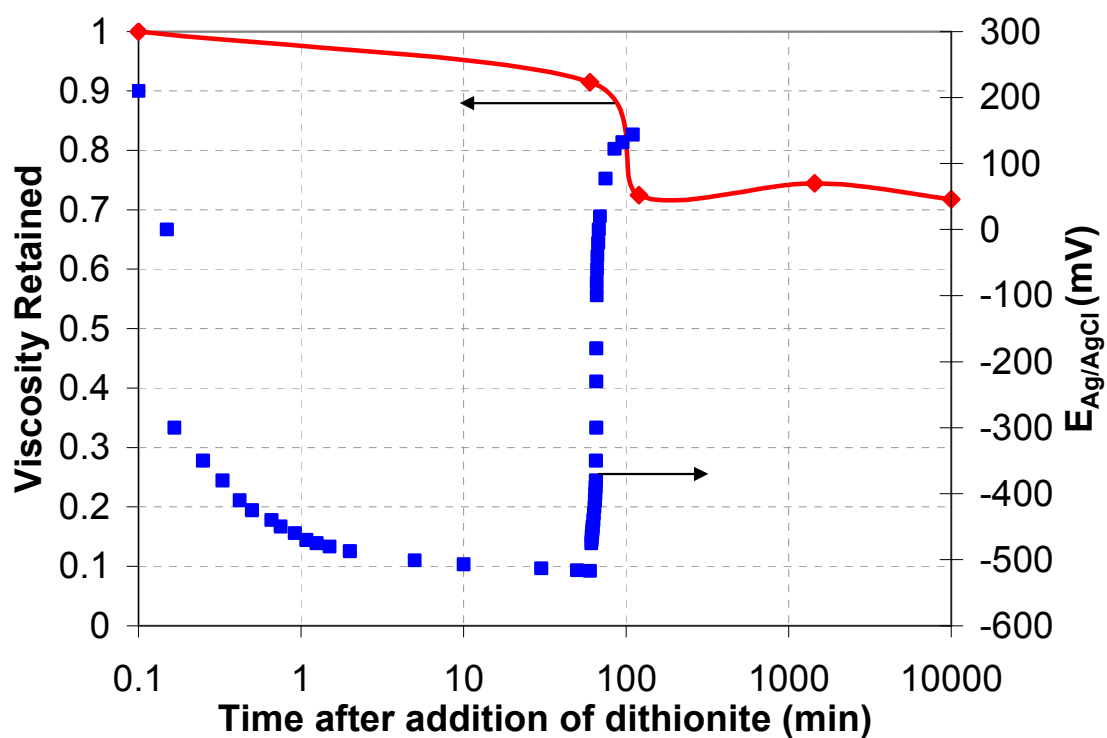


Figure 5.13: $E_{Ag/AgCl}$ and viscosity of 2500 ppm FA 920 SH in 3 wt% NaCl reduced with 100 ppm dithionite initially under N_2 then exposed to O_2

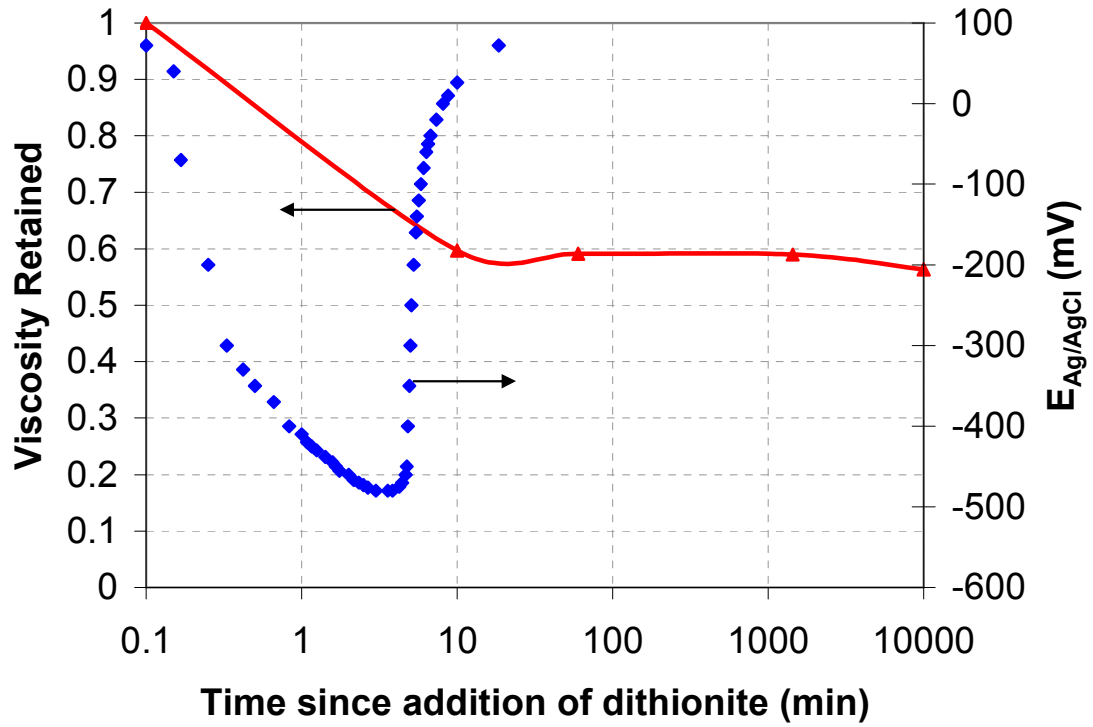


Figure 5.14: $E_{Ag/AgCl}$ and viscosity of 2500 ppm 3630S in 3 wt% NaCl reduced with 100 ppm dithionite and exposed to O_2

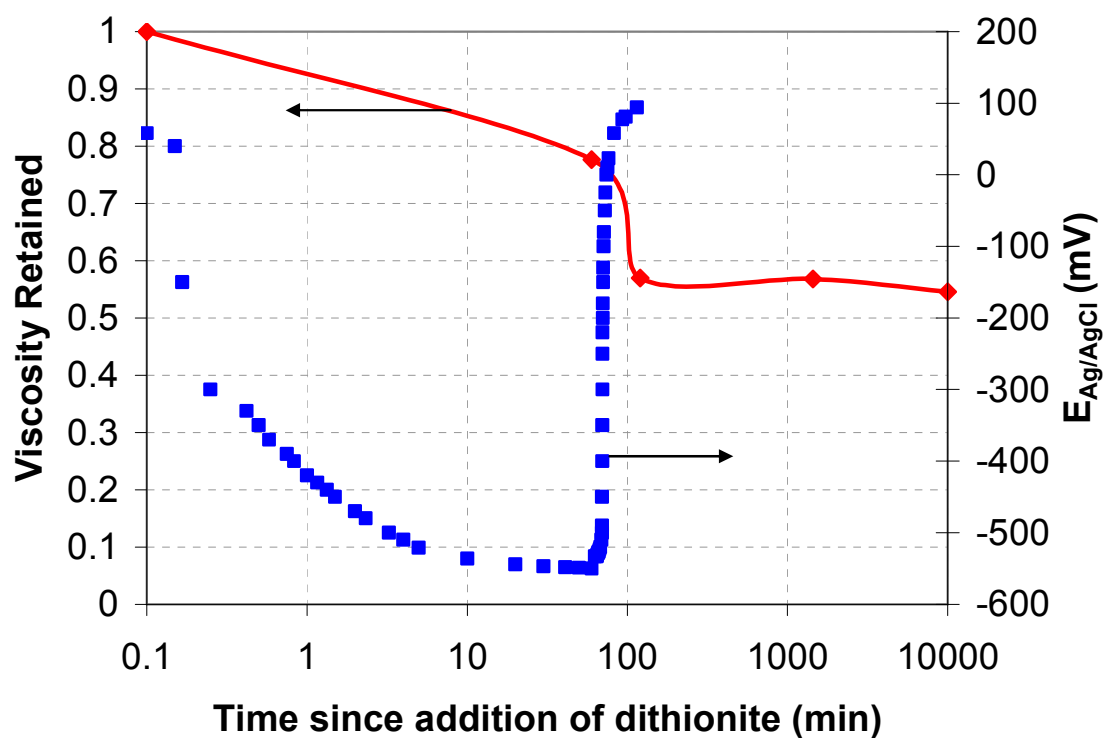


Figure 5.15: $E_{Ag/AgCl}$ and viscosity of 2500 ppm 3630S in 3 wt% NaCl reduced with 100 ppm dithionite initially under N_2 then exposed to O_2

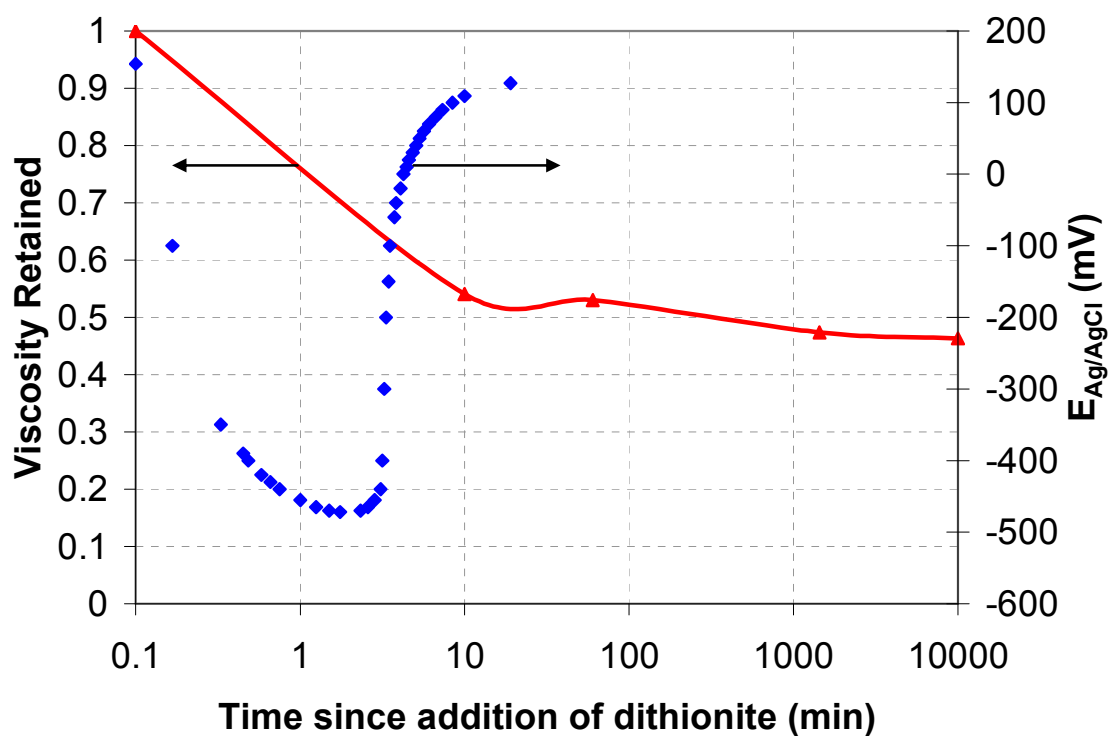


Figure 5.16: $E_{Ag/AgCl}$ and viscosity of 2500 ppm AN 923 in 3% NaCl reduced with 100 ppm dithionite and exposed to O_2

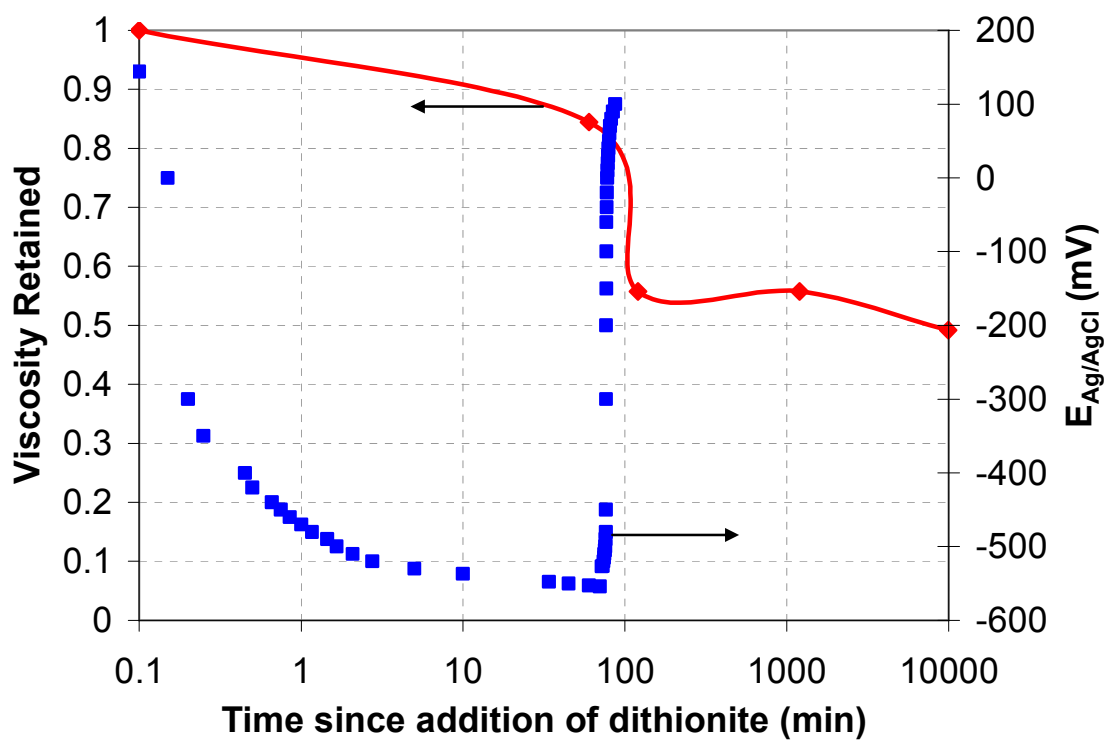


Figure 5.17: $E_{Ag/AgCl}$ and viscosity of 2500 ppm AN 923 in 3 wt% NaCl reduced with 100 ppm dithionite initially under N_2 then exposed to O_2

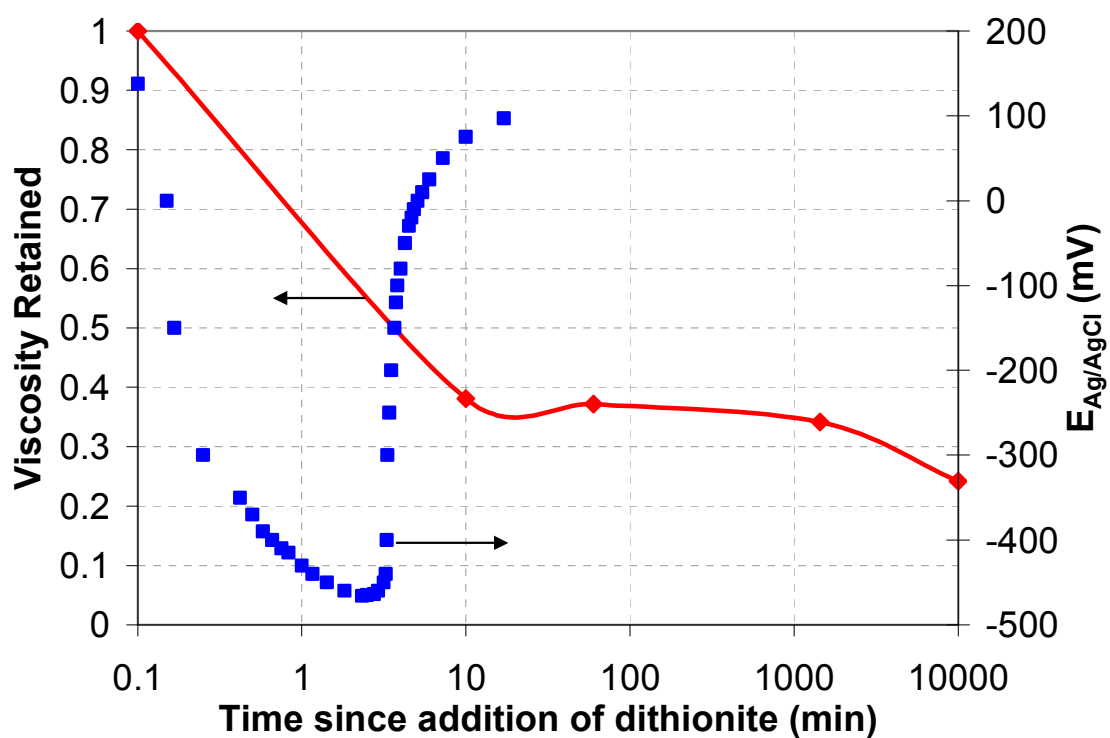


Figure 5.18: $E_{Ag/AgCl}$ and viscosity of 2500 ppm ALP 99 in 3% NaCl reduced with 100 ppm dithionite and exposed to O_2

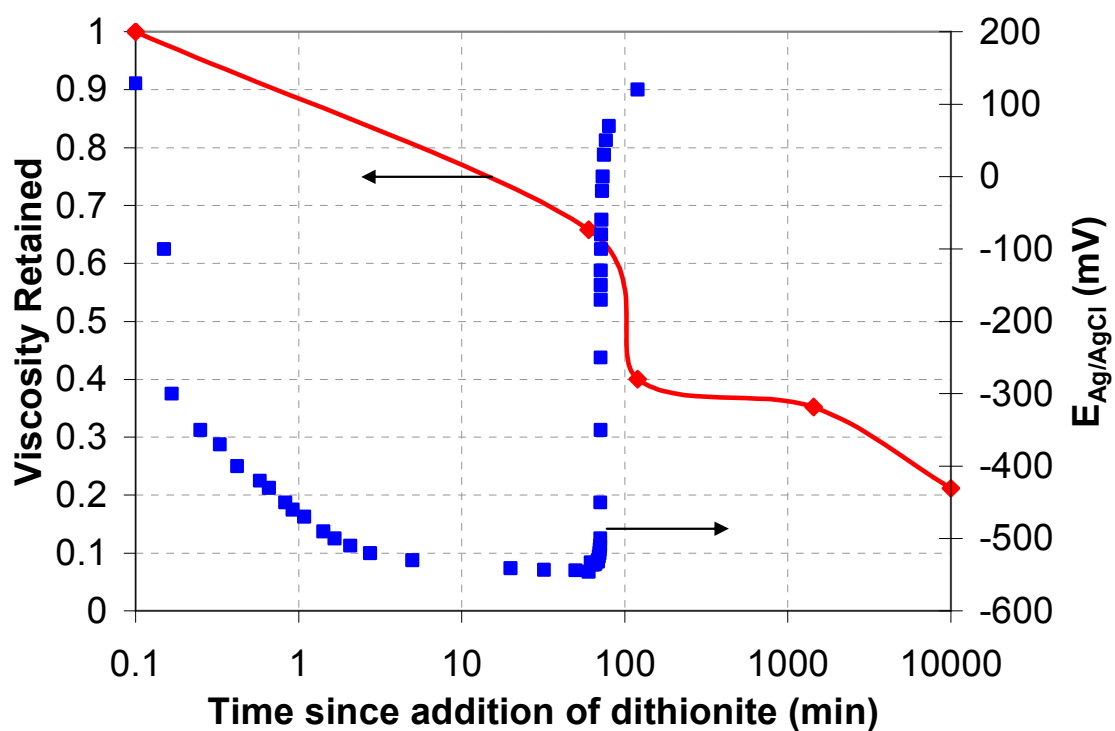


Figure 5.19: $E_{Ag/AgCl}$ and viscosity of 2500 ppm ALP 99 in 3 wt% NaCl reduced with 100 ppm dithionite initially under N_2 then exposed to O_2

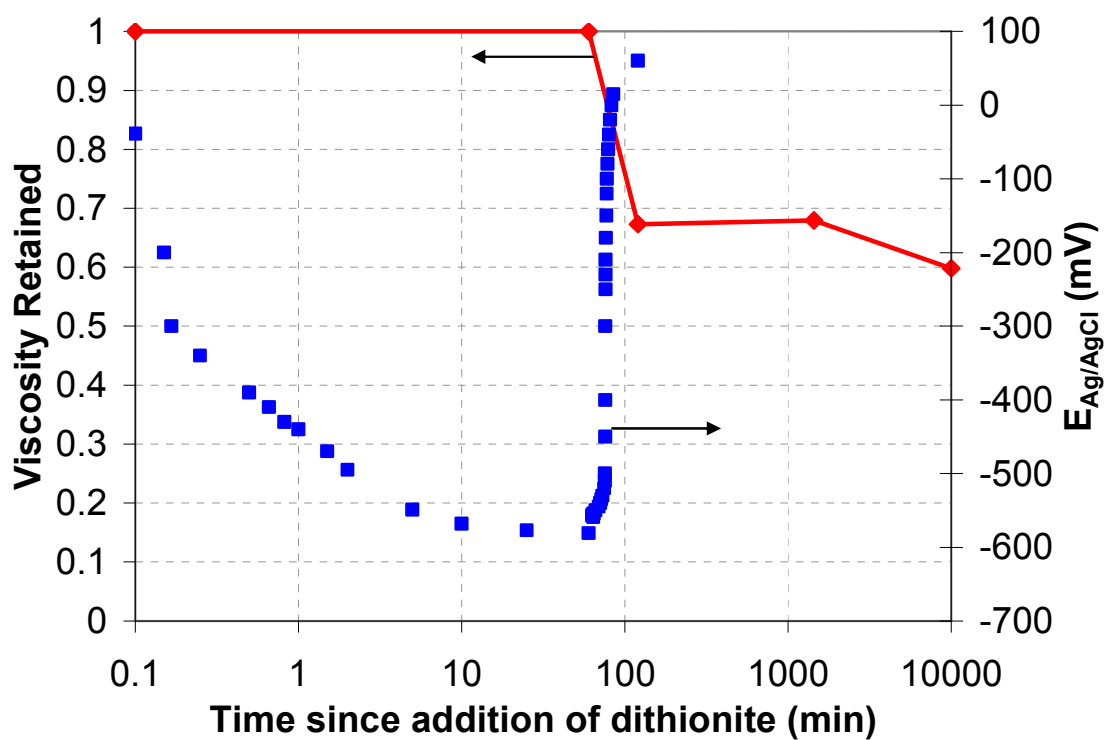


Figure 5.20: $E_{Ag/AgCl}$ and viscosity of 2500 ppm 3630S in 3 wt% NaCl deoxygenated then reduced with 100 ppm dithionite initially under N_2 then exposed to O_2

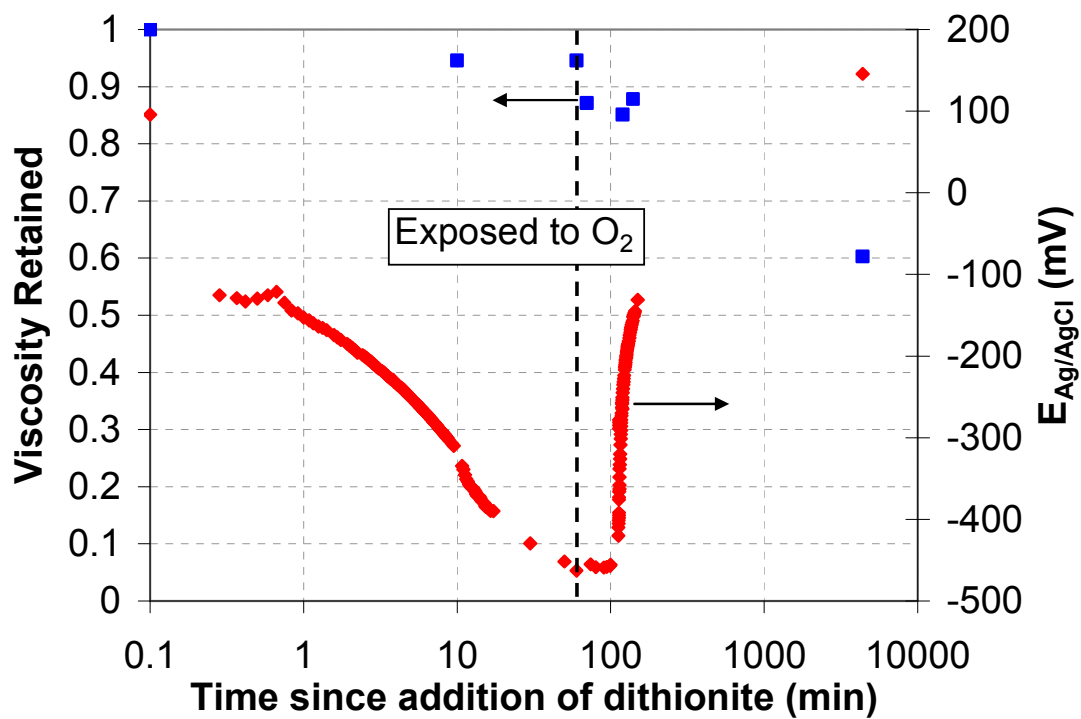


Figure 5.21: $E_{Ag/AgCl}$ and viscosity of 2500 ppm 3630S in 3% NaCl reduced with dithionite (using Montbrite 1240) initially under Ar then exposed to O_2

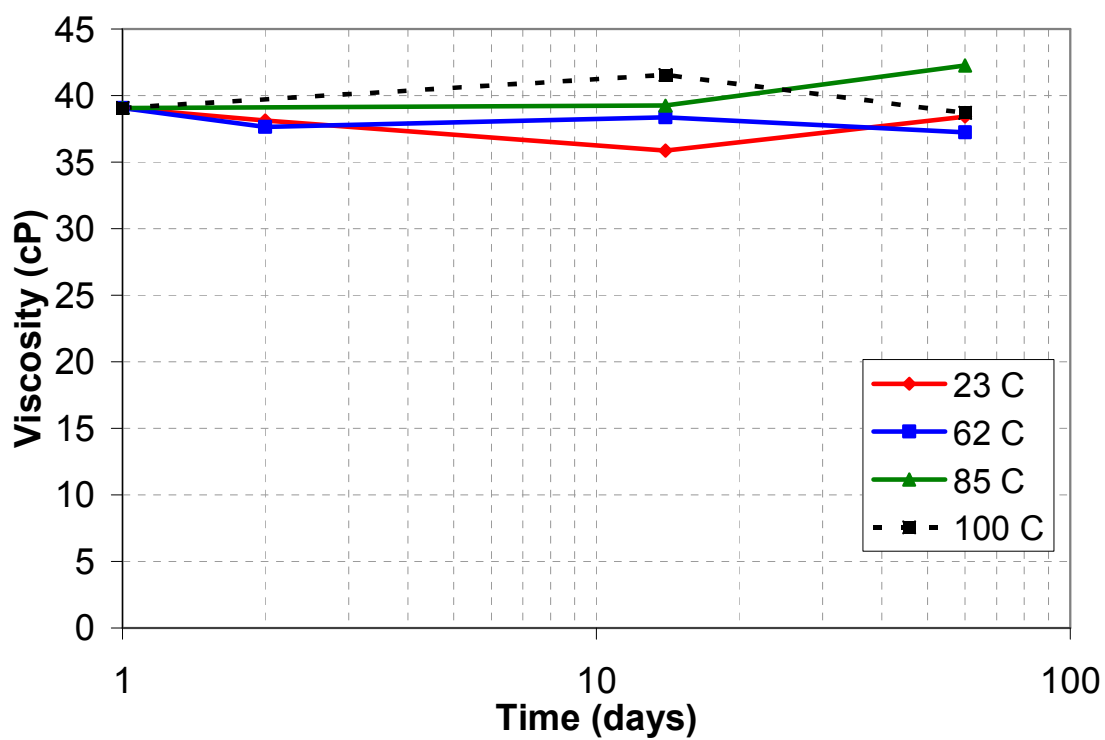


Figure 5.22: 2500 ppm 3630S in 3% NaCl reduced with dithionite (using powder) viscosity data for aged samples at various temperatures

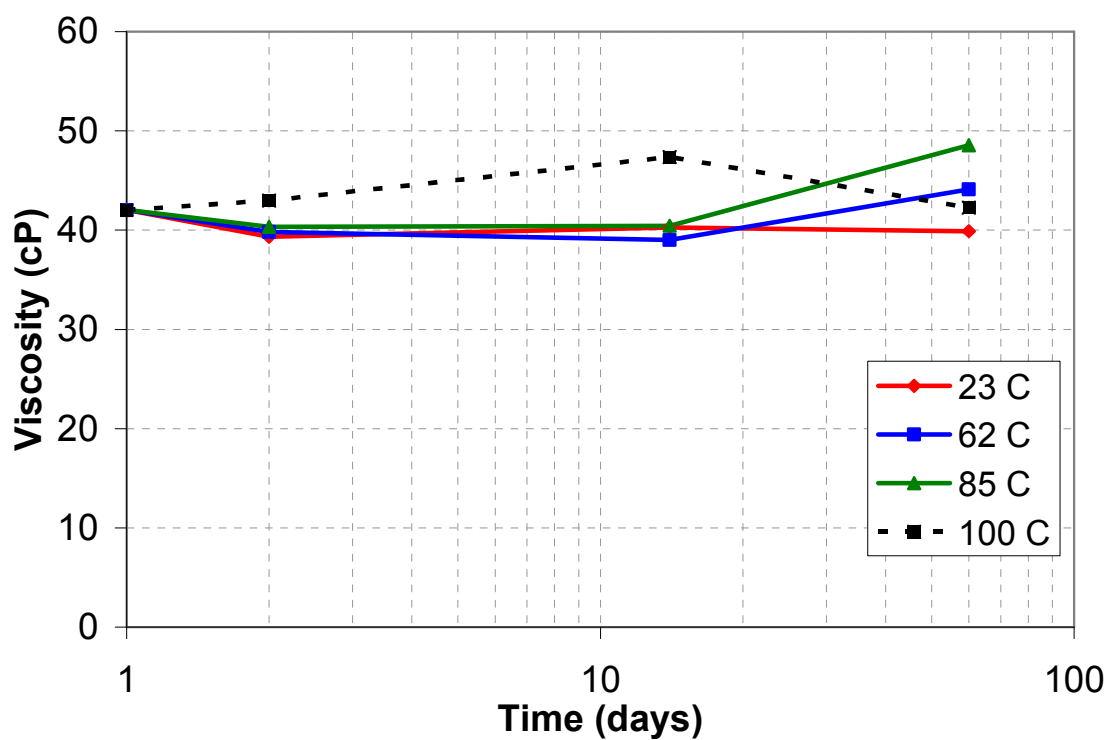


Figure 5.23: 2500 ppm 3630S in 3% NaCl reduced with dithionite (using Montbrite 1240) viscosity data for aged samples at various temperatures

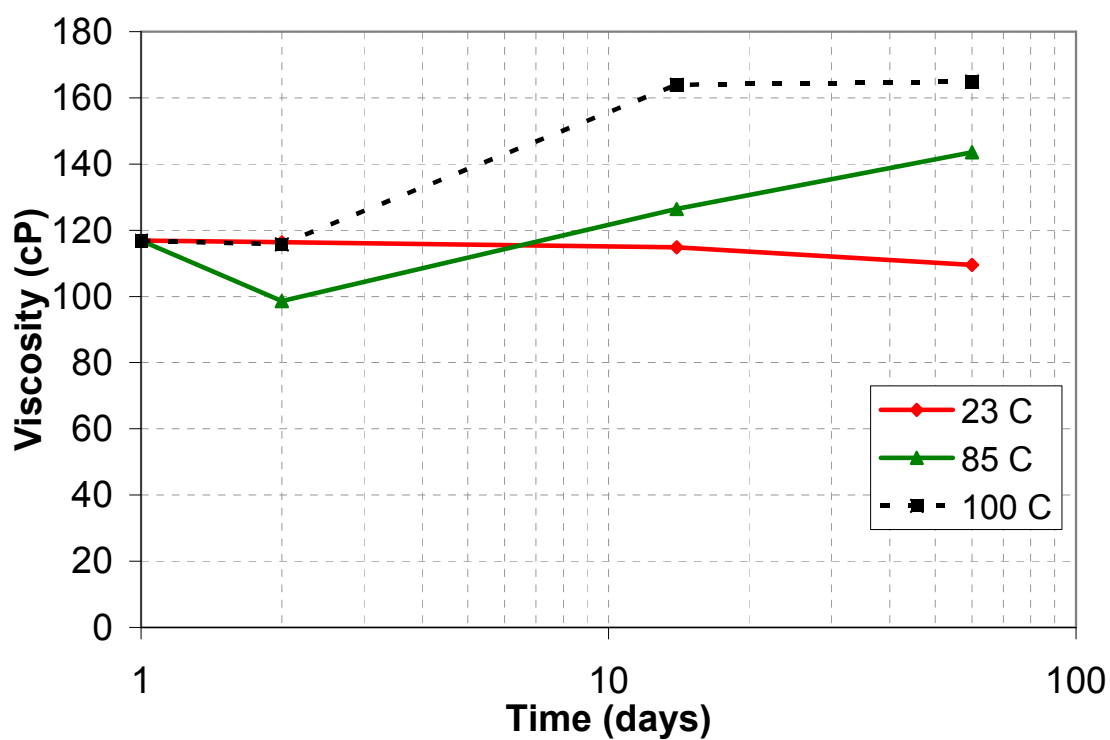


Figure 5.24: 2500 ppm 3330S in synthetic brine with 100 ppm dithionite (using Montbrite 1240) and 2 ppm Fe^{++} viscosity data for aged samples at various temperatures

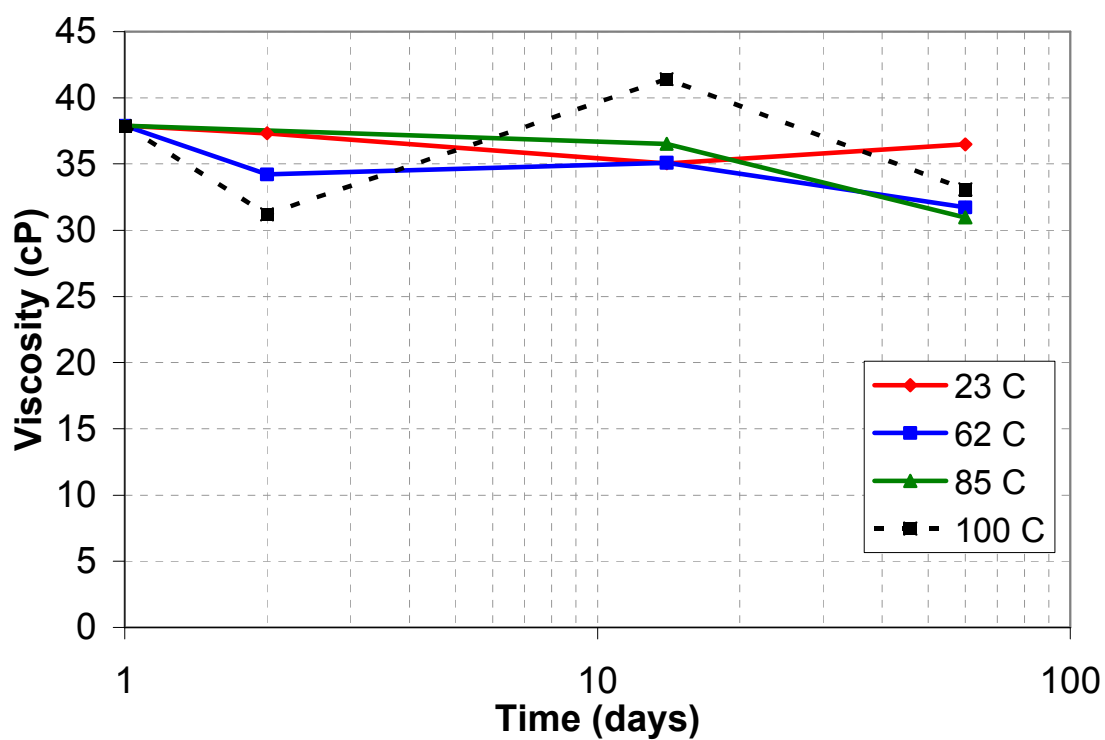


Figure 5.25: 2500 ppm 3630S in 3% NaCl with bisulfite and 2 ppm Fe^{++} viscosity data for aged samples at various temperatures

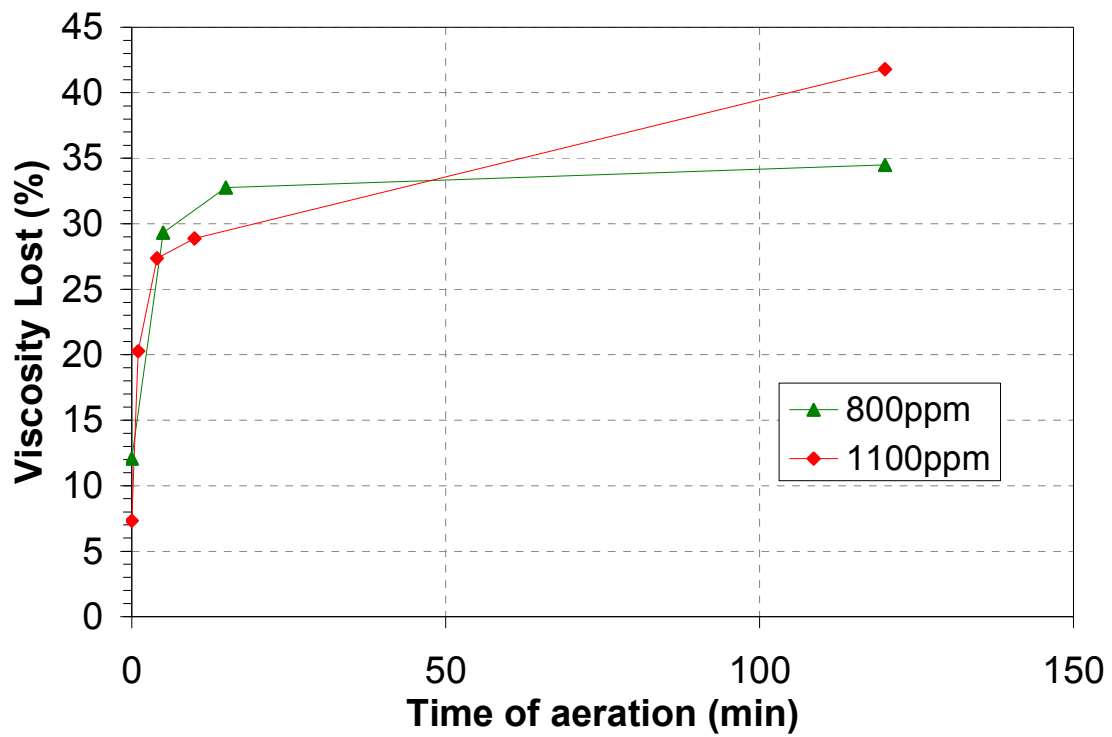


Figure 5.26: Degradation experienced in the field when iron-laden source water is allowed to aerate after addition of polymer, 2 different polymer concentrations

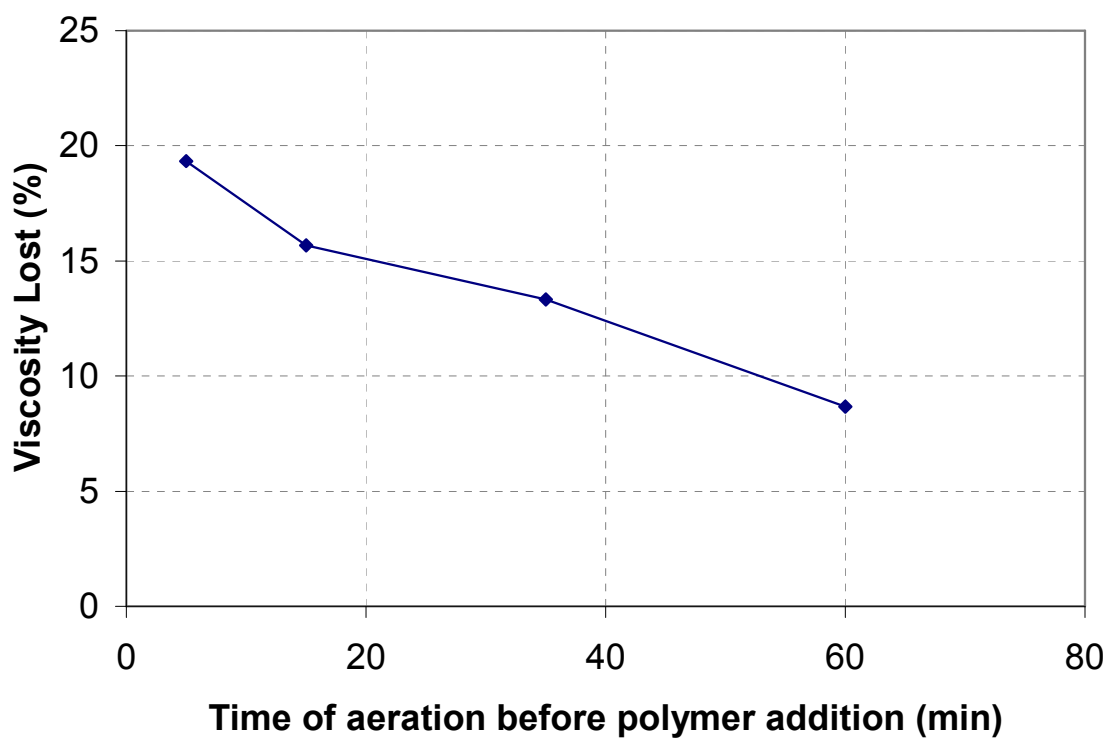


Figure 5.27: In the case where contact with air during polymer hydration is unavoidable, degradation is lower if source brine is aerated prior to addition of polymer

CHAPTER 6: COREFLOODING RESULTS & DISCUSSION

6.1 POLYMER INJECTIVITY TESTS

Whenever a new reservoir is evaluated in the lab, it is always a good to start the coreflooding process with some polymer injectivity tests. This is especially true for low permeability reservoirs such as the case presented here. Polymer injectivity tests are relatively quick, can save time, and help to develop an optimum coreflood.

Many times, a surrogate rock, such as Berea sandstone or Texas cream limestone, will be used initially to develop a chemical formulation that works in order to conserve reservoir rocks. However, reservoir core plugs were used for all coreflooding tests for this research. A list of the porosity (ϕ) and air permeability (k_{air}) of all the available core plugs is detailed in Table 6.1. Reservoir rock and fluid properties are listed in Table 6.2. All corefloods were conducted at reservoir temperature, 69 C.

The results discussed here are from the successful injectivity tests. The results from the first few experiments are outlined in Appendix A. Previous cores seemed to be plugging at the face based upon a comparison of the pressure drop across the first and second half of the cores. The plugging was initially attributed to the polymer, but the same behavior was seen later with brine only before any polymer was injected into a new core, so we changed from Nylon tubing and stainless steel valves to Teflon tubing and inert plastic valves in an attempt to prevent the problem. Brine was then injected into a core for many pore volumes without any plugging.

High Salinity Polymer Injection

As can be seen in Table 6.3, two possible sources of injection water existed for this particular reservoir. Since polymer properties vary greatly between the two salinities, it was necessary to conduct injectivity tests at both salinities. The synthetic softened high salinity brine (SSHSB) was used instead of the synthetic hard high salinity brine (SHHSB) in order to simplify the procedure. Core plug #332 was chosen and initially saturated with the SSHSB. Figure 6.1 shows the pressure drop for the brine flood. The brine permeability (k_{brine}) was determined to be 3.1 md and the pore volume (PV) was determined to be 11.2 mL.

SNF's AN 125 VLM, a polymer of similar consistency to AN 125 but molecular weight of only about 2 million Daltons, was the first polymer used. Figure 6.2 shows the pressure drop for 2500 ppm AN 125 VLM in SSHSB for two different flow rates. Table 6.4 shows the injected and produced viscosities were the same after steady state was reached. The polymer was filtered through a 0.22 μm Millipore membrane before injection. Viscosities are reported at a shear rate of 500 sec^{-1} and at 25 C unless otherwise noted. There seems to be no degradation of the polymer at any time before or after filtration or injection as indicated by viscosity measurements.

Since the polymer viscosity is relatively low, shear rate shows little effect on decreasing viscosity, which is illustrated in Figure 6.3. The viscosity at a shear rate of 10 sec^{-1} is 4.74 cP while the corresponding viscosity for 500 sec^{-1} is 4.24 cP.

Low Salinity Polymer Injections

2500 ppm AN 125 VLM in the synthetic softened low salinity brine (SSLSB) was injected into the same core plug immediately following the high salinity polymer injection. Again, the softened brine was chosen instead of the hard brine to simplify the process. The results of this polymer flood can be reviewed in Figures 6.4 and 6.5 as well as Table 6.5. The flow rate was changed in order to study its effects on the polymer resistance factor (R_f) and permeability reduction factor (R_k) which remained constant.

With two successful core floods completed, several other polymers were tested for injectivity. A new core plug (#341) was chosen for these tests. SNF's AB 305 VLM, an HPAM with a molecular weight of 500,000 Daltons, was chosen because it has a lower molecular weight than AN 125. After a successful injection of the AB 305 VLM, two more HPAM polymers, AB 305 MPM, molecular weight of about 2 million Daltons, and Flopaam 3230S, molecular weight of about 5 million Daltons, were injected successfully. The details of these floods are summarized in Table 6.6. Polymer concentration was varied such that each solution had a viscosity of around 5 cP at 25 C and 500 sec⁻¹.

Initially, core plug #341 was saturated with SSLSB. Figure 6.6 illustrates the brine flood and Figure 6.7 shows the polymer flood with AB 305 VLM. The brine permeability of core plug #341 was determined to be 3.8 md with a PV of 15 mL. The polymer properties are summarized in Table 6.7. For the first time, degradation of the polymer was seen in the effluent sample. This is interesting because the permeability reduction factor of 1.16 is not excessive.

It was determined that the next two polymers, AB 305 MPM and FP 3230S, would be pre-sheared prior to injection. Viscosities as well as a screen factors were

measured before and after the shearing as is summarized in Table 6.8 and viscosity profiles can be viewed in Figures 6.8 and 6.9. After shearing and filtering (but before injection), AB 305 MPM retained 95% of its viscosity while FP 3230S retained 86% of its original viscosity. Pre-shearing helped to reduce the SF of AB 305 MPM by almost half while the reduction for FP 3230S was four-fold. This trade-off was deemed acceptable in so long as it allowed for polymer to be injected into the core without plugging or massive shear degradation.

The second polymer injection, illustrated in Figure 6.10, consisted of 2500 ppm AB 305 MPM in SSLSB. Between around 1.25 to 1.5 pore volumes injected, the setup developed a leak, which was fixed. At around 2.75 pore volume injected, the core was shut in. AB 305 MPM lost little more viscosity in the effluent. The third polymer injection consisted of 2000 ppm FP 3230S in SSLSB. Figure 6.11 presents pressure data for this polymer flood. The noise in the pressure data can be attributed to an unintentional kink in the inlet line around 1.75 pore volume injected. The fact that the flood with FP 3230S appears to have reached a steady state pressure outweighs the fact that the polymer showed further degradation in the effluent sample.

6.2 CHEMICAL FLOODS

Many attempts were made at developing a successful chemical coreflood for this reservoir. This proved to be especially difficult for reasons including high salinity (>200,000 ppm TDS), low permeability (~3 md), and moderately high temperature (69 C). The successful formulation will be discussed here while the rest of the data is presented in Appendix A.

Coreflood L-9 began with 6 reservoir core plugs stacked together to form approximately a 1 foot section and loaded into the core holder. The purpose of L-9 was to use reservoir core plugs to test the chemical formulation that was developed in L-8 which resulted in 98% oil recovery in a Berea sandstone. During the chemical flood (after approximately 0.5 PV injected) the pressure drop in the first half of the core indicated severe plugging, which was attributed to using unsheared polymer. The results presented herein are thus two-fold. For up to and including the water flood, the full section of 6 plugs was used. For the chemical flood, only the 3 plugs in the last half of the core were used. All properties were assumed to be half of the total (like the pore volume and the residual oil saturation to water flood), and it was assumed that the chemical flood had not yet reached the second half of the core when it was stopped the first time. This is important in reviewing the following results.

From the phase behavior experiments (Yang, 2010), the formulation containing 0.3% Isofol C32-7PO-6EO sulfate, 0.3% Petrostep S-3A, 0.1% TDA 30, 0.4% Aerosol MA-80 showed high solubilization ratios varying from 15 to 30 at the optimum salinity in the range of 10,000 ppm to 25,000 ppm Na_2CO_3 in 1% NaCl. These results are presented in Table 6.9 and Figures 6.12 to 6.16. Reservoir L crude oil is considered to be reactive oil, thus expected to give varying solubilization ratios and optimum salinities to different water to oil ratios. The phase behavior experiments confirm that premise. However, the solubilization curves still have signs of un-equilibrated data points after 55 days.

Core plugs #277, 278, and 282 were used for the chemical flood. Table 6.10 lists the details from the coreflood. As can be seen, the permeability is very low by polymer flooding standards. Figure 6.17 shows an illustration of the orientation of the pressure transducers, the direction of flow, and the core plugs. Inlet pressure is the pressure drop

over the first half of the core, the outlet pressure is over the second half of the core, and the whole pressure is the pressure differential over the whole core.

After the core was loaded into the core holder, it was evacuated and saturated with the SSLSB (~1 wt% NaCl). The core was flushed with approximately 200 mL of SSLSB until the effluent ran clear. Next, a tracer test was done by injecting approximately 50 mL of 4% NaCl brine at an effluent flow rate of about 0.25 mL/min (~4 ft/day). Tracer brine was injected until the TDS of the effluent was equivalent to 40 g/L. The pore volume was determined as 41.0 mL. The core was again flushed with several pore volumes of 1% NaCl until the TDS of the effluent was equivalent to 10 g/L. 1% NaCl brine was injected at 0.25 mL/min until the equilibrium state to measure a brine permeability (k_{brine}) of 2.24 md. The pressure data from the brine flood is shown in Figure 6.18.

Reservoir L crude oil was filtered using 0.22 μm filter at constant pressure of 50 psi at 69 C. Then, the core was saturated with oil at constant pressure of 275 psi at 69 C. Initial oil saturation (S_{oi}) was measured to be 0.84 and therefore, the residual water saturation (S_{wr}) was 0.16. Then the crude oil was injected at a constant flow rate of 0.1 mL/min (~1.5 ft/day) to determine the oil permeability of the core. Oil permeability (k_o) was determined to be 1.02 md, and the relative oil permeability (k_{ro}) to be 0.45. Figures 6.19 and 6.20 show the oil flood pressure drops at constant pressure and constant flow rate, respectively.

The core was aged for 72 hours at 69 C, and then water flooded with SSLSB at 69 C at ~2.5 ft/day until 99% water cut was reached. From that, the residual oil saturation to water (S_{orw}) was determined to be 0.20, and water relative permeability (k_{rw}) was determined to be 0.09. The pressure data from the water flood can be seen in Figure 6.21.

Chemicals injected in ASP flood (both the slug and the subsequent drive) consisted of FP 3230S polymer sheared on "high" setting for 6 minutes using a Waring blender then passed through 0.22 μm filter under 30 psi pressure. Viscosity of unsheared and sheared/filtered polymer is given in the Figure 6.22. This process dramatically reduced the viscosity of the polymer solution, thus the concentrations had to be increased to get the target viscosity of 6 cP.

0.3 PV of ASP slug was injected at 0.06 ml/min (~ 1 ft/day) and 69 C using the formulation shown below:

ASP slug ($\text{PV} \times \text{C} = 18$)

Slug size 0.3 PV

0.3% C32-7PO-6EO Sulfate (U32-P706E-2)

0.3% Petrostep S3A (*Lot # 18239-091907*)

0.1% TDA-30 (*Lot # 2097082107*)

0.4% Aerosol MA 80-I (Sodium dihexyl sulfosuccinate)

2.5% Na_2CO_3

5000 ppm sheared FP3230S in SSLSB

The ASP slug was followed by polymer drive with 4000 ppm sheared FP3230s in SSLSB at the same flow rate and temperature until no more oil or emulsion were produced. Pressure data from the chemical flood is shown in Figure 6.23. Whole pressure drop is 230 psi at a flow rate of 1 ft/day. Again, this is for a 0.5 ft section of core. Effluent samples were collected in graduated test tubes every 50 minutes with a sample size of ~ 3.0 mL. Oil recovery was measured immediately after collection, and again at 69 C after centrifuging the tubes for 2 min at 1000 rpm after 24 hours. Cumulative oil recovery, oil saturation, and oil cut are plotted as a function of PV injected in Figure 6.24. Notice the small, drawn out oil cut. Nonetheless, 90% oil recovery is achieved. pH and ionic concentration of the effluent were analyzed and

reported in Figures 6.25 and 6.26, respectively. Core plugs were later removed from the core holder and visually checked for indication of remaining oil and its location.

6.3 DISCUSSION

Several polymers were successfully injected into a low permeability carbonate core plug. A chemical formulation was also developed that recovered more than 90% of the oil remaining after water flooding. For most reservoirs, this fact alone would be enough to recommend traditional chemical flooding using polymer for mobility control. However, the pressure drops during the core flood were extremely high (on the order of 500 psi/ft corresponding to a flow rate of ~ 1 ft/day) and scaling to the field would be either mean excessively low injectivity or an impossibly high pressure gradient. Also, the polymer used for the chemical flood was pre-sheared for six minutes in a Waring blender and passed through a $0.2\ \mu\text{m}$ filter, which may not be feasible in a field setting.

Table 6.1 k_{air} and ϕ of reservoir core plugs

Core Plug #	Porosity ϕ	Air permeability k_{air} (md)
144	0.28	2.0
150	0.282	1.7
152	0.246	1.4
153	0.261	1.1
155	0.24	1.2
156	0.248	1.0
323	0.273	3.8
324	0.276	3.6
326	0.289	4.8
327	0.293	5.1
328	0.294	5.4
330	0.278	4.0
331	0.287	4.0
332	0.304	5.4
339	0.296	4.2
340	0.281	3.5
341	0.288	3.8
343	0.288	4.3

Table 6.2: Reservoir rock and fluid properties

Rock Type	Chalky limestone
Reported permeability	1-20 md (5 md average)
Porosity	0.28
Temperature	69 C
Oil viscosity (live oil)	0.8 cP
API gravity	38°
Type	reactive
Formation brine	220,000 ppm TDS

Table 6.3: Formation and injection water make-up

	Low salinity hard injection brine (mg/l)	Synthetic softened low salinity brine (SSLSB) (mg/l)	High salinity hard injection brine (mg/l)	Synthetic softened high salinity brine (SSHBS) (mg/l)	Reservoir brine (mg/l)
Na ⁺	2719	3898	59970	77385	64893
K ⁺	64	64	Not determined	Not determined	500
Mg ²⁺	220	0	2153	0	2227
Ca ²⁺	665	0	11618	0	16578
Sr ²⁺	7	0	Not determined	Not determined	1300
Cl ⁻	4731	4731	118791	118791	136408
SO ₄ ²⁻	1830	1830	689	689	201
HCO ₃ ⁻	170	170	9	9	84
TDS	10406	10693	193230	196874	222191

Table 6.4: 2500 ppm AN 125 VLM in SSHSB, injected and produced viscosities, 25 C

Viscosity (pre-filter)	4.24 cP
Filter size	0.22 μm
Viscosity (after filter)	4.24 cP
Viscosity (core effluent)	4.24 cP

Table 6.5: 2500 ppm AN 125 VLM in SSLSB, injected and produced viscosities, 25 C

Viscosity (pre-filter)	4.3 cP
Filter size	0.22 μm
Viscosity (after filter)	4.3 cP
Viscosity (core effluent)	4.3 cP

Table 6.6: Summary of polymer injectivity tests for core plug #341

Polymer	Sheared	Brine	Injected Viscosity at 500 s ⁻¹ (cP)	Result	Effluent Viscosity at 500 s ⁻¹ (cP)	Resistance Factor R _F	Permeability Reduction Factor R _k
10,000 ppm AB 305 VLM	no	SSL SB	5.36	success	4.7	6.5	1.16
2500 ppm AB 305 MPM	yes	SSL SB	5.47	success	5.15	5.8	1
2000 ppm FP 3230S	yes	SSL SB	5.53	success	4.2	5.52	0.95

Table 6.7: 10,000 ppm AB 305 VLM in SSLSB, injected and produced viscosities, 25 C

Viscosity (pre-filter)	5.5 cP
Filter size	0.22 μm
Filter ratio	1
Viscosity (after filter)	5.36 cP
Viscosity (core effluent)	4.7 cP

Table 6.8: AB 305 MPM & FP 3230S in SSLSB, pre-sheared, sheared and produced viscosities, 25 C

	2500 ppm AB 305 MPM	2000 ppm FP 3230S
Viscosity (unsheared)	5.77 cP	6.43 cP
SF (unsheared)	15	52
Viscosity (sheared 20 sec)	5.5 cP	5.6 cP
SF (sheared 20 sec)	9	14
Filter size	0.45 μ m	0.45 μ m
Filter ratio	1	1
Viscosity (after filter)	5.47 cP	5.52 cP
Viscosity (core effluent)	5.15 cP	4.21 cP

Table 6.9: L-9 phase behavior data for varying WOR

Oil Scan	WOR	Solubilization Ratio	Optimum Salinity Na ₂ CO ₃
10%	9	17	2.30%
20%	4	24	1.90%
30%	2.33	27	1.40%
40%	1.5	16	1.10%
50%	1	35	0.90%

Table 6.10: Summary of L-9 coreflood

Rock	Reservoir
Mass	635.5 g
PV	41 mL
Porosity	0.257
Length	14.35 cm
Diameter	3.73 cm
Area	11.1 cm ²
Temperature	69 C
Injection Brine	SSL SB
k_{brine}	1.55 md
S_{oi}	0.84
S_{wr}	0.16
k_{oil}	0.71 md
k_{ro}	0.47
S_{orw}	0.40
k_{water}	0.16 md
k_{rw}	0.11
S_{orc}	0.019

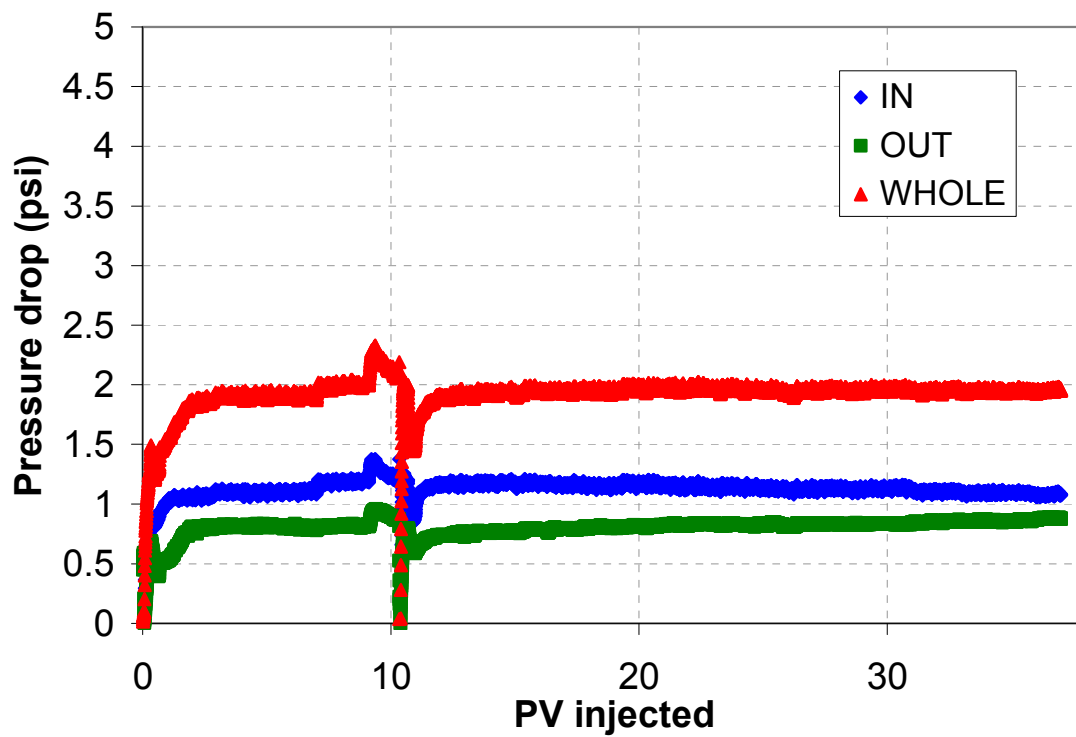


Figure 6.1: High salinity polymer injectivity test brine flood pressure drop (#332); 69 C; 2 ft/day

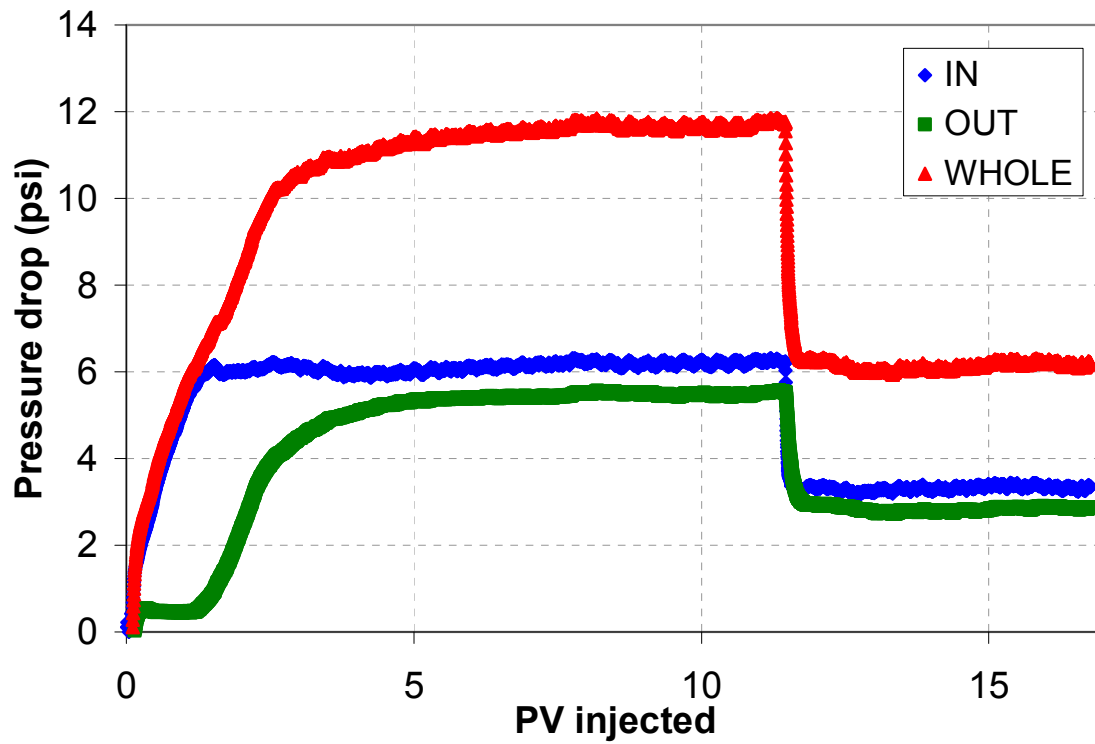


Figure 6.2: High salinity polymer injectivity test polymer flood pressure drop, 2500 ppm AN 125 VLM in SSHSB (#332); 69 C; 1 & 2 ft/day

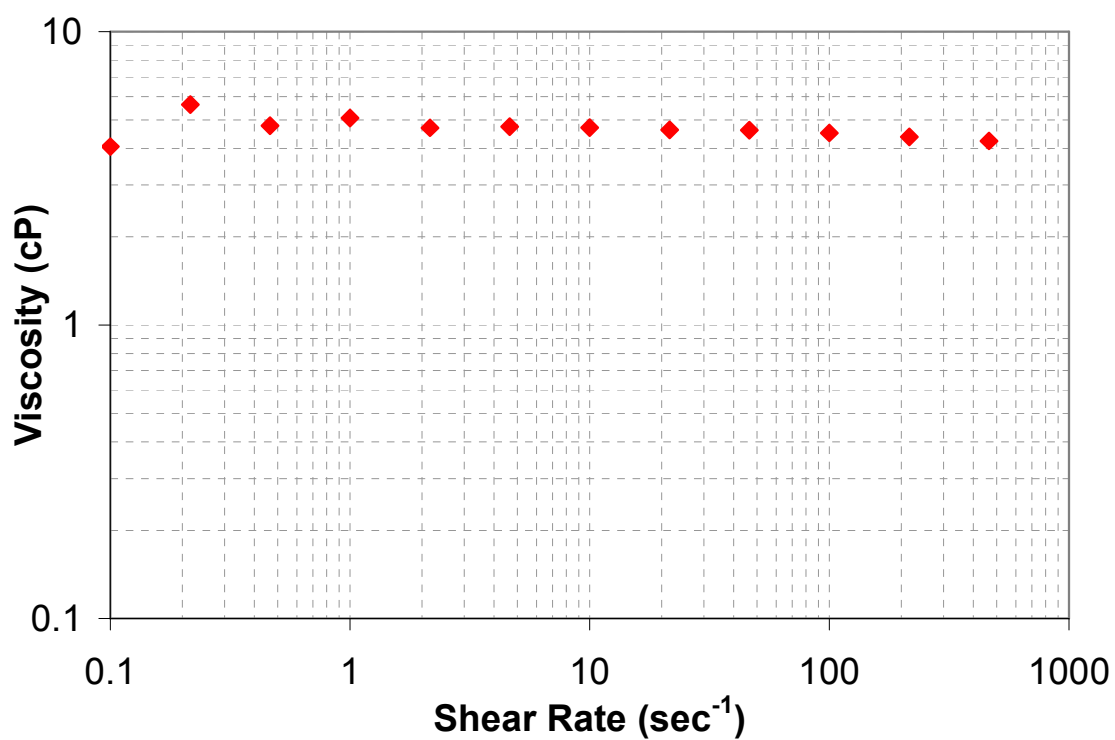


Figure 6.3: 2500 ppm AN 125 VLM in SSHSB, injected viscosity profile at 25 C

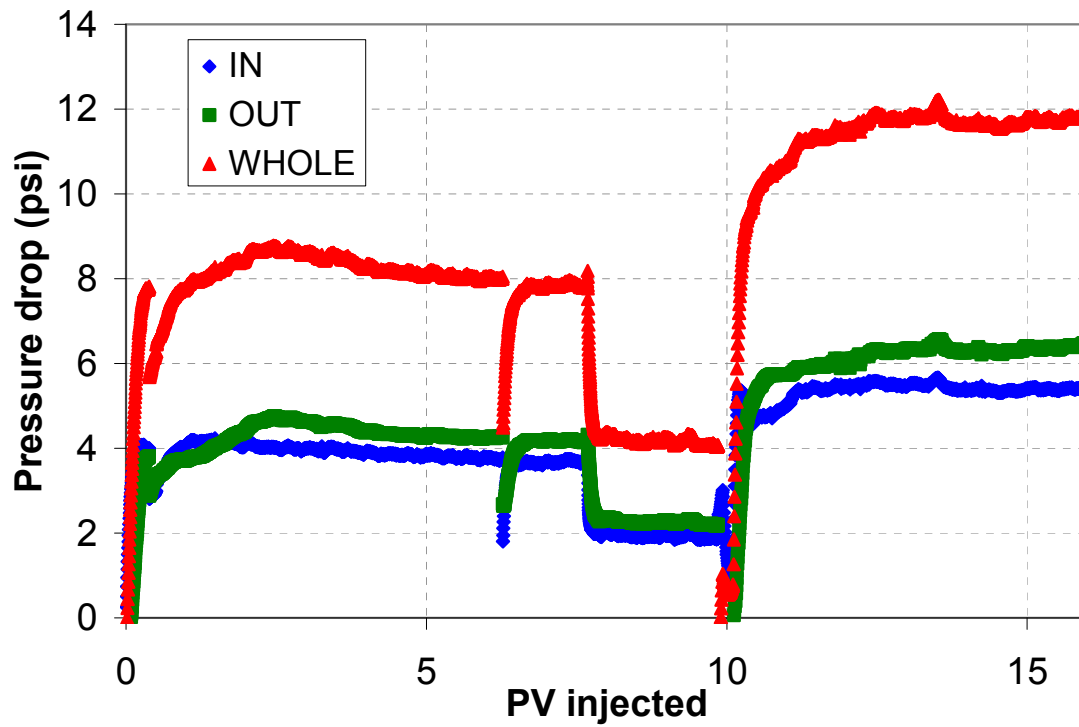


Figure 6.4: Low salinity polymer injectivity test polymer flood pressure drop, 2500 ppm AN 125 VLM in SSLSB (#332); 69 C; 1, 2, & 3 ft/day

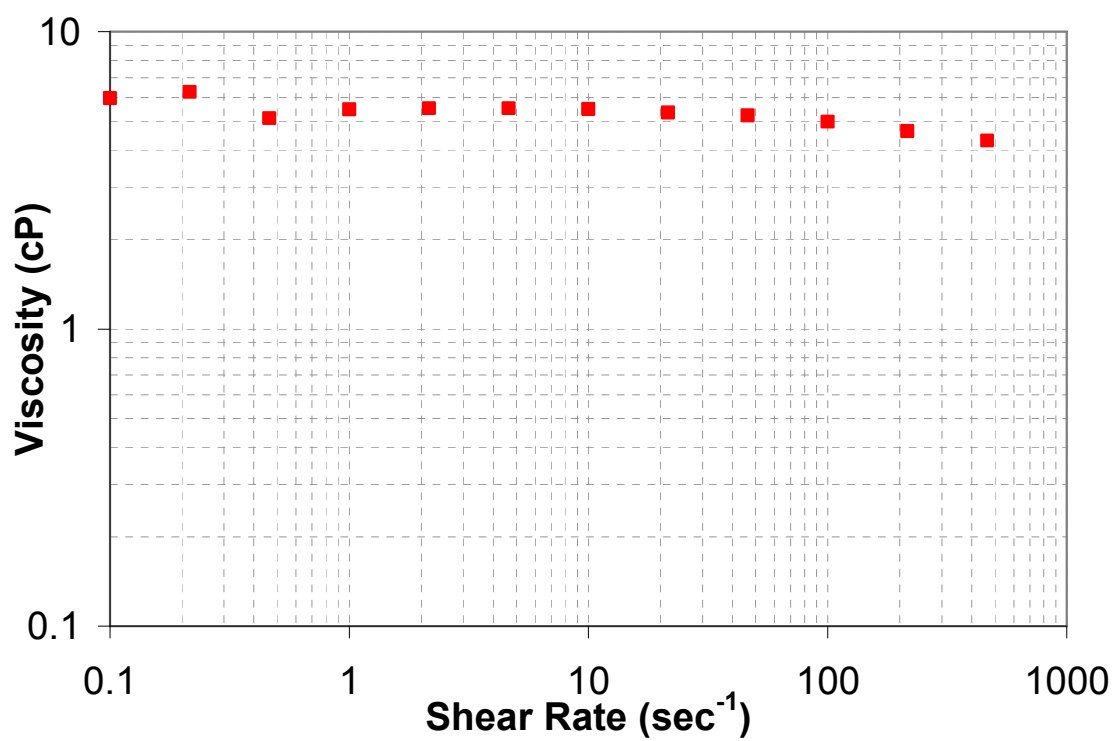


Figure 6.5: 2500 ppm AN 125 VLM in SSLSB, viscosity profile at 25 C

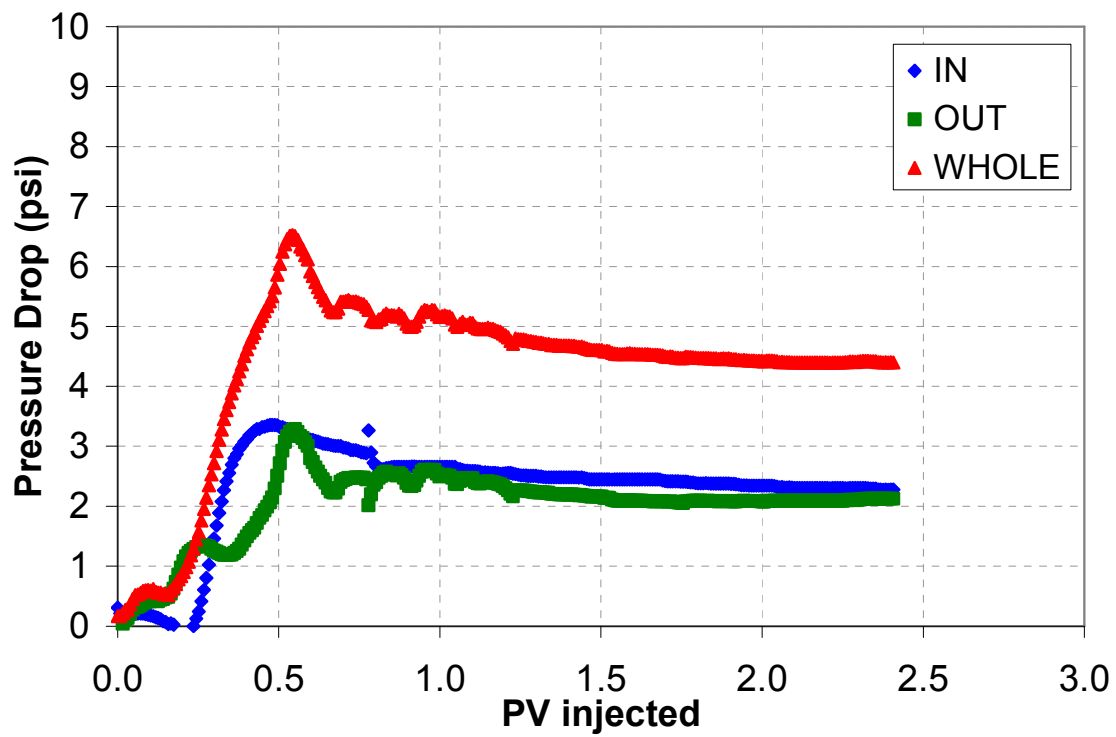


Figure 6.6: Low salinity polymer injectivity test brine flood pressure drop (#341); 69 C; 4 ft/day

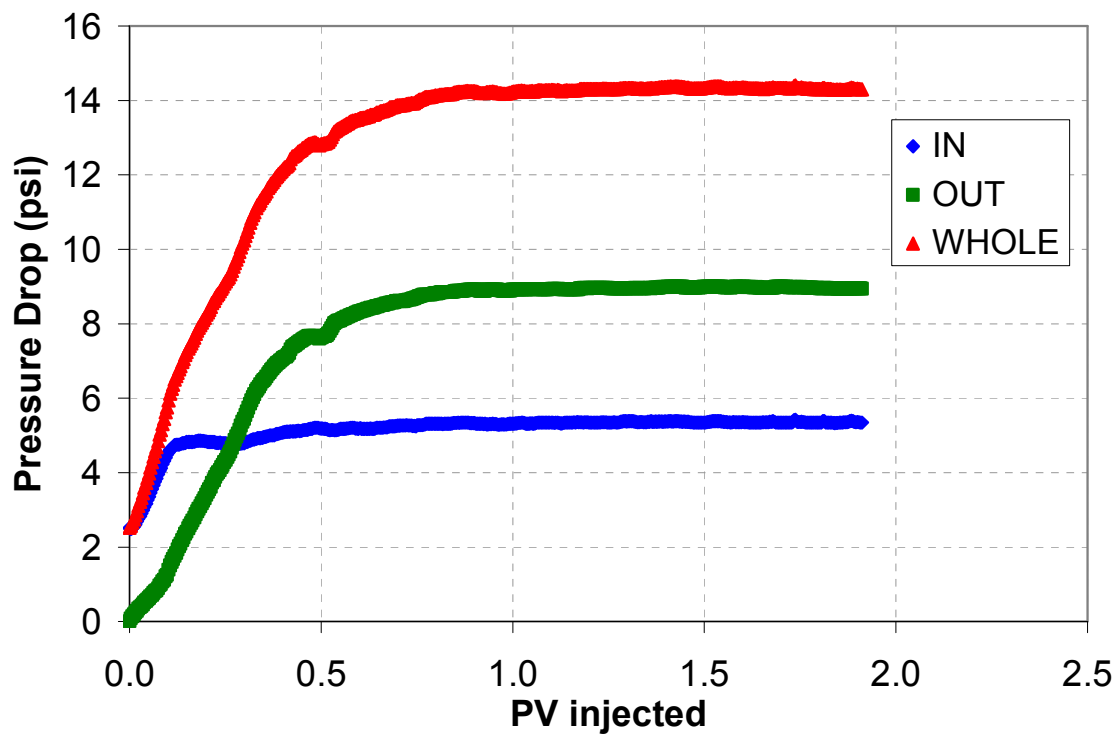


Figure 6.7: Low salinity polymer injectivity test polymer flood pressure drop, 10,000 ppm AB 305 VLM in SSLSB (#341); 69 C; 2 ft/day

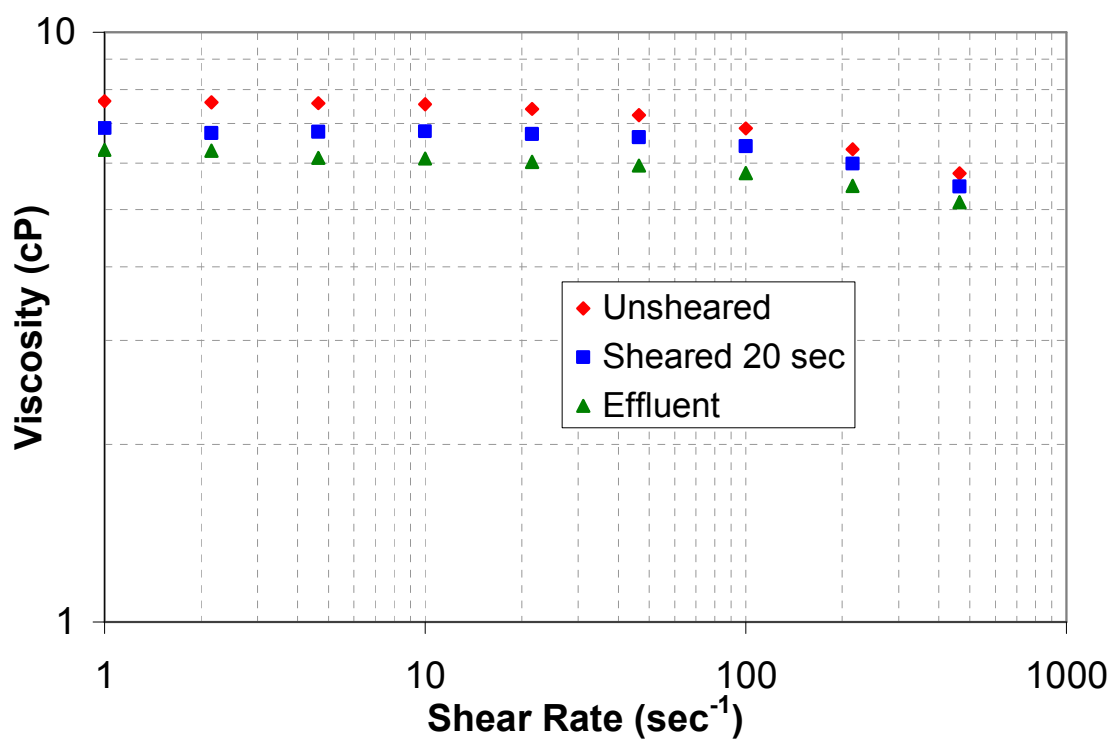


Figure 6.8: 2500 ppm AB 305 MPM in SSLSB, viscosity profile at 25 C

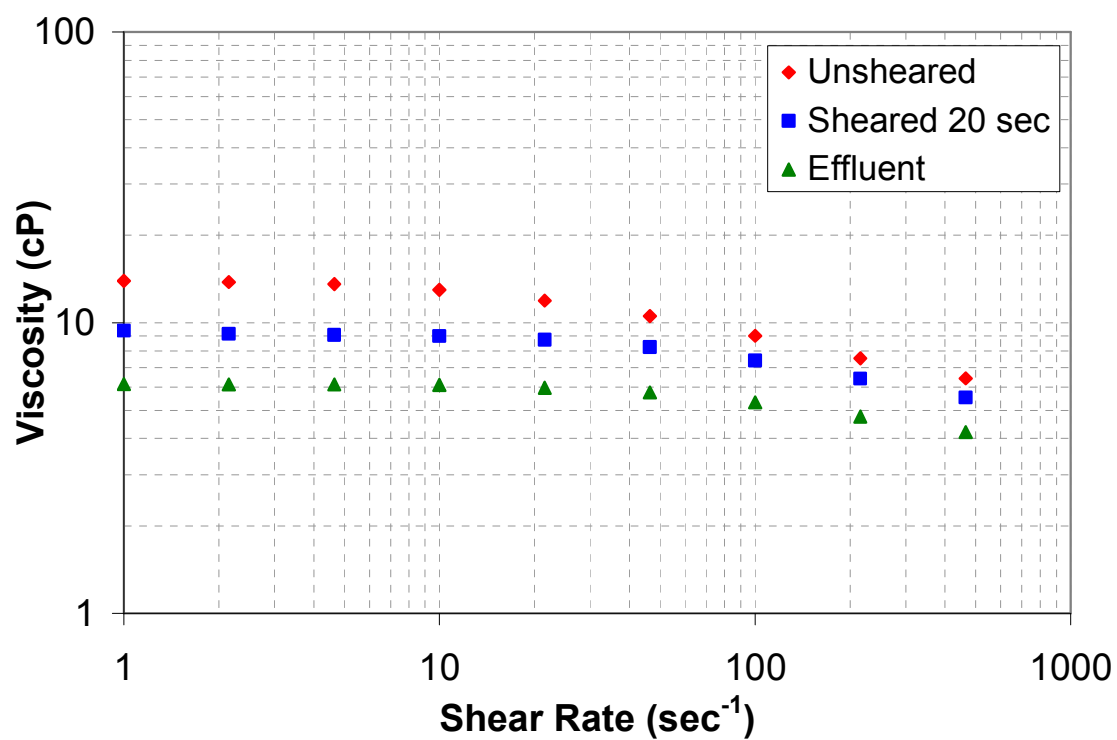


Figure 6.9: 2000 ppm FP 3230S in SSLSB, viscosity profile at 25 C

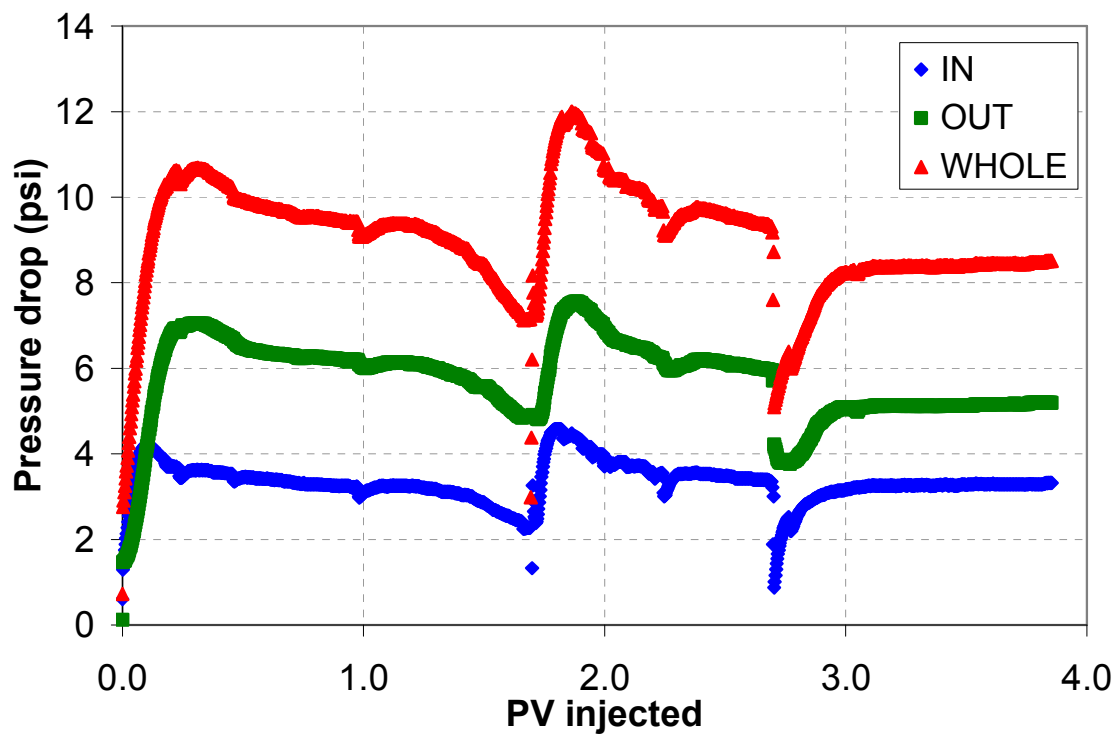


Figure 6.10: Low salinity polymer injectivity test polymer flood pressure drop, 2500 ppm AB 305 MPM in SSLSB (#341); 69 C; 1.33 ft/day

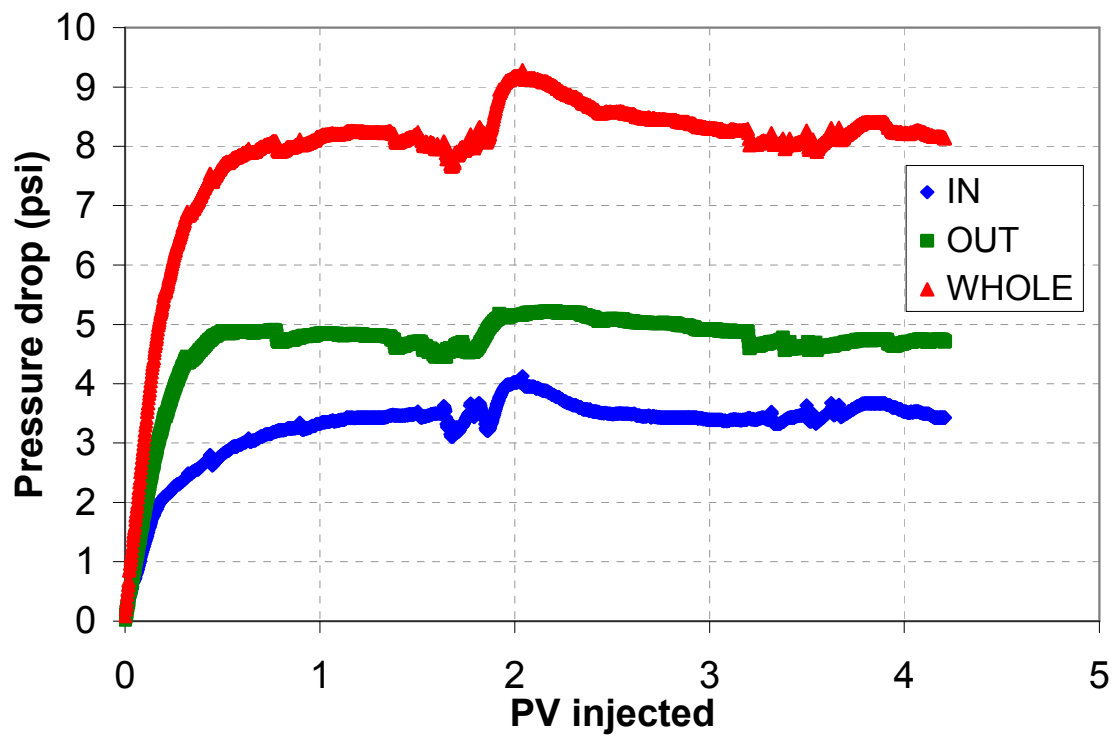


Figure 6.11: Low salinity polymer injectivity test polymer flood pressure drop, 2000 ppm FP 3230S in SSLSB (#341); 69 C; 1.33 ft/day

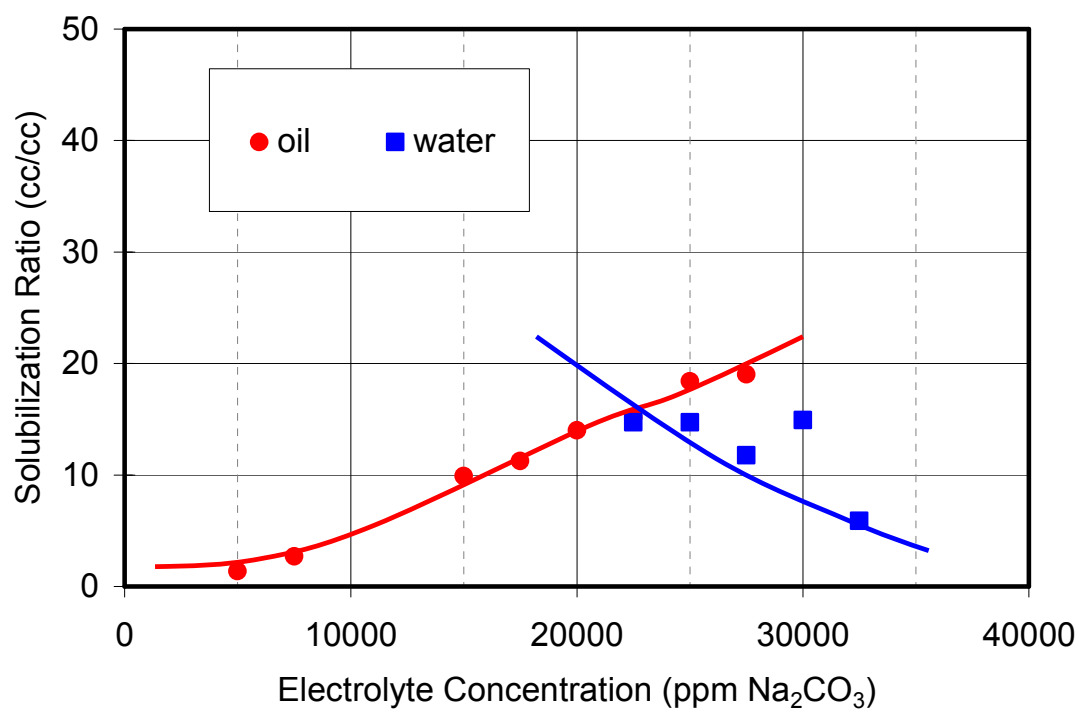


Figure 6.12: L-9 phase behavior plot after 55 days, 10% oil

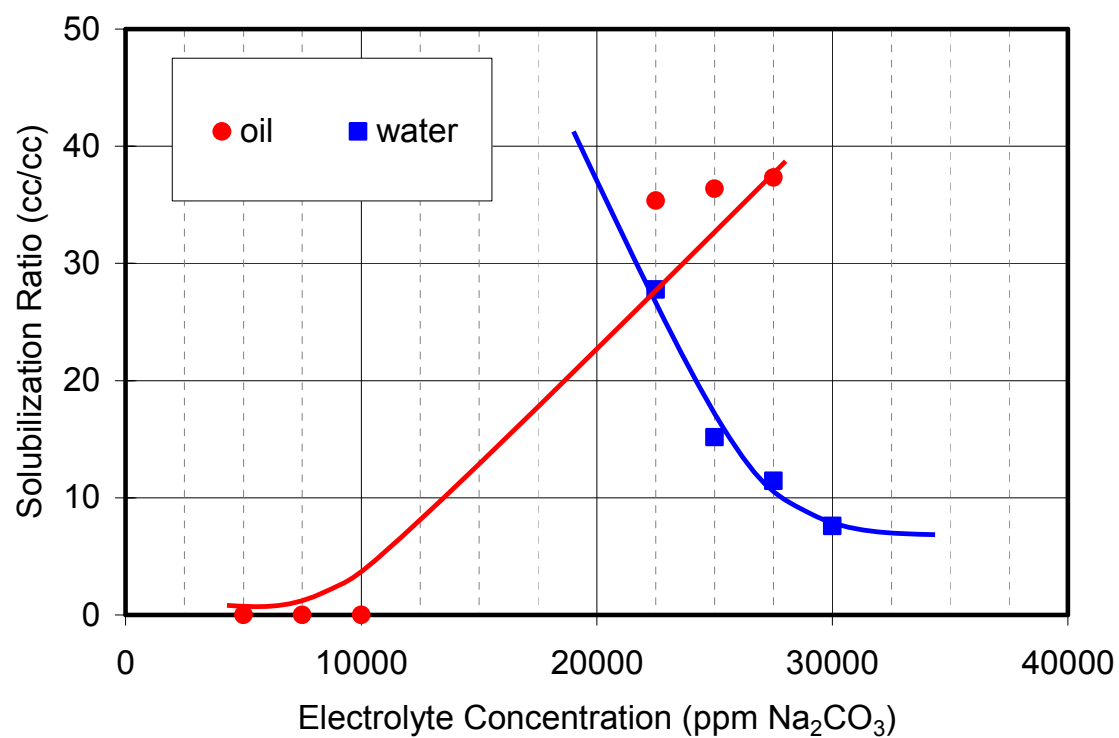


Figure 6.13: L-9 phase behavior plot after 55 days, 20% oil

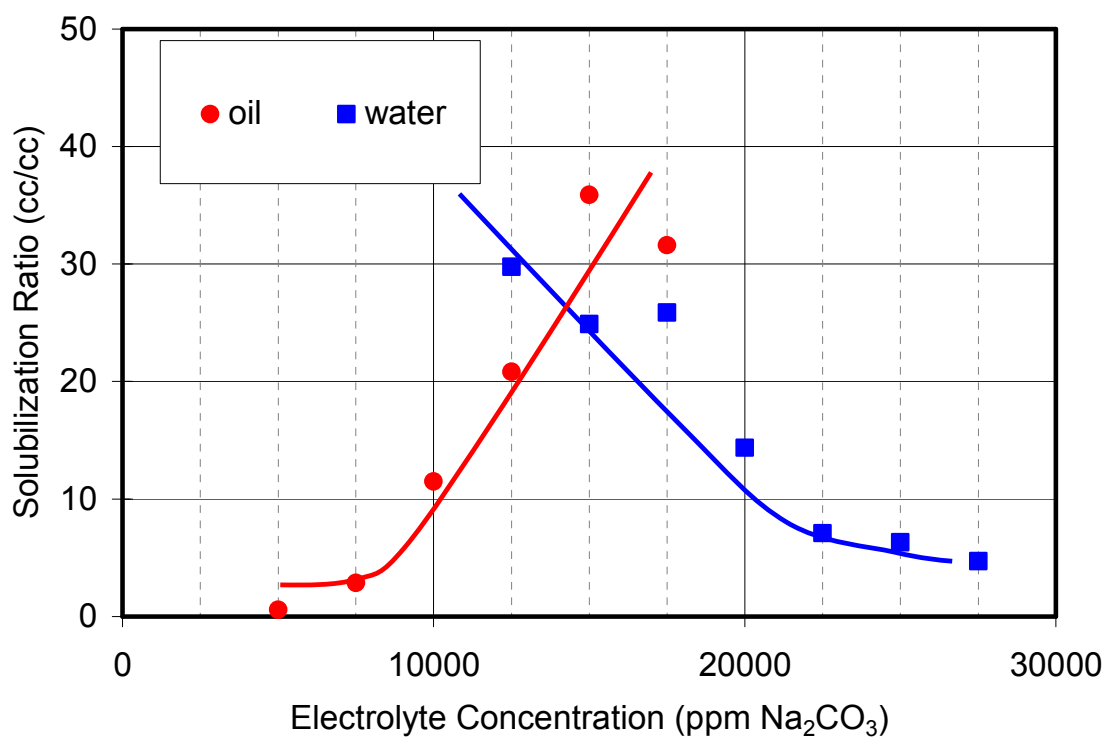


Figure 6.14: L-9 phase behavior plot after 55 days, 30% oil

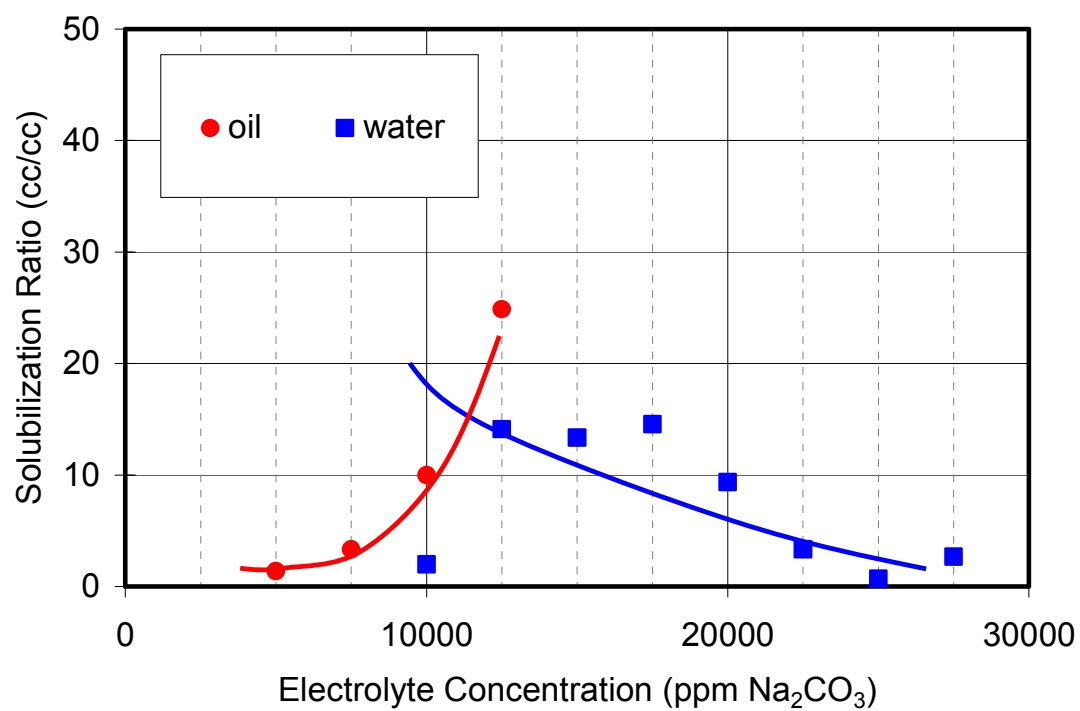


Figure 6.15: L-9 phase behavior plot after 55 days, 40% oil

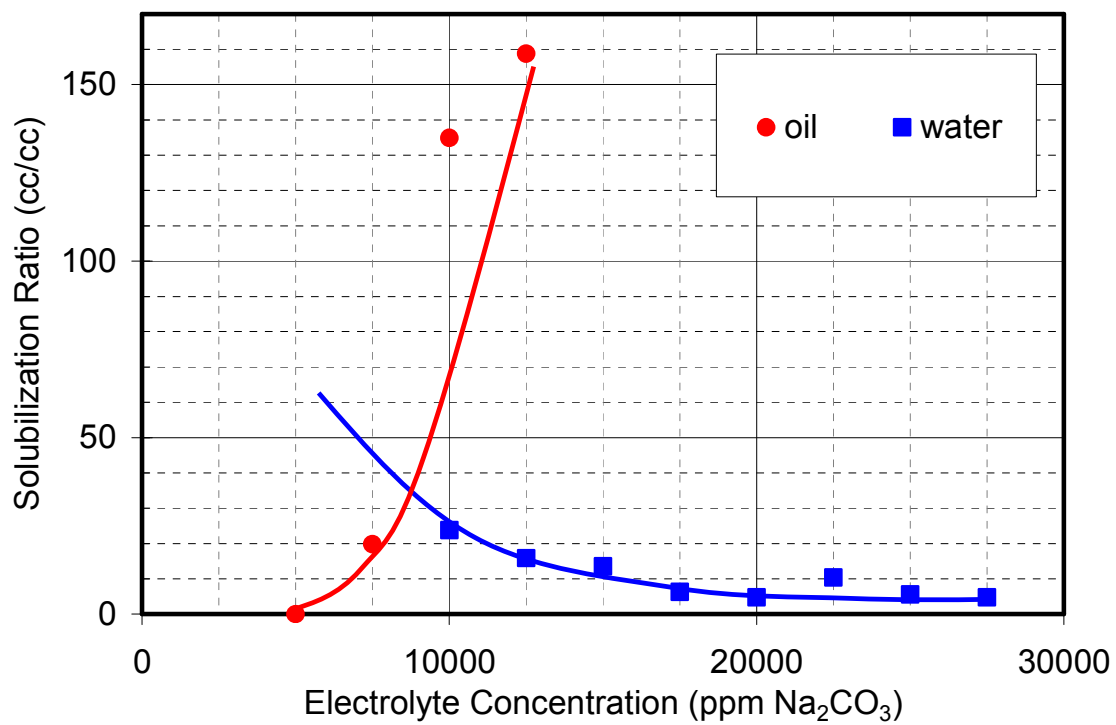


Figure 6.16: L-9 phase behavior plot after 55 days, 50% oil

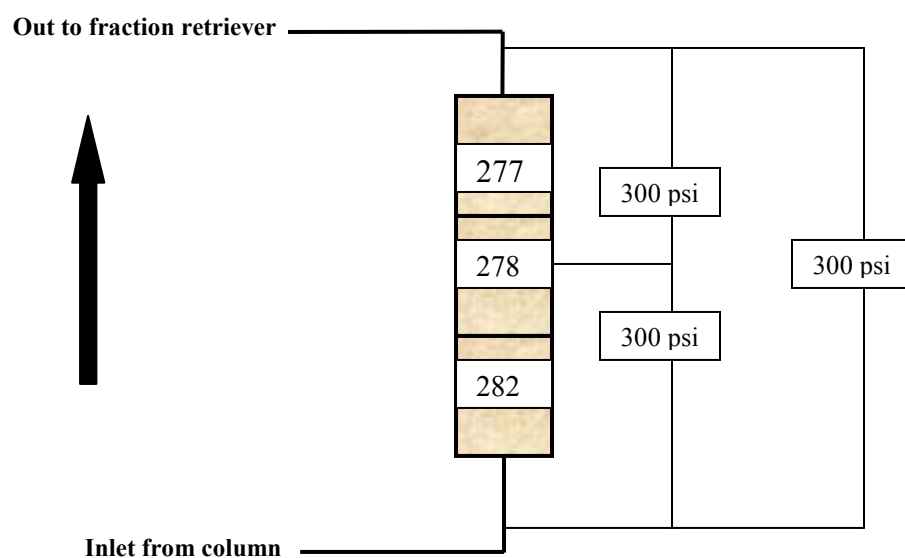


Figure 6.17: Pressure transducer setup and orientation of core

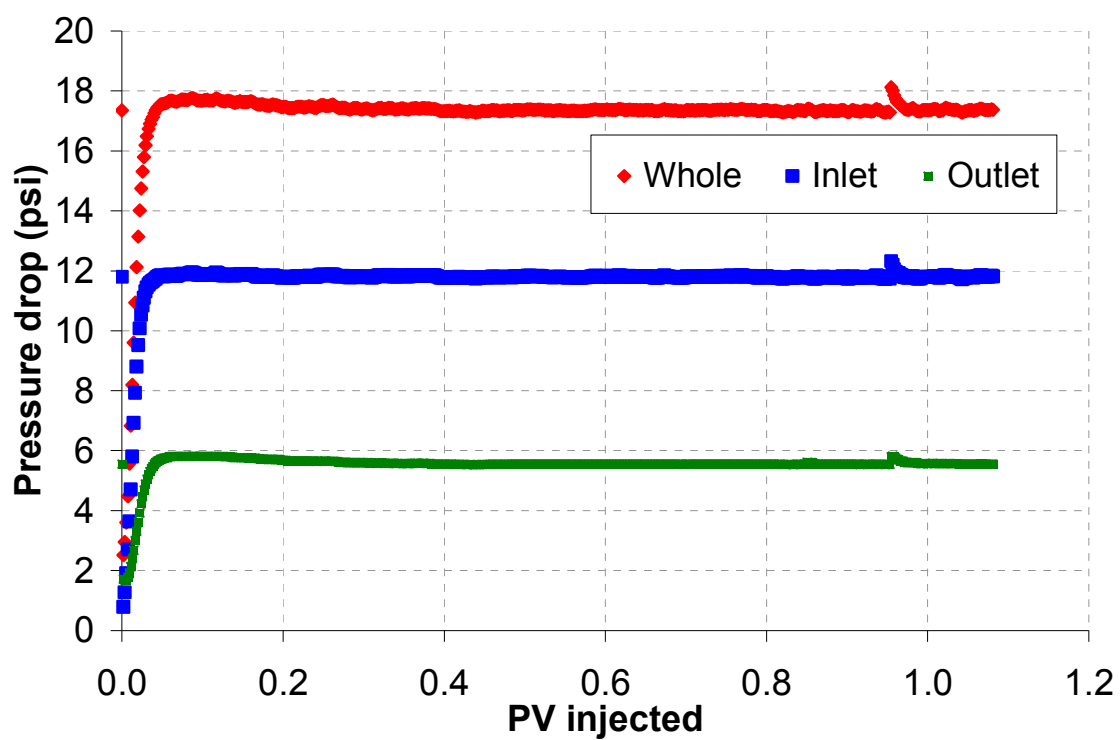


Figure 6.18: L-9 brine flood pressure data; 69 C; ~4 ft/day

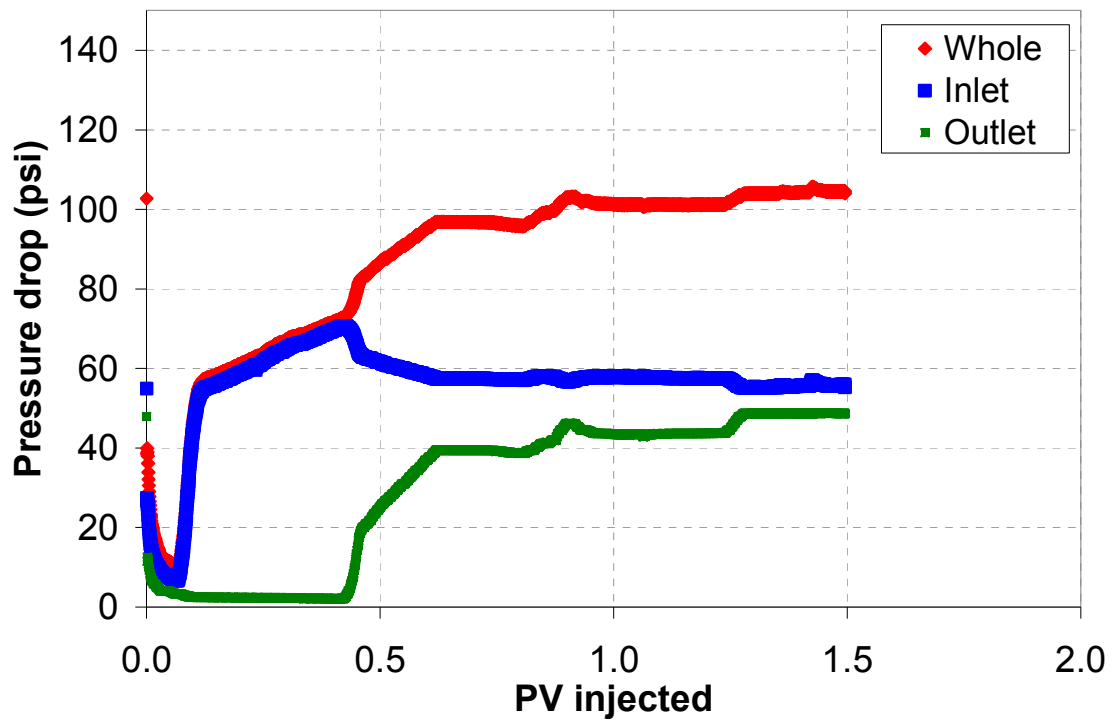


Figure 6.19: L-9 oil flood pressure data (constant pressure); 69 C; 275 psi

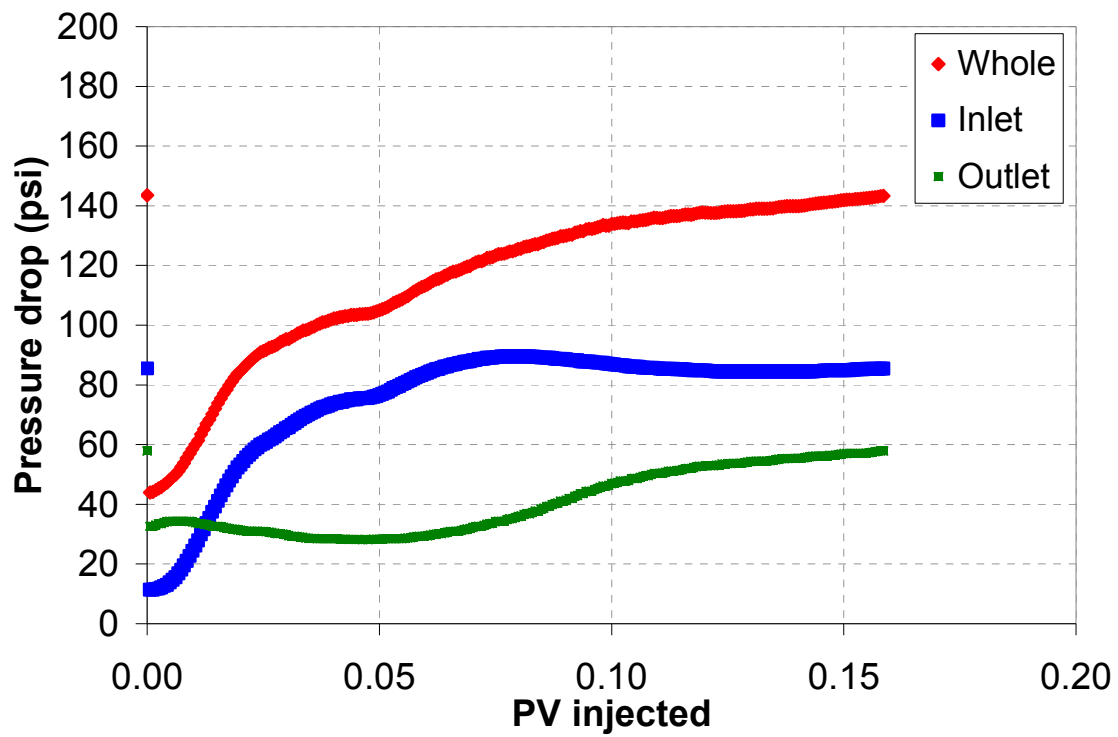


Figure 6.20: L-9 oil flood pressure data (constant flow rate); 69 C; ~1.5 ft/day

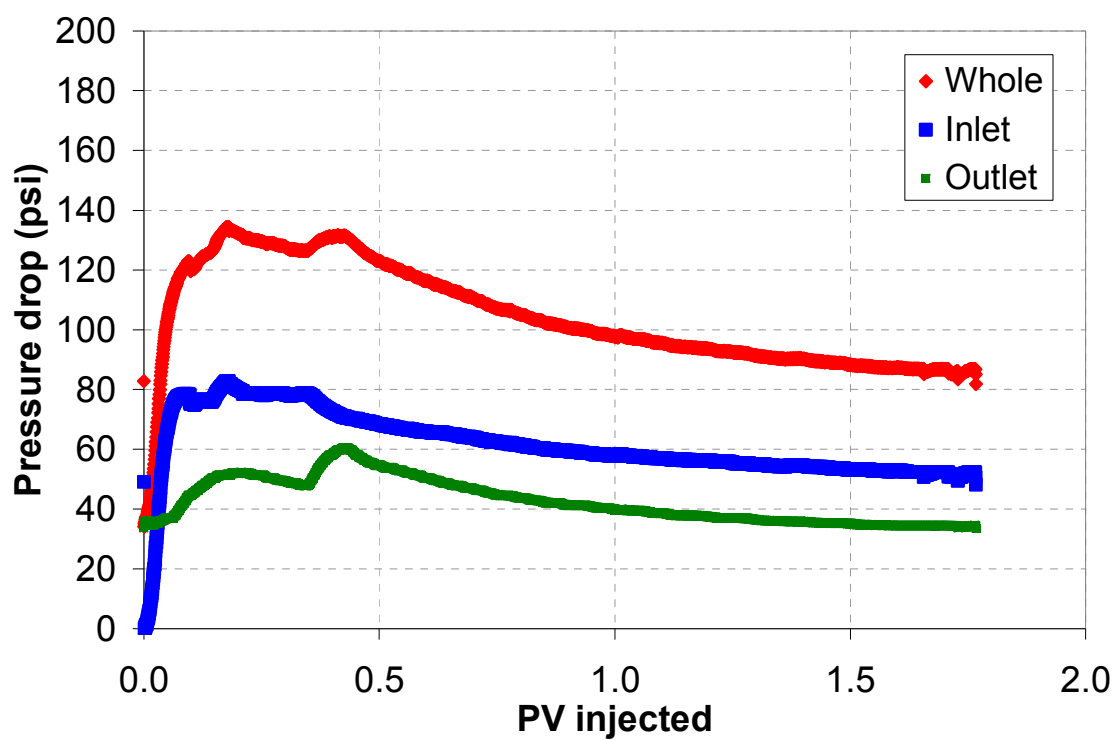


Figure 6.21: L-9 water flood pressure data; 69 C; ~2.5 ft/day

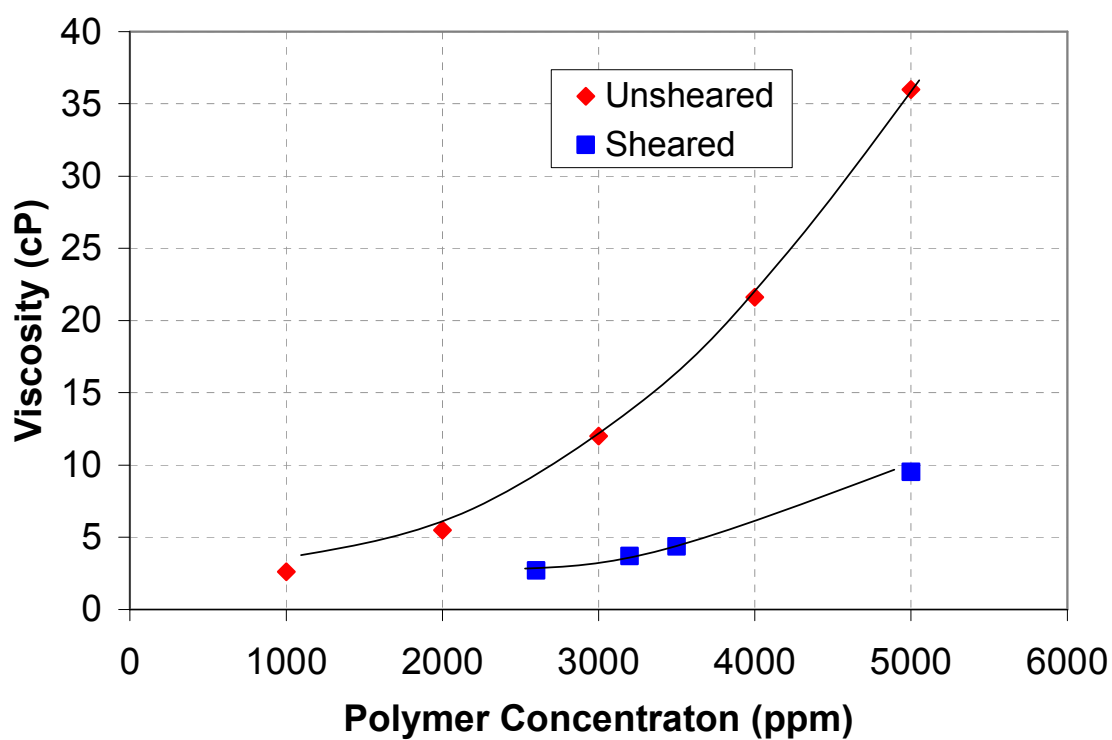


Figure 6.22: FP 3230S in SSLSB, viscosity vs. concentration before and after shearing for 6 min in Waring blender, 25 C

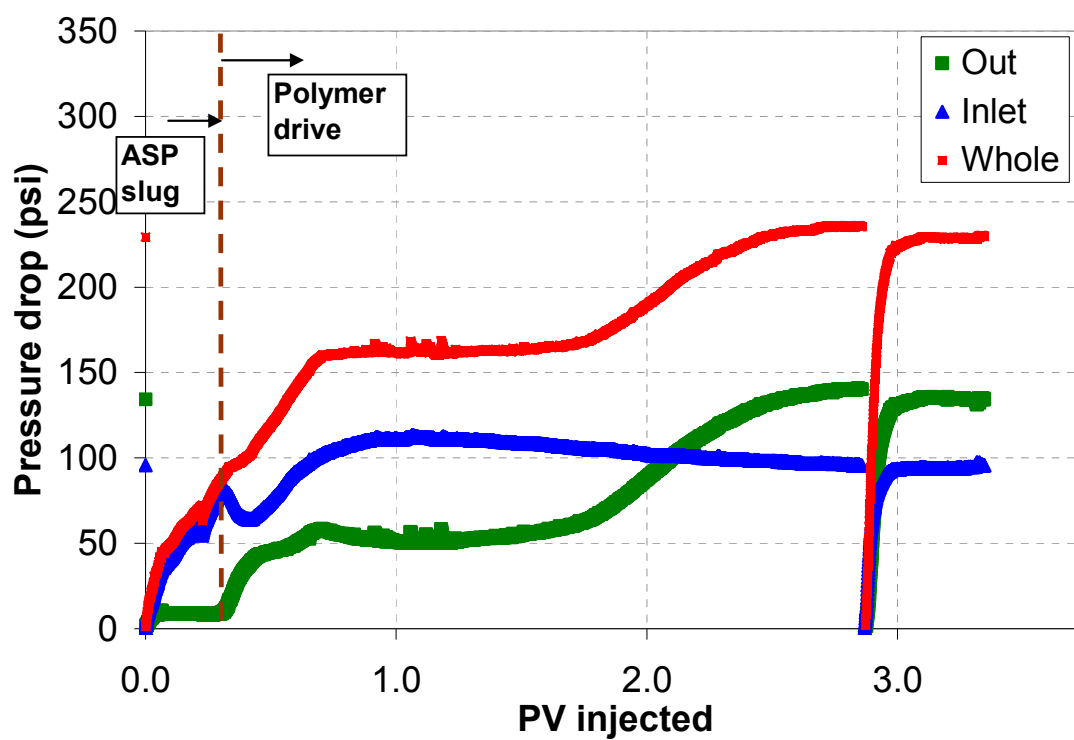


Figure 6.23: L-9 chemical flood pressure data; 69 C; ~1 ft/day

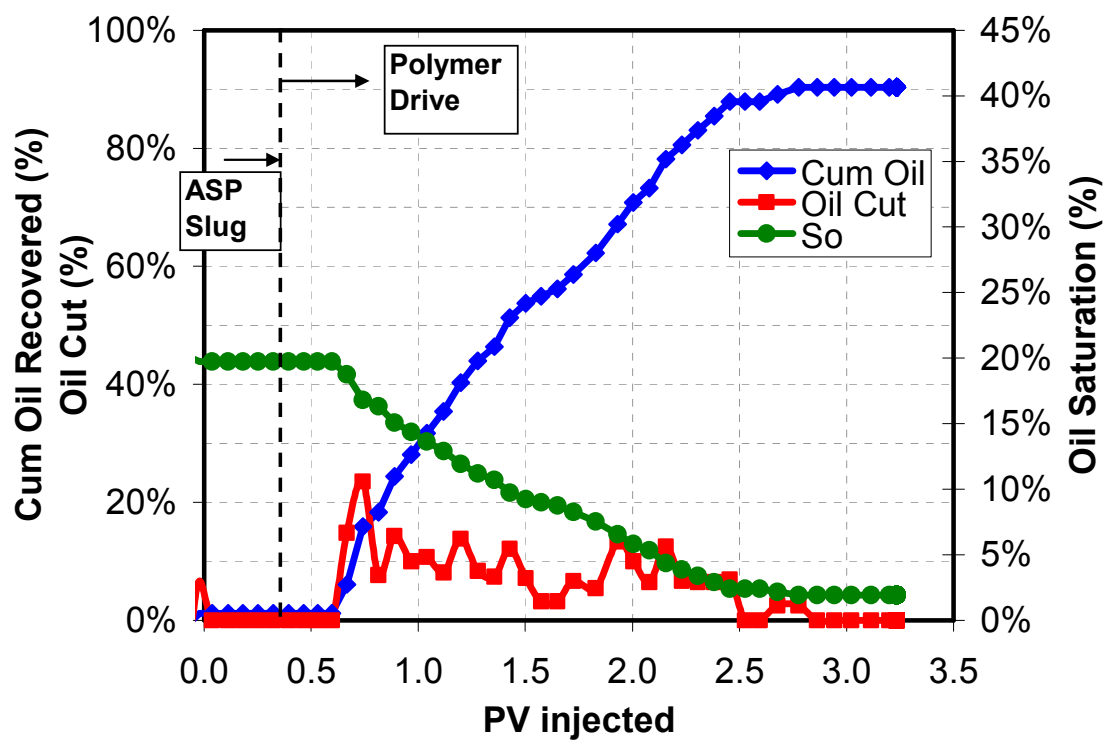


Figure 6.24: Oil recovery, saturation, and cut for L-9 chemical flood

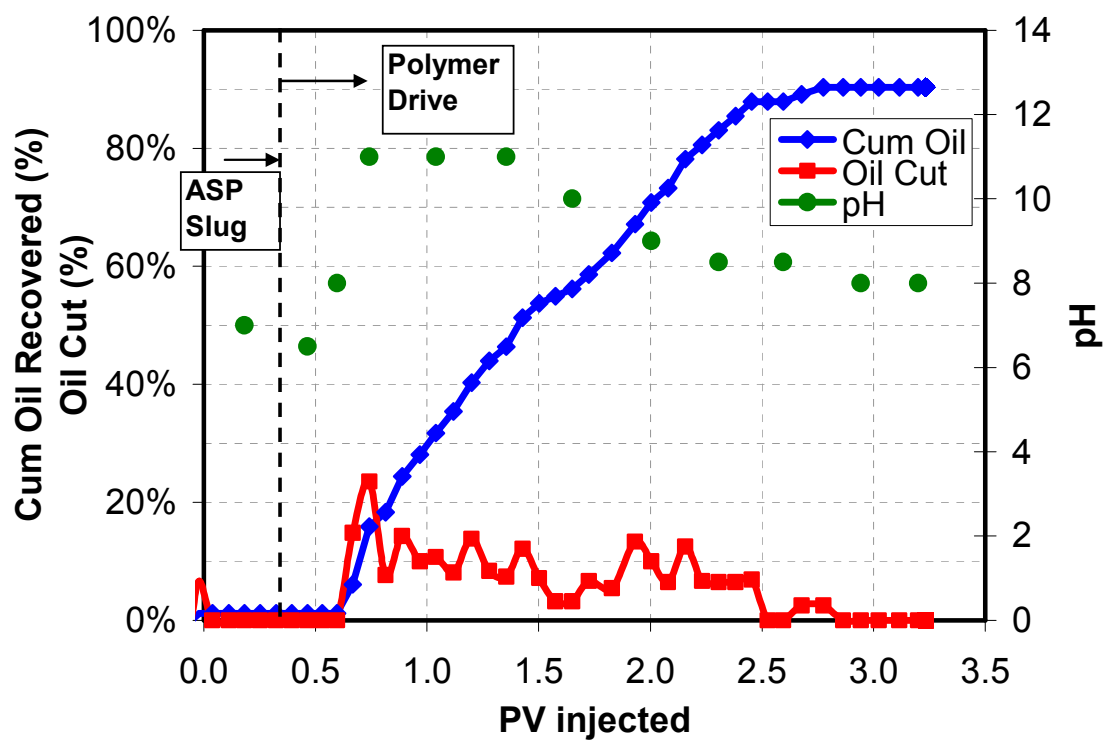


Figure 6.25: pH of effluent for L-9 chemical flood

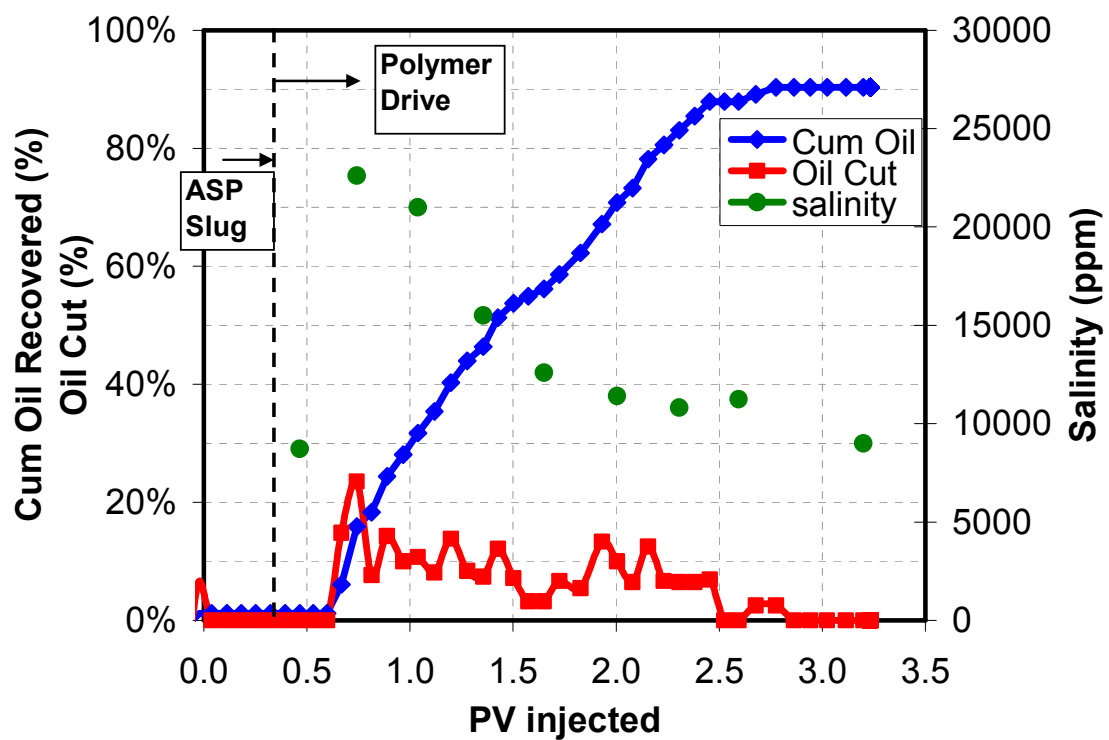


Figure 6.26: Ion concentration of effluent for L-9 chemical flood

CHAPTER 7: CONCLUSIONS AND RECOMMENDATIONS

Acrylic polymers are used because of their viscosifying effects for mobility control in chemical enhanced oil recovery because they are widely available in various forms at low cost, but they are easily susceptible to degradation. It is important to know what causes degradation as well as how to retard or eliminate it. Three main types of degradation were identified and studied: chemical, thermal, and mechanical. Of these, mechanical is the easiest to prevent while chemical and thermal both require much more attention in order to inhibit.

Results of this research were similar to those found by Levitt (2009) with respect to chemical stability of acrylic polymers, or more specifically calcium tolerance. Three polymers, PAM, poly(AM-co-AMPS), and poly(AM-co-ATBS-co-NVP), were post-hydrolyzed to $\tau \sim 0.6$. Poly(AM-co-ATBS-co-NVP) displayed the best results in both maintaining the highest viscosity and tolerating the most amount of calcium before showing signs of precipitation. Poly(AM-co-AMPS) retained significantly higher viscosity than PAM as it reached the onset of turbidity, but they both shared similar cloud points, the calcium concentration corresponding to the approach of precipitation, for several NaCl background concentrations. These results suggest that the NVP monomer may be shielding the ATBS monomer.

SNF Floerger has developed these NVP ter-polymers, but one limitation of the current product is that it is proving extremely difficult to synthesize anything larger than about 5 million Dalton. If made available at a reasonable cost, these polymers may have a market in some reservoirs (high temperature, low to moderate permeability, and

presence of divalent cations), but until larger chains can be manufactured their use will be limited.

The chelator, EDTA, was studied as a possible solution to the issue of calcium tolerance. Experiments using EDTA to sequester Ca^{++} ions showed mixed results. When post-hydrolyzed poly(AM-co-AMPS) was used, almost 100% viscosity was retained when EDTA was implemented, and much higher Ca^{++} concentrations were tolerated. This was only true at elevated pH as the scans with neutralized EDTA showed no effect on improving viscosity. Also, salinity tolerance became an issue at low salinities when EDTA was used. For the experiments involving post-hydrolyzed PAM, viscosity retention was improved and the onset of precipitation was delayed, but the results were not nearly as pronounced as the experiments with AMPS.

Initial results indicate that EDTA is a good technical solution for the chemical stability of polymer in the presence of divalent cations. The main issue going forward will be the cost of EDTA. One solution could be to soften water to some extent then use EDTA to sequester any remaining divalent cations. Another issue is that EDTA is only soluble in water at a concentration greater than a molar equivalence to divalent cations. This becomes relevant because the concentration of divalent cations in the formation brine may need to be accounted for when formulating the amount of EDTA to use. In any case, much more work needs to be done with EDTA and other potential sequestering agents.

Several discrepancies in the literature in reference to thermal degradation were resolved by this research, though some still remain. Carbonate and bicarbonate ions have been shown to have been a hidden factor in degradation experiments involving the addition of sodium dithionite to polymer solutions without the exclusion of oxygen, resolving a conflict in the literature between the results of Shupe (1981), who included

these ions, and others who did not. However, it has proven difficult to show whether this degradation is a result of redox cycling of iron impurities in the polymer or if it is due to a direct reaction between dithionite and oxygen. Another explanation could be that iron is playing a catalytic role in the process, but future work is necessary to clarify. Irrespective to the result of the latter, carbonate and bicarbonate ions corresponding to field conditions should be included in any study of oxidative polymer degradation.

A commercial HPAM polymer (Flopaam 3630S) has been shown to be stable in the presence of ferrous iron in the absence of oxygen, clarifying an apparent discrepancy in the literature between the results of Yang and Treiber (1985) and Kheradmand (1987). One plausible explanation for the inconsistency is that, because Kheradmand was using lab-prepared polymer, some impurities existed which are normally absent in commercially synthesized polymers.

The sensitivity study on polymer stability with respect to sodium dithionite produced some interesting results. After exposure to oxygen, a polymer's degree of hydrolysis plays a role in amount of degradation when dithionite is present. Delayed exposure to oxygen seems to have no effect on the level of degradation. However, as shown by Levitt (2009), the initial level of dissolved oxygen does play an important role, even after the polymer solution is exposed to oxygen. A polymer solution that was initially deoxygenated was subjected to less degradation upon addition of dithionite, both initially and after subsequent exposure to oxygen. The rapid cessation of degradation when DTPA is present, which can be explained by the chelator's ability to prevent further redox cycling of iron, supports the theory that redox cycling of trace amounts of iron play a decisive role in the degradation of the polymer backbone. However, the increase in degradation seen when additional dithionite is added, despite the absence of further change in redox potential, indicates additional complexity.

Aqueous solutions of sodium borohydride (Montbrite 1240) mixed with sodium bisulfite to produce sodium dithionite and sodium metaborate has proven to be a superior method to that of the traditional use of powder sodium dithionite. The degradation experienced is equivalent, but the benefit that it is much safer to handle than powder makes it the preferred choice in the field as an oxygen scavenger.

The results of the experiment with sodium bisulfite as an oxygen scavenger are puzzling. It is apparent that the experiment was not a good representation of what would occur in the field, which would be a non-reduced solution continuously encountering reduced fluids, so further tests should be conducted with this in mind.

Exposing reduced brines to oxygen as polymer is hydrated or afterwards risks serious degradation to the polymer, even when iron concentrations are less than 1 ppm. One method to mitigate this is oxygenation of the brine before polymer is added, however care must be taken to ensure subsequent degradation is not caused by the injection of a polymer solution containing oxygen into a formation containing iron. For instance, sodium dithionite can be added downstream of the last exposure to oxygen. The addition of sodium carbonate to the brine prior to polymer could also mitigate the presence of iron (II).

Several polymers were successfully injected into a low permeability carbonate core plug. A chemical formulation was also developed that recovered more than 90% of the oil remaining after water flooding. For most reservoirs, this would be enough to recommend chemical flooding using polymer for mobility control. However, the pressure drops during the core flood were extremely high (on the order of 500 psi/ft corresponding to a flow rate of ~1 ft/day) and scaling to the field would be either mean excessively low injectivity or an impossibly high pressure gradient. Also, the polymer

used for the chemical flood was pre-sheared for six minutes in a Waring blender and passed through a 0.2 μm filter, which may not be feasible in a field setting.

APPENDIX A

The purpose of this appendix is to provide a summary of the coreflooding experiments not included in the main body of this thesis.

Table A.1: Summary of L-1 Coreflood

Rock	Reservoir
Mass	632.0 g
PV	92.0 mL
Porosity	0.284
Length	28.96 cm
Diameter	3.73 cm
Area	11.1 cm ²
Temperature	69 C
Injection Brine	SSL SB
k_{brine}	3.25 md
S_{oi}	0.75
S_{wr}	0.25
k_{oil}	1.50 md
k_{ro}	0.46
S_{orw}	0.37
k_{water}	0.40 md
k_{rw}	0.12
S_{orc}	0.20

ASP slug

0.3 PV

0.3% Avanel S-150

0.3% Neodol sulfate

4000 ppm FP 3230S

10,000 ppm Na₂CO₃ and 190,000 ppm NaCl

Frontal velocity : ~1 ft/day (=0.0625 ml/min)

Polymer drive

4000 ppm FP 3230S

SSL SB

Frontal velocity : ~1 ft/day (=0.0625 ml/min)

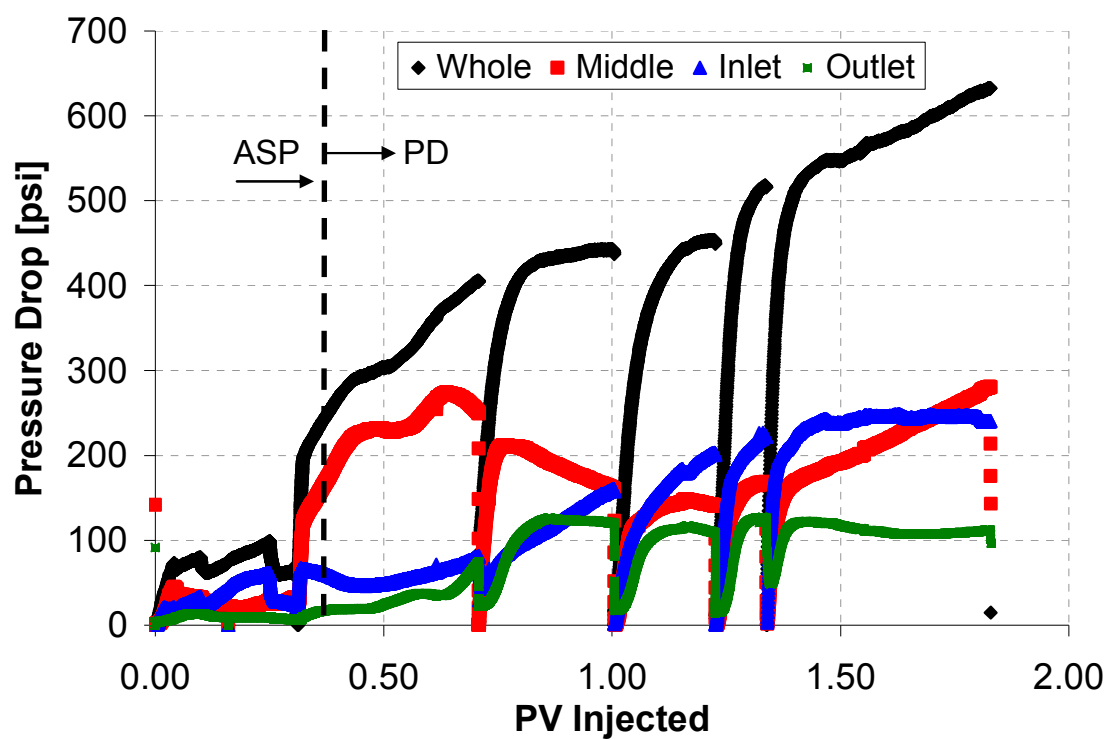


Figure A.1: L-1 chemical flood pressure data; 69 C; ~1 ft/day

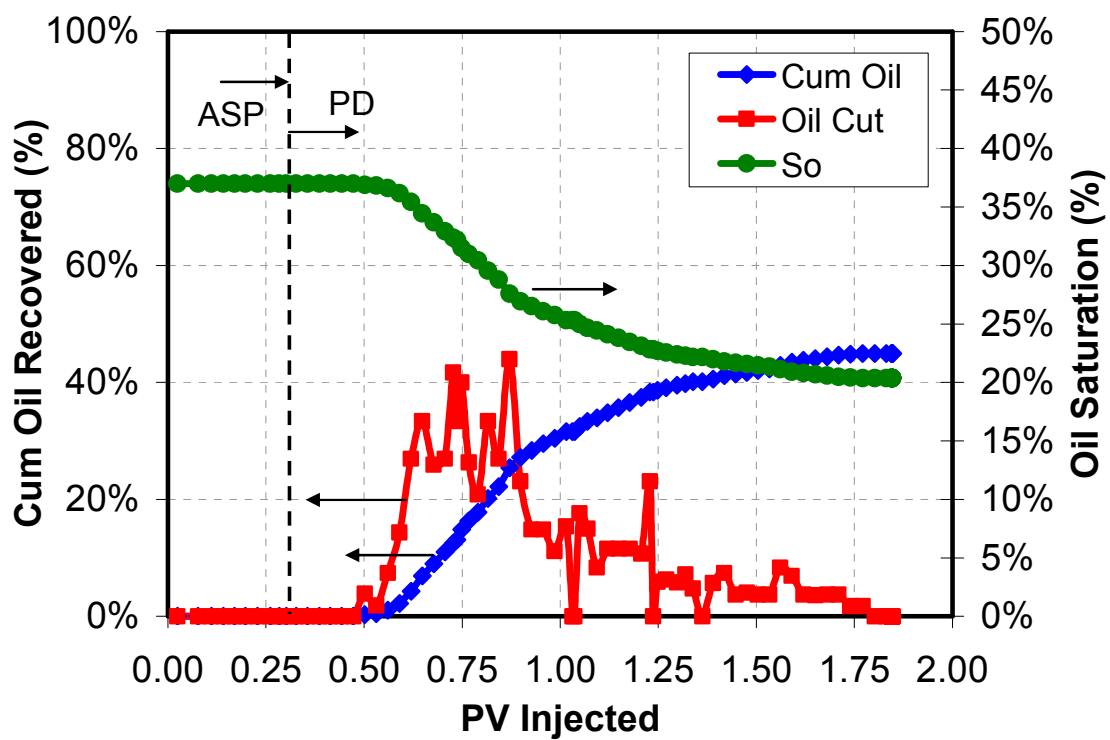


Figure A.2: Oil recovery, saturation, and cut for L-1 chemical flood

Table A.2: Summary of L-2 Coreflood

Rock	Reservoir
Mass	525.0 g
PV	78.0 mL
Porosity	0.284
Length	24.13 cm
Diameter	3.73 cm
Area	11.1 cm ²
Temperature	69 C
Injection Brine	SSLB
k_{brine}	3.06 md
S_{oi}	0.73
S_{wr}	0.27
k_{oil}	1.94 md
k_{ro}	0.63
S_{orw}	0.35
k_{water}	0.30 md
k_{rw}	0.10
S_{orc}	0.26

ASP slug

0.3 PV

0.5% BASF sulfate (C17-12EO-sulfate)

0.5% Neodol sulfate (C12~15-12EO-sulfate)

2500 ppm FP 3230S

10,000 ppm Na₂CO₃ and 190,000 ppm NaCl

Frontal velocity : ~1 ft/day (=0.0625 ml/min)

Polymer drive

2500 ppm FP 3230S

in 180,000 ppm NaCl

Frontal velocity : ~1 ft/day (=0.0625 ml/min)

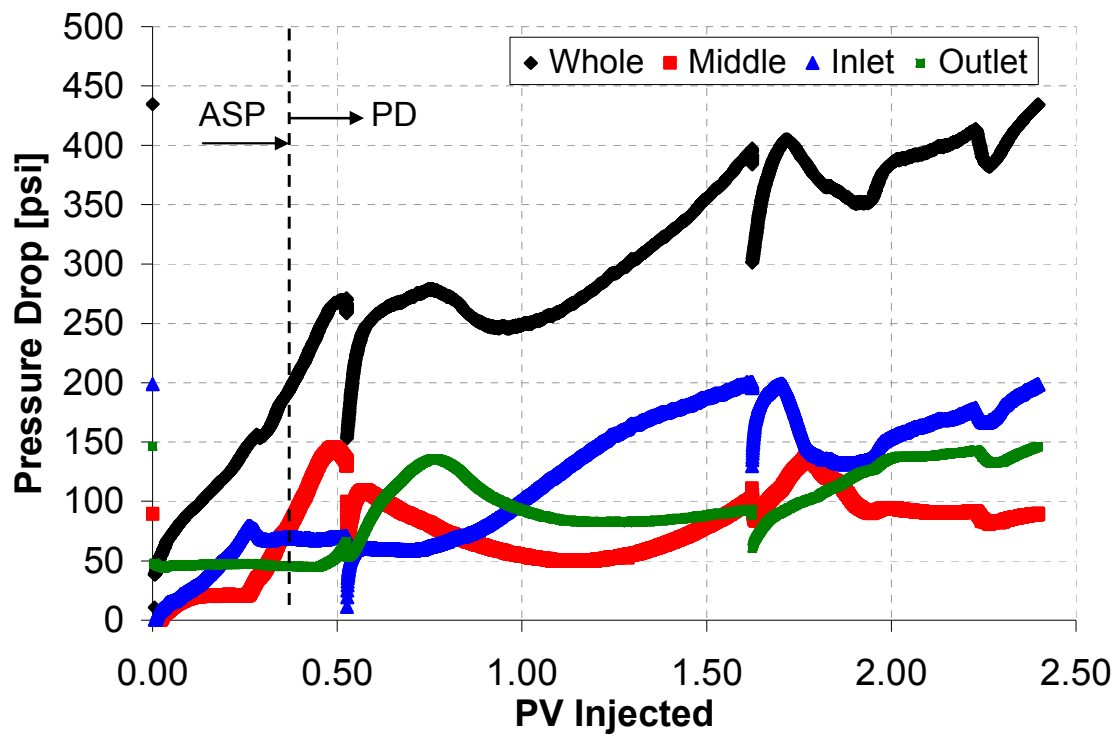


Figure A.3: L-2 chemical flood pressure data; 69 C; ~1 ft/day

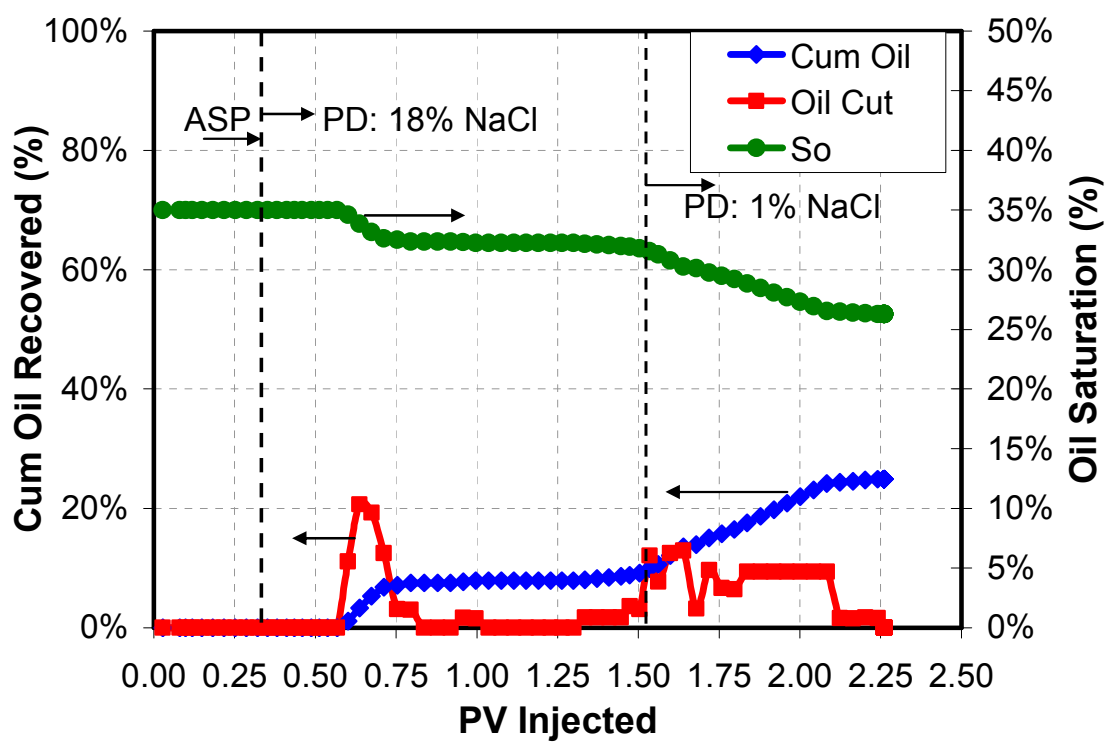


Figure A.4: Oil recovery, saturation, and cut for L-2 chemical flood

Table A.3: Summary of L-3 Coreflood

Rock	Berea
Mass	1200.0 g
PV	118.0 mL
Porosity	0.200
Length	29.08 cm
Diameter	5.08 cm
Area	20.27 cm ²
Temperature	69 C
Injection Brine	SSLB
k_{brine}	465.4 md
S_{oi}	0.61
S_{wr}	0.39
k_{oil}	292.6 md
k_{ro}	0.63
S_{orw}	0.35
k_{water}	22.2 md
k_{rw}	0.04
S_{orc}	0.23

ASP slug

0.3 PV

0.5% BASF sulfate (C17-12EO-sulfate)

0.5% Neodol sulfate (C12~15-12EO-sulfate)

2500 ppm FP 3230S

10,000 ppm Na₂CO₃ and 170,000 ppm NaCl

Frontal velocity : ~2 ft/day (=0.167 ml/min)

Polymer drive

2500 ppm FP 3230S

in 180,000 ppm NaCl

Frontal velocity : ~2 ft/day (=0.167 ml/min)

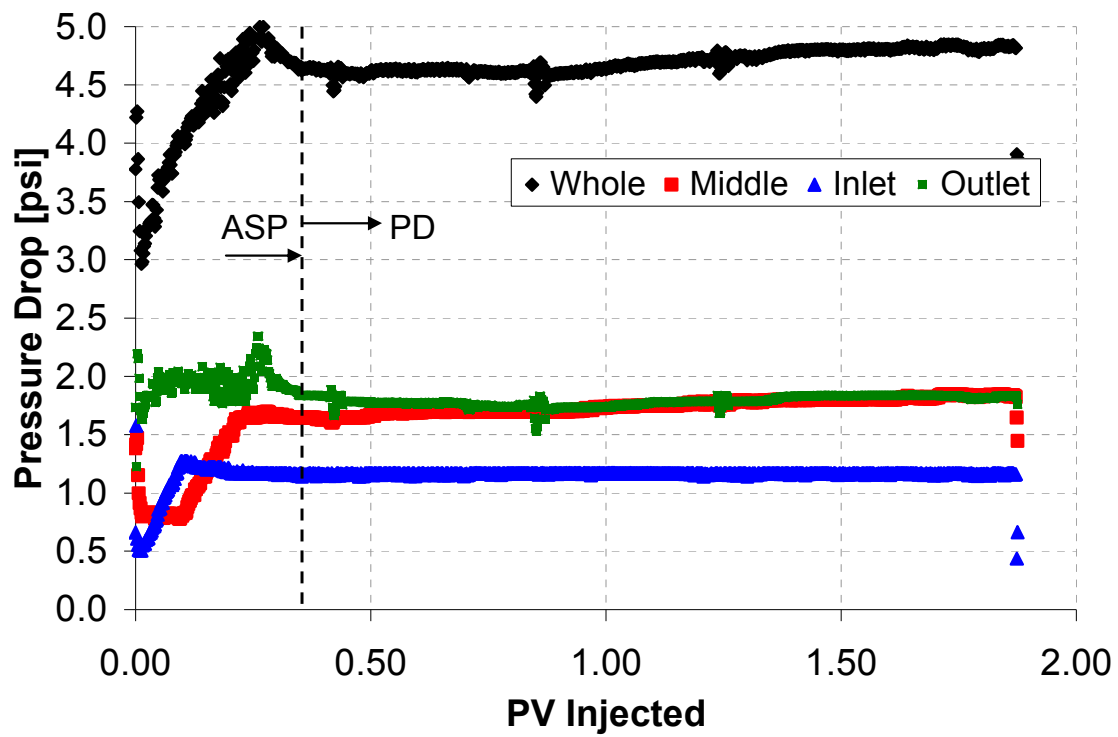


Figure A.5: L-3 chemical flood pressure data; 69 C; ~2 ft/day

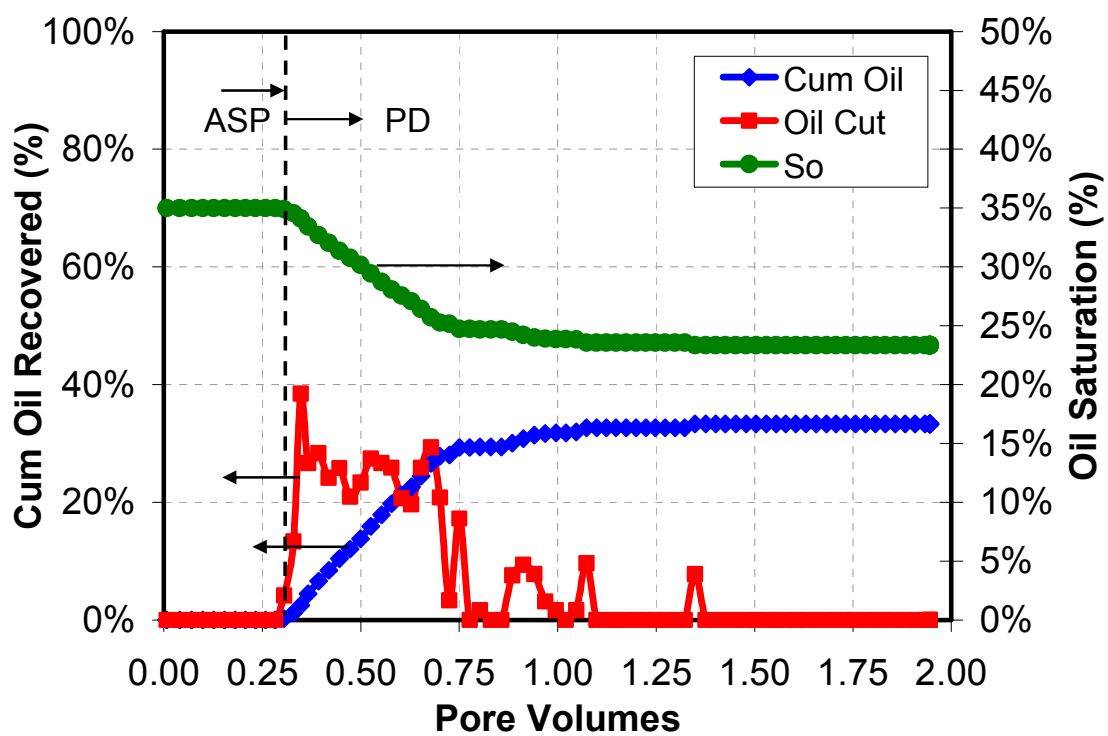


Figure A.6: Oil recovery, saturation, and cut for L-3 chemical flood

Table A.4: Summary of L-4 Coreflood

Rock	Berea
Mass	1203.7 g
PV	129.0 mL
Porosity	0.218
Length	29.21 cm
Diameter	5.08 cm
Area	20.27 cm ²
Temperature	69 C
Injection Brine	SSLBS
k_{brine}	423.0 md
S_{oi}	0.55
S_{wr}	0.45
k_{oil}	385.0 md
k_{ro}	0.91
S_{orw}	0.35
k_{water}	19.82 md
k_{rw}	0.05
S_{orc}	0.17

ASP slug

0.3 PV

0.15% Petrostep S-3A (*Lot # 18239-091907*)

0.15% Petrostep S-1 (Lot: 17A)

0.2% TDA-30

20000 ppm Na₂CO₃

2500 ppm FP3230S

@ SSLBS (1% NaCl)

Viscosity: ~ 6 cP @ 10 s⁻¹

Frontal velocity: ~2 ft/day (=0.167 ml/min)

Polymer drive

2000 ppm FP3230S

@ SSLBS (1% NaCl)

Viscosity: ~ 6 cP @ 10 s⁻¹

Frontal velocity: ~2 ft/day (=0.167 ml/min)

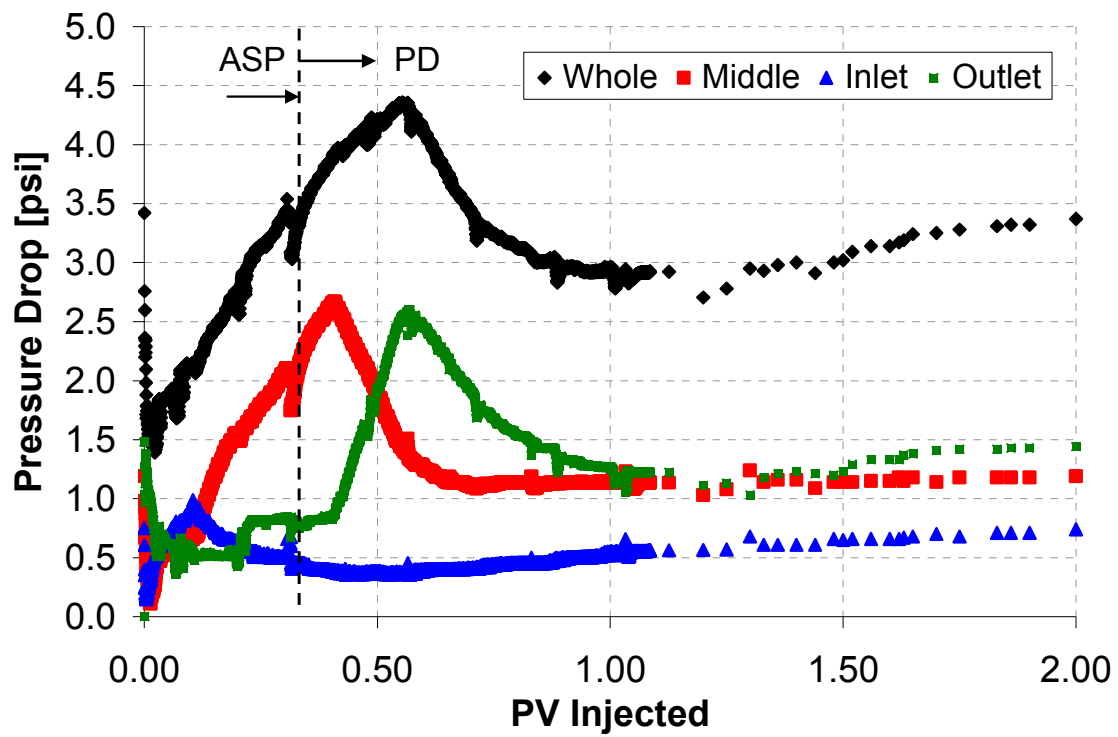


Figure A.7: L-4 chemical flood pressure data; 69 C; ~2 ft/day

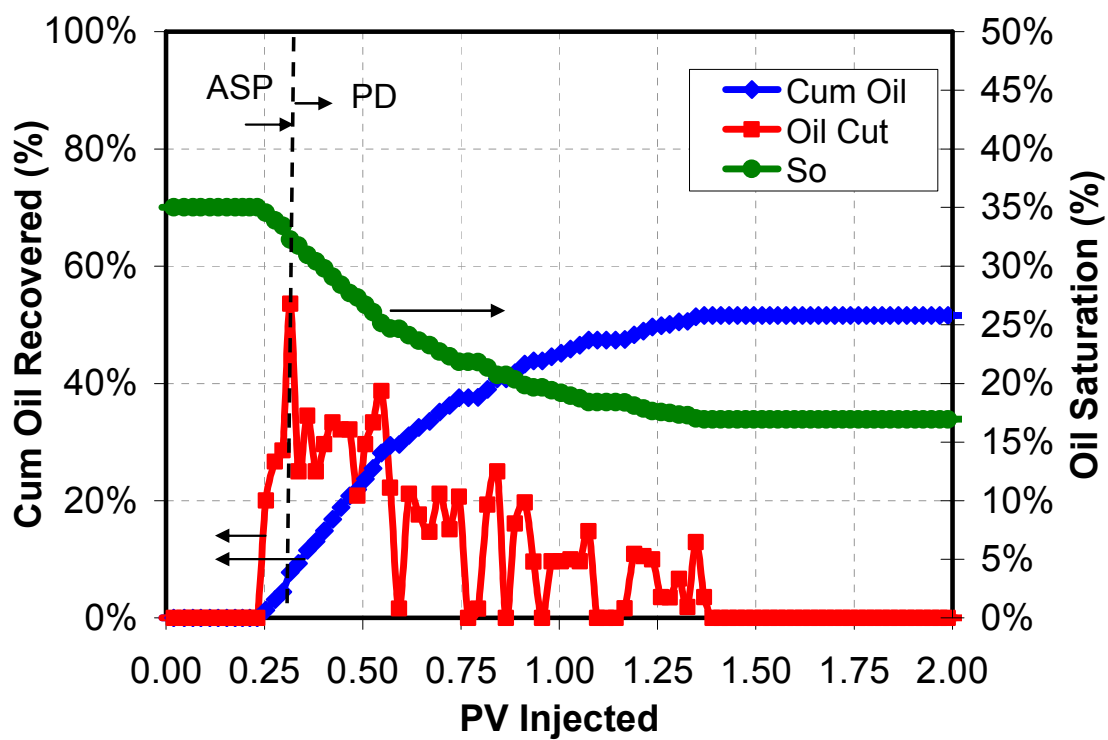


Figure A.8: Oil recovery, saturation, and cut for L-4 chemical flood

Table A.5: Summary of L-5 Coreflood

Rock	Berea
Mass	1200.1 g
PV	115.0 mL
Porosity	0.194
Length	29.21 cm
Diameter	5.08 cm
Area	20.27 cm ²
Temperature	69 C
Injection Brine	SSLB
k_{brine}	498.0 md
S_{oi}	0.63
S_{wr}	0.37
k_{oil}	298.0 md
k_{ro}	0.59
S_{orw}	0.40
k_{water}	22.0 md
k_{rw}	0.04
S_{orc}	0.13

ASP slug (PV*C = 15)

0.5 PV

0.15% Petrostep S-3A (*Lot # 18239-091907*)

0.15% Petrostep S-1 (*Lot # 18302-17A*)

0.2% TDA-30 (*Lot # 2097082107*)

25000 ppm Na₂CO₃

2500 ppm FP3230S in 1% NaCl

Viscosity: 5.5 cP@ 10s⁻¹ and 69 C

Frontal velocity: ~1 ft/day (=0.09 ml/min)

Polymer drive

2500 ppm FP3230S in 1% NaCl

Viscosity: 7.8 cP@ 10s⁻¹ and 69 C

Frontal velocity: ~1 ft/day (=0.09 ml/min)

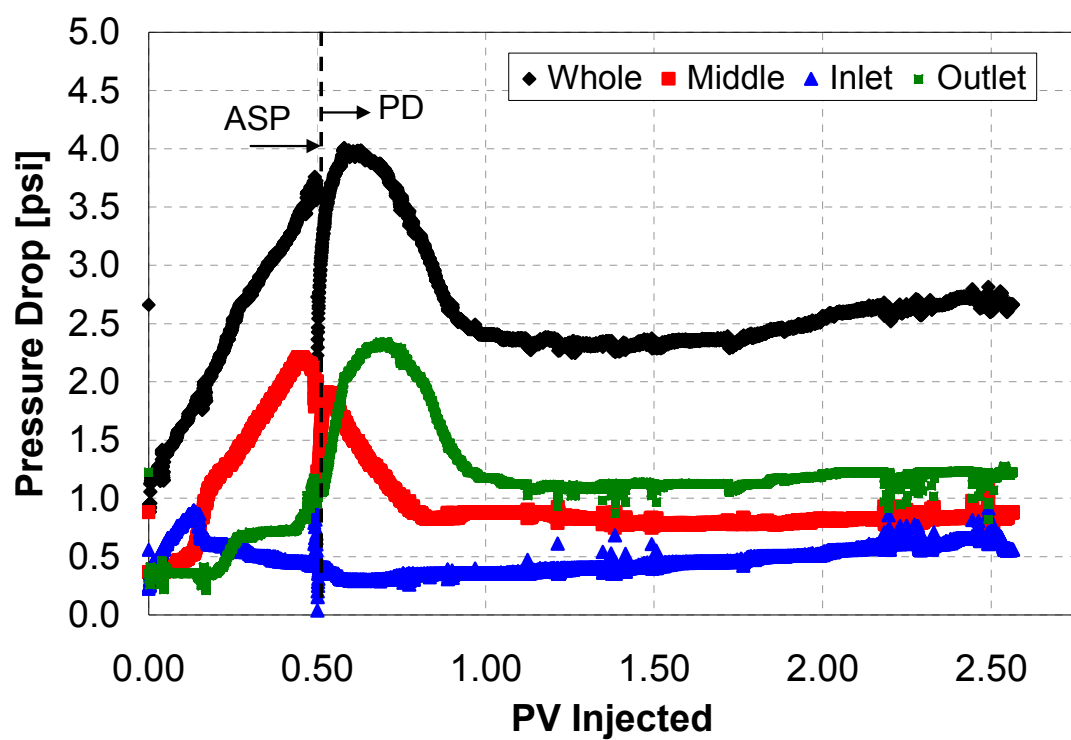


Figure A.9: L-5 chemical flood pressure data; 69 C; ~1 ft/day

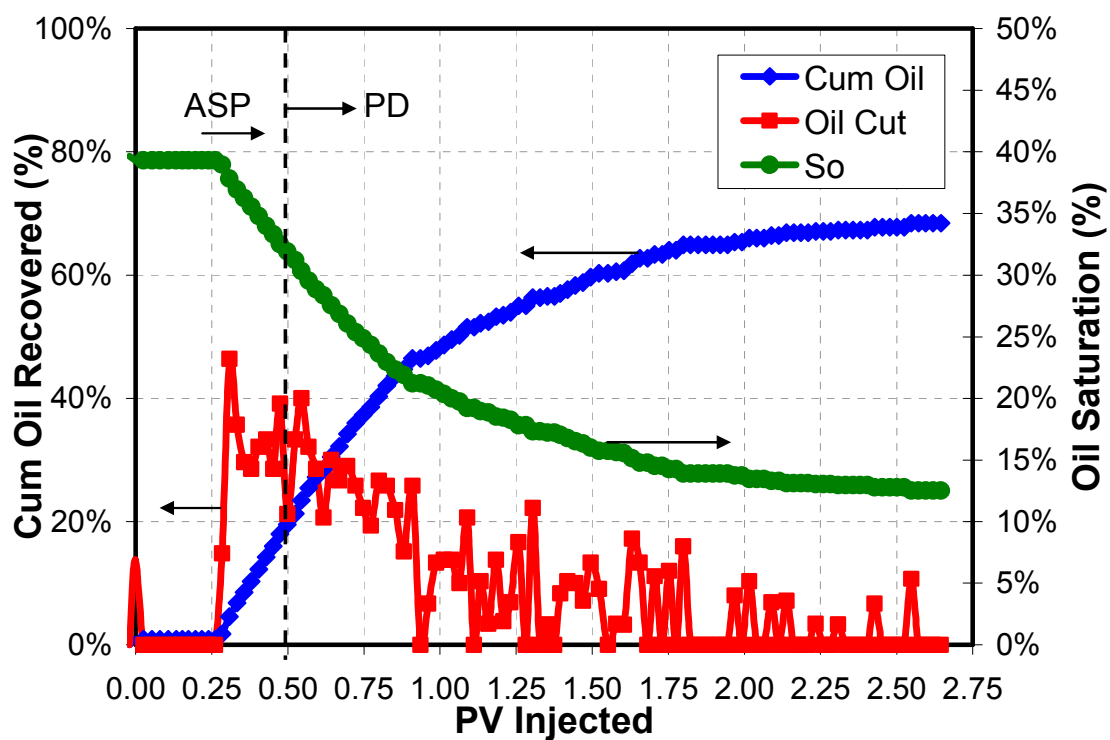


Figure A.10: Oil recovery, saturation, and cut for L-5 chemical flood

Table A.6: Summary of L-6 Coreflood

Rock	Berea
Mass	1200.0 g
PV	105.4 mL
Porosity	0.178
Length	29.21 cm
Diameter	5.08 cm
Area	20.27 cm ²
Temperature	69 C
Injection Brine	SSLBS
k_{brine}	476.0 md
S_{oi}	0.62
S_{wr}	0.38
k_{oil}	371.0 md
k_{ro}	0.78
S_{orw}	0.36
k_{water}	17.0 md
k_{rw}	0.04
S_{orc}	0.08

ASP slug (PV*C = 18)

0.3 PV

0.3% C28-7PO-2EO-sulfate

0.3% Petrostep S3A (*Lot # 18239-091907*)

0.3% TDA-30 (*Lot # 2097082107*)

0.3% Aerosol MA 80-I

3.25% Na₂CO₃

3500 ppm FP3230S in 1% NaCl

Viscosity: 9.8 cP@ 10s⁻¹ and 69 C

Frontal velocity: ~2 ft/day (=0.16 ml/min)

Polymer drive

3000 ppm FP3230S in 1% NaCl

Viscosity: 13.6 cP@ 10s⁻¹ and 69 C

Frontal velocity: ~2 ft/day (=0.16 ml/min)

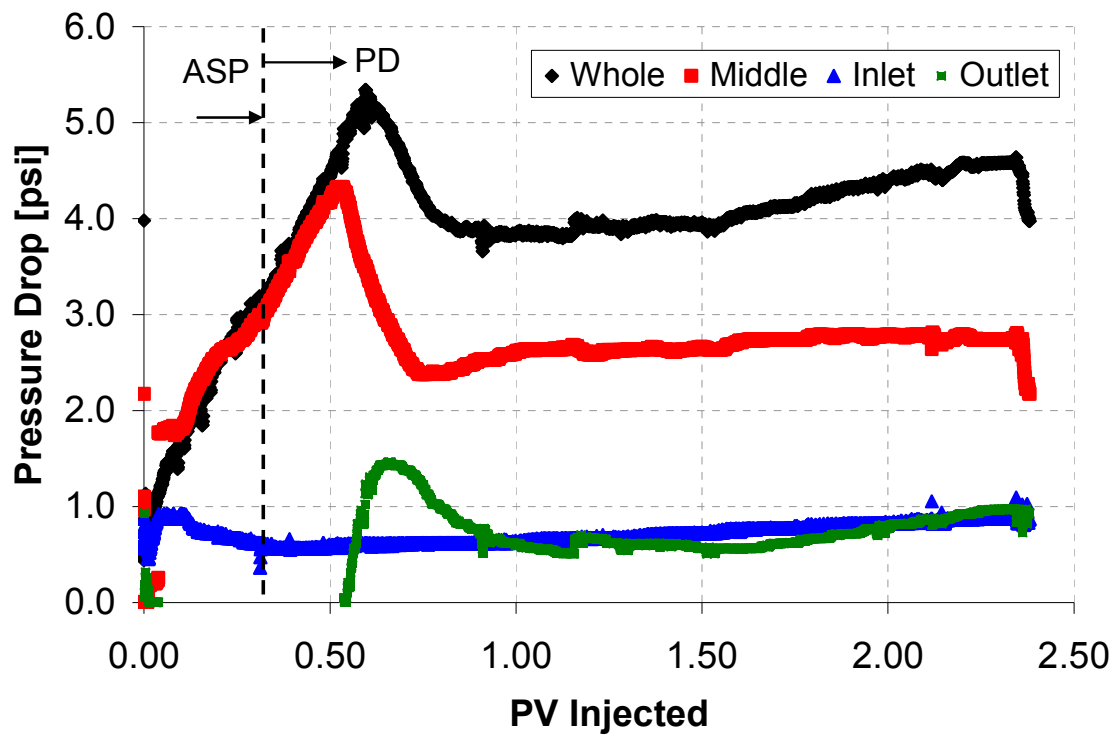


Figure A.11: L-6 chemical flood pressure data; 69 C; ~2 ft/day

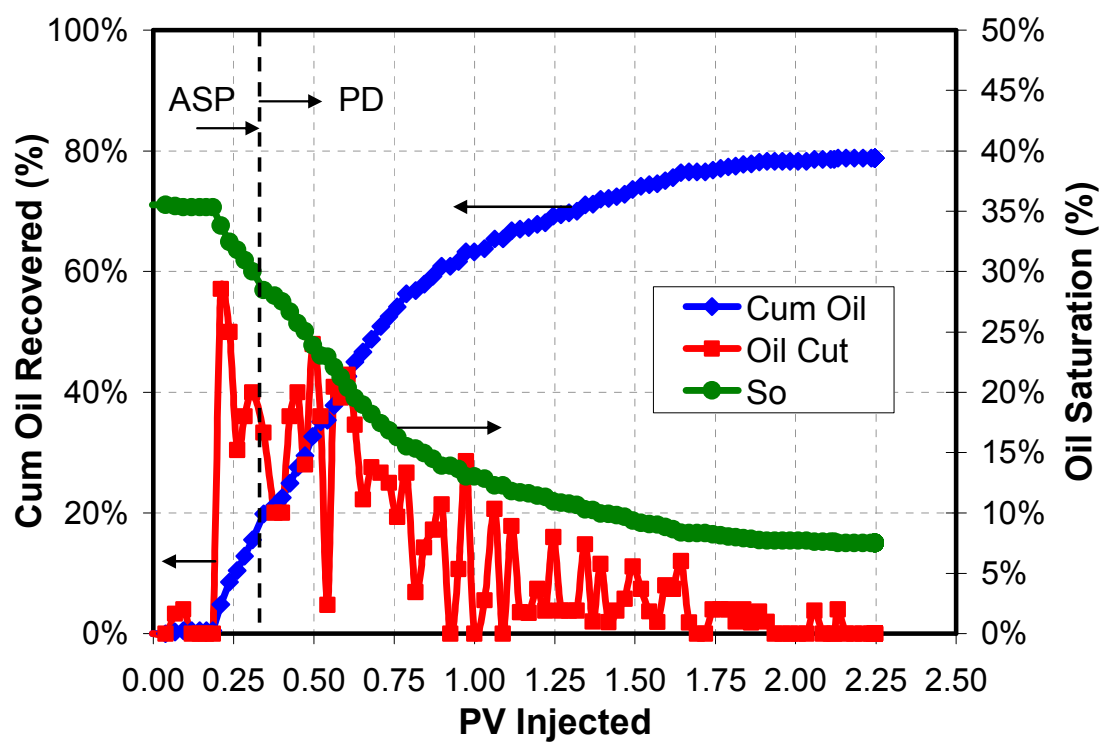


Figure A.12: Oil recovery, saturation, and cut for L-6 chemical flood

Table A.7: Summary of L-7 Coreflood

Rock	Berea
Mass	1200.0 g
PV	116.2 mL
Porosity	0.199
Length	29.06 cm
Diameter	5.05 cm
Area	20.07 cm ²
Temperature	69 C
Injection Brine	SSLB
k_{brine}	587.0 md
S_{oi}	0.65
S_{wr}	0.35
k_{oil}	506.0 md
k_{ro}	0.86
S_{orw}	0.37
k_{water}	20 md
k_{rw}	0.04
S_{orc}	0.01

ASP slug (PV*C = 18)

0.3 PV

0.3% C32-7PO-6EO Sulfate

0.3% Petrostep S3A (*Lot # 18239-091907*)

0.1% TDA-30 (*Lot # 2097082107*)

0.4% Aerosol MA 80-I

2.5% Na₂CO₃

3000 ppm FP3330S in 1% NaCl

Viscosity: 13.6 cP@ 10s-1 and 69 C

Frontal velocity: ~2 ft/day (=0.16 ml/min)

Polymer drive

2500 ppm FP3330S in 1% NaCl

Viscosity: 14.9 cP@ 10s-1 and 69 C

Frontal velocity: ~2 ft/day (=0.16 ml/min)

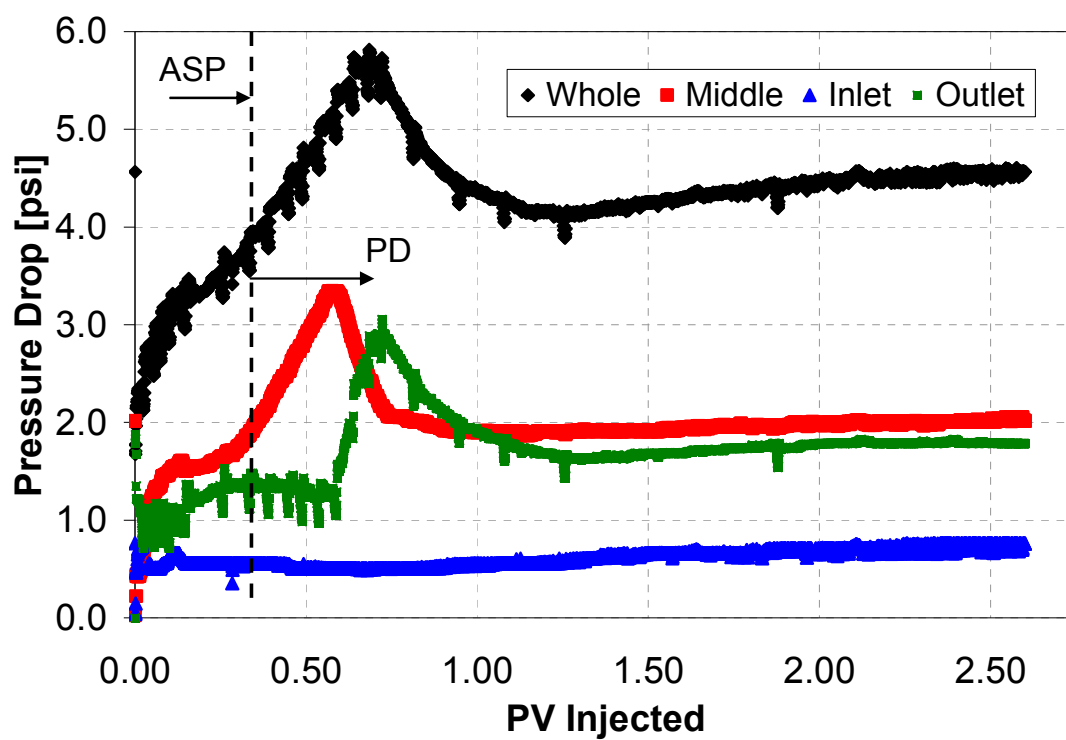


Figure A.13: L-7 chemical flood pressure data; 69 C; ~2 ft/day

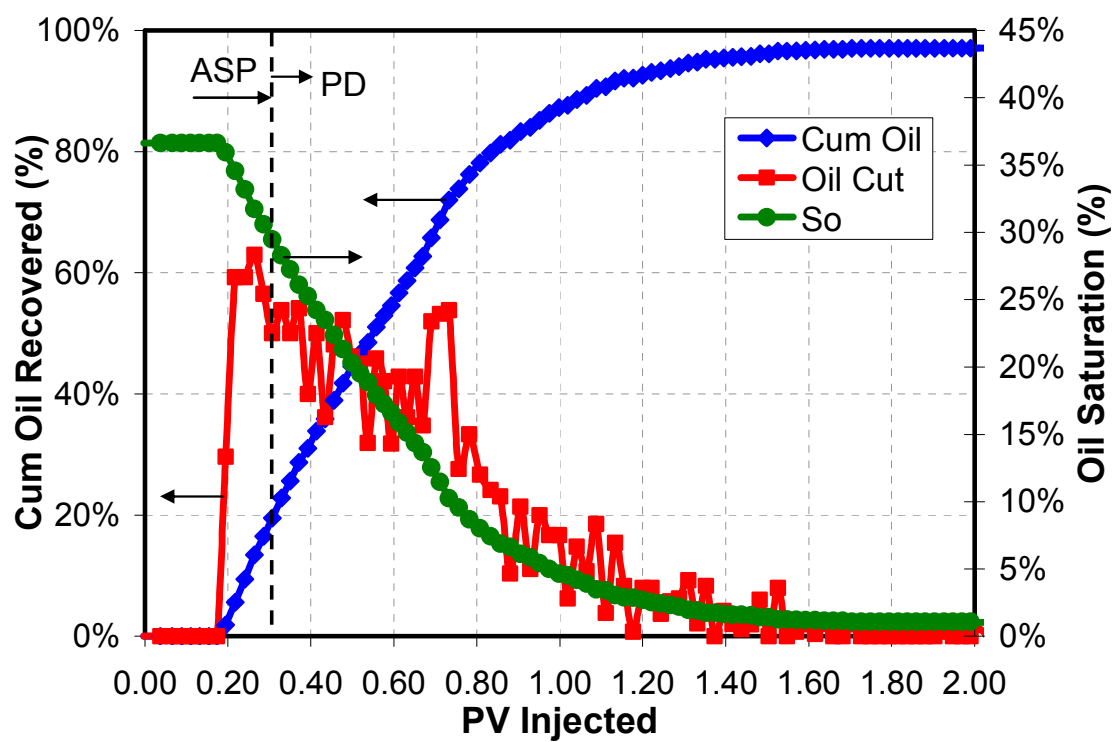


Figure A.14: Oil recovery, saturation, and cut for L-7 chemical flood

Table A.8: Summary of L-8 Coreflood

Rock	Berea
Mass	1199.2 g
PV	119.4 mL
Porosity	0.205
Length	29.06 cm
Diameter	5.05 cm
Area	20.07 cm ²
Temperature	69 °C
Injection Brine	SSLB
k_{brine}	517.0 md
S_{oi}	0.66
S_{wr}	0.34
k_{oil}	475.0 md
k_{ro}	0.92
S_{orw}	0.35
k_{water}	15.0 md
k_{rw}	0.03
S_{orc}	0.01

ASP Slug (PV*C=18):

Slug size 0.3 PV

0.3% Isofol C32-7PO-6EO Sulfate (U32-P706E-2)

0.3% Stepan Petrostep S-3A (*Lot # 18239-091907*)

0.1% TDA-30 (*Lot # 2097082107*)

0.4% Aerosol MA 80-I (Sodium dihexyl sulfosuccinate)

2.5% Na₂CO₃

1600 ppm FP 3330S in 1% NaCl

Frontal Velocity: 2 ft/day (0.16 ml/min)

Viscosity: 5.6 cP at 10 s⁻¹ and 69 °C

Filtration Ratio: 1.0

Polymer Drive:

2 PV or until emulsion stops being produced

1300 ppm FP 3330S in 1% NaCl

Frontal Velocity: 2 ft/day (0.16 ml/min)

Viscosity: 5.9 cP at 10 s⁻¹ and 69 °C

Filtration Ratio: 1.1

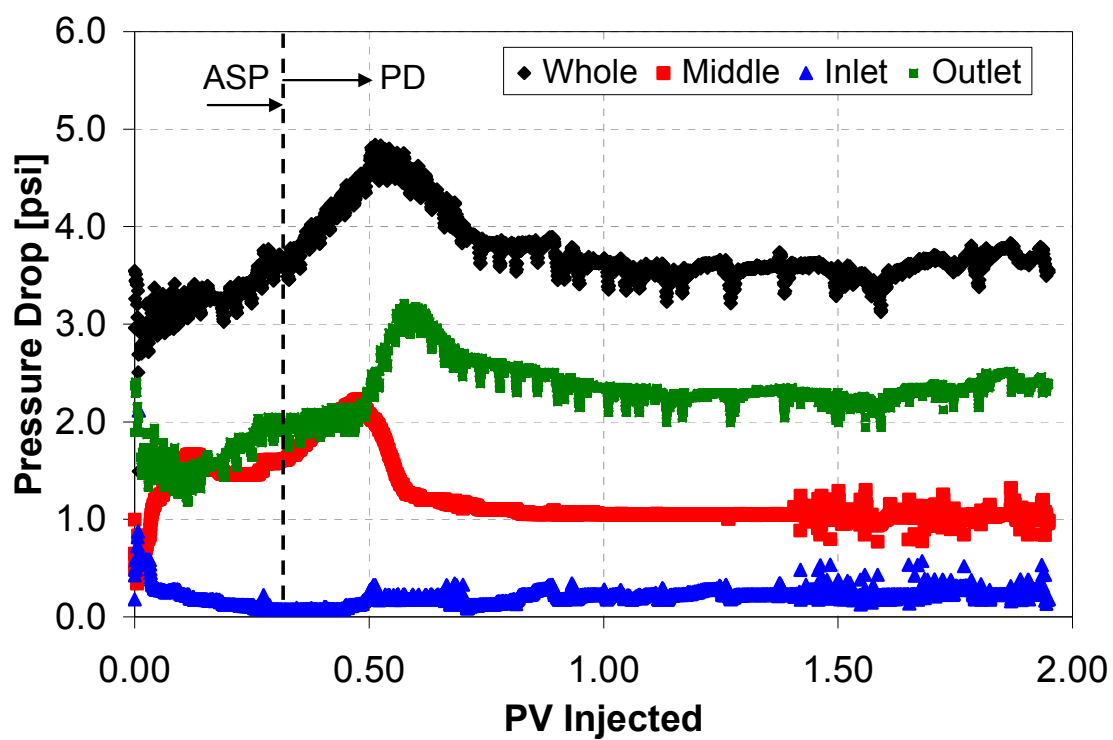


Figure A.15: L-8 chemical flood pressure data; 69 C; ~2 ft/day

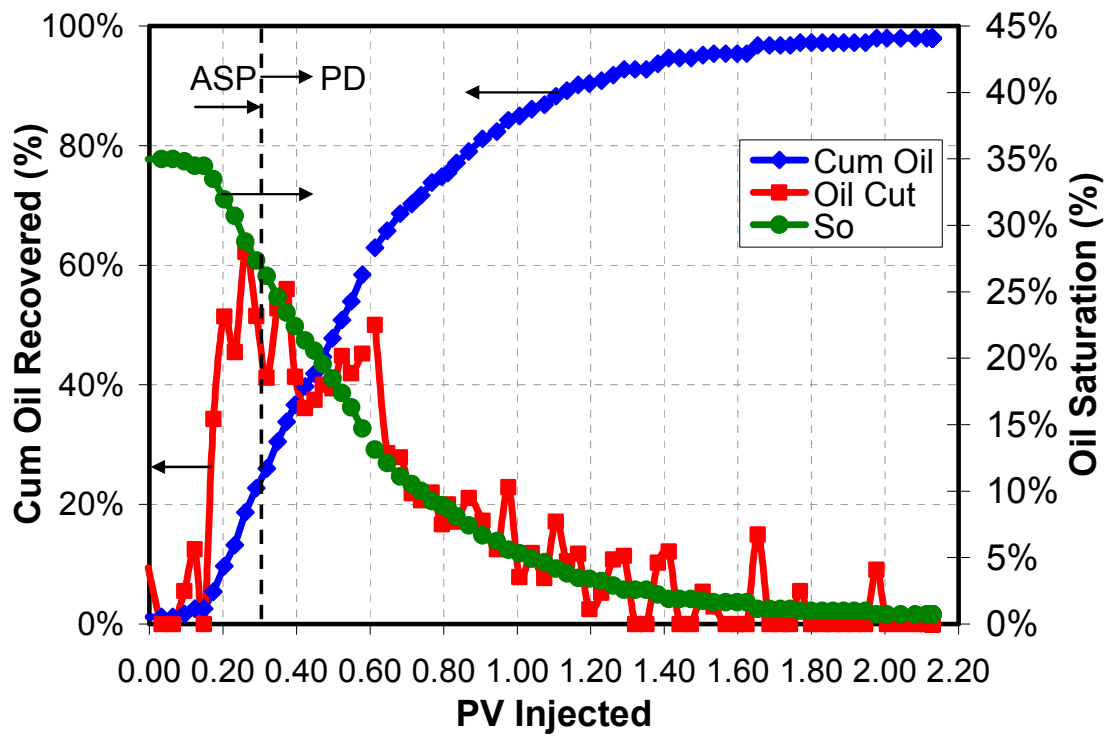


Figure A.16: Oil recovery, saturation, and cut for L-8 chemical flood

Bibliography

- Baas Becking, L.G.M., Kaplan, I.R. and Moore, D. 1960. "Limits of the Natural Environment in Terms of pH and Oxidation-Reduction Potentials," *Journal of Geology* 68 (3): 243-284.
- Cohen, G., and Sinet, M. P. 1982. The Fenton Reaction Between Ferrous Diethylenetriaminepentaacetic Acid and Hydrogen Peroxide. *FEBS Letters*, Vol 138 No. 2, February. 258-260.
- Davidson, P. and Mentzer, E. 1982. Polymer Flooding in North Sea Reservoirs. Paper SPE 9300 presented at the 1982 SPE Annual Technical Conference and Exhibition, Dallas, TX, 21-24 September.
- Dria, M.A., Schechter, R.S., and Lake, L.W. 1988. "An Analysis of Reservoir Chemical Treatments," *SPE Production Engineering*, February, 52-62.
- Flaaten, A.K. 2007. "Experimental Study of Microemulsion Characterization and Optimization in Enhanced Oil Recovery: A Design Approach for Reservoirs with High Salinity and Hardness," M.S. Thesis, University of Texas at Austin, Austin Texas, December.
- Flaaten, A.K., Nguyen, Q.P., Zhang, J., Mohammadi, H., Pope, G.A. 2008. "ASP Chemical Flooding without the Need of Soft Water," SPE 116754, paper presented at the SPE IOR Symposium, Tulsa, OK, 19-23 April.
- Fernandez, I.J., 2005, "Evaluation of Cationic Water-Soluble Polymers With Improved Thermal Stability," SPE 93003, paper presented at the SPE International Symposium on Oilfield Chemistry, Houston, TX, 2-4 February.
- Foshee, W.C., Jennings, R. R., and West, T. J. 1976. "Preparation and Testing of Partially Hydrolyzed Polyacrylamide Solutions." SPE 6202, paper presented at the 1976 SPE Annual Technical Conference and Exhibition, New Orleans, LA, 3-6 October.
- Jackson, A.C. 2006. "Experimental Study of the Benefits of Sodium Carbonate on Surfactants for Enhanced Oil Recovery" M.S. Thesis, University of Texas at Austin, Austin Texas, December.

- Jennings, R. R., J. H. Rogers and T. J. West. 1971. "Factors Affecting Mobility Control by Polymer Solutions," *Journal of Petroleum Technology*, March, 391- 401.
- Kheradmand, H. 1987. Contribution A L'Etude De La Degradation Et La Stabilisation De Polyacrylamides En Solution Aqueuse. These Pour Obtenir Le Grade De Docteur D'Etat Es Sciences Physiques, Universite Louis Pasteur De Strasbourg, Strasbourg, France.
- Knight, B. L. 1973. "Reservoir Stability of Polymer Solutions," *Journal of Petroleum Technology*, May: 618-626.
- Lake, L.W. Enhanced Oil Recovery. Prentice-Hall, Upper Saddle River, NJ, 1989.
- Levitt, D.B. 2006. "Experimental Evaluation of High Performance EOR Surfactants for a Dolomite Oil Reservoir," M.S. Thesis, University of Texas at Austin, Austin Texas, December.
- Levitt, D.B. 2009. "The Optimal Use of Enhanced Oil Recovery Polymers Under Hostile Conditions," PhD Dissertation, University of Texas at Austin, Austin Texas, May.
- Levitt, D.B., and Pope, G.A. 2008. "Selection and Screening of Polymers for Enhanced Oil Recovery," SPE 113845, paper presented at the SPE IOR Symposium, Tulsa, OK, 19-23 April.
- Martin, F.D. 1974. "Laboratory Investigations in the Use of Polymers in Low Permeability Reservoirs," SPE 5100, paper presented at Fall Meeting of the Society of Petroleum Engineers of AIME, Houston, Texas, 6-9 October.
- Martin, F.D., Hatch, M.J., Shepitka, J.S., and Ward, J.S. 1983. "Improved Water-Soluble Polymers for Enhanced Recovery of Oil," SPE 11786, paper presented at the International Symposium on Oilfield and Geothermal Chemistry, Denver, CO 1-3 June.
- Moradi-Araghi, A., Cleveland, D.H., Jones, W.W., and Westerman, I.J. 1987. "Development and Evaluation of EOR Polymers Suitable for Hostile Environments: II-Copolymers of Acrylamide and Sodium AMPS," SPE 16273, paper presented at the International Symposium on Oilfield Chemistry, San Antonio, TX 4-6 February.
- Moradi-Araghi, A. and Doe, P.H. 1987. "Hydrolysis and Precipitation of Polyacrylamides in Hard Brines at Elevated Temperatures," *SPE* 189-198.
- Muller, G. 1981a. "Thermal Stability of High-molecular-weight Polyacrylamide Aqueous Solutions," *Polymer Bulletin* **5**: 31-37.

- Muller, G. 1981b. "Thermal Stability of Polyacrylamide Solutions: Effect of Residual Impurities in the Molecular-weight-degradation Process upon Heating," *Polymer Bulletin* **5**: 39-45.
- Muller G., Fenyo, J.C., and Selegny, E. 1980. "High Molecular Weight Hydrolyzed Polyacrylamides. III. Effect of Temperature on Chemical Stability," *J. Applied Polymer Science* **25**: 627-633.
- Parker Jr , W. O. and Lezzi, A. 1993. "Hydrolysis of Sodium-2-acrylamido-2 methylpropanesulfonate Copolymers at Elevated Temperature in Aqueous Solution via ^{13}C n.m.r. Spectroscopy," *Polymer* **34** (23) 4913-4918.
- Pye, D. J. 1967. Water Flooding Process. US Patent No. 3,343,601.
- Ramsden, D.K. and McKay, K. 1986. "The Degradation of Polyacrylamide in Aqueous Solutions Induced by Chemically Generated Hydroxyl Radicals: Part I – Fenton's Reagent," *Polymer Degradation and Stability* **14**: 217-229.
- Sahni, V.M. 2009. "Experimental Evaluation of Co-Solvents in Development of High Performance Alkali/Surfactant/Polymer Formulations for Enhanced Oil Recovery," M.S. Thesis, University of Texas at Austin, Austin Texas, December.
- Schurz, G. 1972. "Field Preparation of Polymer Solutions Used to Improve Oil Recovery," SPE 4254, paper presented at the SPE Symposium on the Handling of Oilfield Waters, Los Angeles, California, 4-5 December.
- Shafer, R. V. and Pirson, S. J. 1969. "Characterization of Oilfield Waters by pH and Oxidation-Reduction Potential," SPE 2592, paper presented at the 1969 SPE Annual Meeting, Denver, Colorado, 28 September – 1 October.
- Shaughnessy, C.M. and Kline, W.E. 1983. "EDTA Removes Formation Damage at Prudhoe Bay," SPE 11188, *Journal of Petroleum Technology*, October: 1783-1791.
- Shupe, R.D. 1981. "Chemical Stability of Polyacrylamide Polymers," *Journal of Petroleum Technology*, August: 1513-1529.
- Sorbie, K. S. 1991. Polymer-Improved Oil Recovery. CRC Press, Inc., Boca Raton, FL.
- Taylor, K. S., and Nasr-El-Din, H. A. 1995. "Water-Soluble Hydrophobically Associating Polymers for Improved Oil Recovery: A Literature Review," SPE 29008, paper presented at the SPE International Symposium on Oilfield Chemistry, San Antonio, TX, 14-17 February.

- Xie, J., Liu, F.-P., 2007, "Degradation and Protection of Polymer used for enhanced Oil Recovery Rate (EOR)," *Journal of Shandong University of Science and Technology*, vol. 26, No 6, 16-20.
- Yang, H.T. 2010. M.S. Thesis (in progress), University of Texas at Austin, Austin Texas.
- Yang, S.H. and Treiber, L.E. 1985. "Chemical Stability of Polyacrylamide Under Simulated Field Conditions," SPE 14232, paper presented at the SPE Annual Technical Conference and Exhibition, Las Vegas, NV 22-25 September.
- Zaitoun, A. and Potie, B. 1983. "Limiting Conditions for the Use of Hydrolyzed Polyacrylamides in Brines Containing Divalent Ions," SPE 11785, paper presented at the International Symposium on Oilfield and Geothermal Chemistry, Denver, CO 1-3 June.
- Zobell, C. E. 1946. "Studies on Redox Potential of Marine Sediments," *Bulletin of the American Association of Petroleum Geologists* **30** (4): 477-513.

Vita

Will Slaughter was born in Houston, Texas March, 8th 1980, the son of Kinneth and Joan Slaughter, and was raised in New Braunfels, Texas. After graduating from New Braunfels High School in New Braunfels, Texas, he attended The University of Texas at Austin, where he earned a Bachelor of Science in Civil Engineering in May 2003. Following a brief period working for an environmental engineering consulting firm in New Orleans, Louisiana and then for separate residential construction contractors in New Orleans, Louisiana and San Antonio, Texas, he began graduate studies at the University of Texas at Austin in June 2008.

Permanent address: 1711 Marigold Dr, New Braunfels, TX 78130

This thesis was typed by the author.